Analysis of Laminated Structures
Course of Lectures

Rolands Rikards
Riga Technical University

Riga, 1999

Preface

Among the modern structural materials, the history of fiber reinforced composites is only some decades old. However, in this short period of time, there has been a tremendous advancement in the science and technology of this new class of materials. The low density, high strength, high stiffness to weight ratio, exellent durability, and design flexibility of fiber reinforced polymers are the primary reasons for their use in many structural components in the aircraft, automotive, marine, building, and other industries. Fiber reinforced polymers are now used in applications ranging from spacecraft frames to ladder rails, from aircraft wings to automobile doors, from oxygen tanks to tennis rackets. Their use is increasing at such a rapid rate that they are no longer considered advanced materials.

In teaching courses on mechanics of composite materials to university students, I have felt a great need for a textbook on the separate subject of composite materials - analysis of laminated composite and sandwich structures. The present textbook is a brief introduction to the subject. In order to show the basic principles of analysis of laminated structures it is not necessary to give in detail the analysis of plates and shells, which is too complicated for the beginners. In the present textbook the basic principles of analysis are explained on laminated composite and sandwich beams. Similarly also the plates and shells can be analyzed.

The present textbook is a revised English version of one chapter of the book published in German in 1996 [1]. Here only laminated and sandwich beams are analized. For introduction into mechanics of composite materials the textbooks of Jones [6] and Gibson [12] can be recommended. Analysis of laminated composite plates is presented in the textbooks of Reddy [20, 21]. Analysis of sandwich structures in detail was outlined by Zenkert [2] and Stamm & Witte [3]. The last book was translated also in Russian. Fundamentals of variational methods were outlined in the book of Washizu [7], which also was translated in Russian. There are many textbooks on the finite element method. For beginners I can recommend the textbook [18]. For advanced users can be reccomended the book of Bathe [5], which is a

second edition. The first edition of this book also was translated in Russian. In detail the references for the finite element method you can find at the Web site http://www.solid.ikp.liu.se/fe suggested by J. Mackerle. A special subject of the present textbook is damping analysis. In detail the damping and the viscoelastic behavior of materials and structures was outlined in the books of Nashif, Johnes & Henderson [9] (translated in Russian), Sun [10] and Christensen [11] (translated in Russian). However, especially on the finite element method many other textbooks can be recommended.

The last information about new developments in the field of mechanics of composite materials and structures can be found in the scientific journals. Leading journals on this subject are as follows.

1. Mechanics of Composite Materials and Structures, Taylor & Francis, London, UK.
2. Journal of Reinforced Plastics and Composites, Technomic Publishing Co., Lancaster, Pennsylvania, USA.
3. Journal of Composite Materials, Technomic Publishing Co., Lancaster, Pennsylvania, USA.
4. Composite Structures, Elsevier Science, Oxford, England, UK.
5. Composites. Part A, Elsevier Science, Oxford, England, UK.
6. Composites. Part B, Elsevier Science, Oxford, England, UK.
7. Composites Science and Technology, Elsevier Science, Oxford, England, UK.
8. Polymer Composites, Society of Plastics Engineers, Brookfeld Center, Connecticut, USA.
9. Mechanics of Composite Materials, Zinatne Publishing House, Riga, Latvia.
10. Journal of Sandwich Structures and Materials, Technomic Publishing Co., Lancaster, Pennsylvania, USA.

The latest information about developments in the field of composite materials and structures can be obtained attending the international conferences on this subject or can be found in the proccedings of these meetings.

Rolands Rikards
Riga, July 1999

Contents

Chapter 1

Modelling of Composite Beams

1.1 Theory of Timoshenko's Beam

It is well known that due to week transverse stiffness the laminated composite and sandwich beams can not be analysed by using the Bernoulli-Euler's beam theory. There are many advanced theories for analysis of the laminated composite and sandwich beams. The simplest theory is the so-called Timoshenko's beam theory or the first order shear deformation theory, which was proposed by Timoshenko in 1921.

In the Timoshenko's beam theory a longitudinal displacement u_1 in the direction of the beam axis x and a transverse displacement u_3 are presented as follows (see Figure 1.1)

$$u_1(x,z) = u(x) + z\gamma_x(x), \quad u_3(x,z) = w(x) \tag{1.1}$$

Here u is longitudinal displacement at $z = 0$, w is deflection of the beam axis and γ_x is rotation of the normal in the x direction. Due to linear approximation of the tangential displacement u_1 Timoshenko's beam theory is called the first order shear deformation theory (FOSDT). Since the approximations (1.1) have been performed for the whole cross section of beam the present theory is called also the single layer theory. Note that this single approximation can be used for homogeneous beams as well as for multilayered beams.

In the Timoshenko's beam theory there are only two nonzero strains

$$\varepsilon_x = \frac{\partial u_1}{\partial x}, \qquad \varepsilon_y = 0, \quad \varepsilon_z = 0, \quad \gamma_{xz} = \frac{\partial u_1}{\partial z} + \frac{\partial u_3}{\partial x}, \quad \gamma_{yz} = 0, \quad \gamma_{xy} = 0 \tag{1.2}$$

Substituting the expressions (1.1) into (1.2) one obtains

$$\varepsilon_x = \epsilon_x + z\kappa_x, \quad \gamma_{xz} \equiv 2\epsilon_{xz} = \gamma_x + \frac{\partial w}{\partial x} \tag{1.3}$$

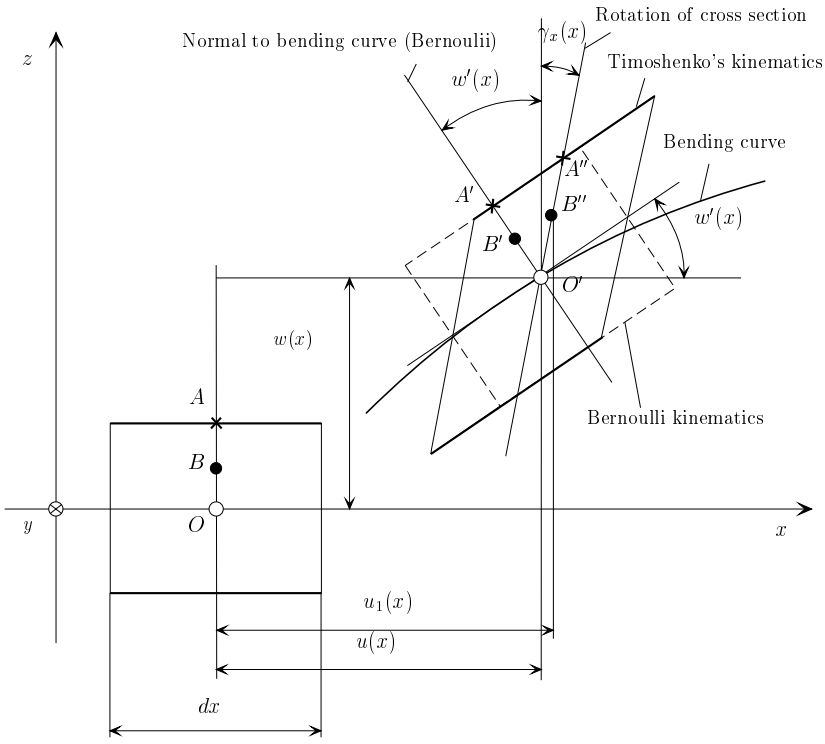

Figure 1.1: Deformations in beam according Bernoulli-Euler's and Timoshenko's theories

Here $\epsilon_x, 2\epsilon_{xz}$ and κ_x are strains and curvature, respectively

$$\epsilon_x = \frac{\partial u}{\partial x}, \quad \kappa_x = \frac{\partial \gamma_x}{\partial x} \tag{1.4}$$

The strain energy functional of the Timoshenko's beam can be written as follows

$$U = \frac{1}{2}\int_V (\sigma_x \varepsilon_x + \sigma_{xz}\gamma_{xz})\, dV \tag{1.5}$$

Substituting the expressions (1.3) in this functional one can obtain

$$U = \frac{1}{2}\int_0^L (N_x \epsilon_x + M_x \kappa_x + 2\, Q_x \epsilon_{xz})\, dx \tag{1.6}$$

Here L is length of the beam and stress resultants are introduced by

$$N_x = \int_F \sigma_x dF, \quad M_x = \int_F \sigma_x z dF, \quad Q_x = \int_F \sigma_{xz} dF \tag{1.7}$$

Here F is a cross section of the beam and $dF = dzdy$. Substituting into (1.7) the Hooke's law and taking into account (1.3) one can obtain the stress-strain relations of the Timoshenko's beam

$$N_x = Q_{11}\epsilon_x + B_{11}\kappa_x, \quad M_x = B_{11}\epsilon_x + D_{11}\kappa_x, \quad Q_x = 2kQ_{55}\,\epsilon_{xz} \tag{1.8}$$

Here k is a shear correction factor (SCF), which is introduced for correction of the transverse shear stiffness. Discussion in details about the shear correction factor and the method of evaluation of the SCF will be presented in the next section. In the expressions (1.8) the beam stiffness coefficients Q_{ij}, B_{ij} and D_{ij} are calculated using the stiffness $A_{ij}^{(k)}$ of the layers of the beam

$$\begin{aligned}
Q_{11} &= b\sum_{k=1}^{K} A_{11}^{(k)}[z_k - z_{k-1}], \\
Q_{55} &= b\sum_{k=1}^{K} A_{55}^{(k)}[z_k - z_{k-1}], \\
B_{11} &= b\frac{1}{2}\sum_{k=1}^{K} A_{11}^{(k)}[z_k^2 - z_{k-1}^2], \\
D_{11} &= b\frac{1}{3}\sum_{k=1}^{K} A_{11}^{(k)}[z_k^3 - z_{k-1}^3]
\end{aligned} \tag{1.9}$$

Here b is width of the beam and z_{k-1} is the bottom coordinate of the kth layer (see Figure 1.2). Since deformations of the beam are not constrained in the transverse directions in the formulae (1.9) the stiffness coefficients $A_{ij}^{(k)}$ of the layers can be expressed through the engineering elastic constants as follows

$$A_{11}^{(k)} = E_x^{(k)}, \quad A_{55}^{(k)} = G_{xz}^{(k)} \tag{1.10}$$

Here $E_x^{(k)}$ is a Young's modulus of the kth layer in the direction of the beam axis and $G_{xz}^{(k)}$ is a transverse shear modulus of the kth layer of the beam.

Substituting eq. (1.8) into the expression (1.6) and taking into account eqs (1.3) and (1.4) the strain energy functional can be expressed through three unknown functions $u(x), w(x)$ and $\gamma_x(x)$ as follows

$$\begin{aligned}
U = \frac{1}{2}\int_0^L [&Q_{11}\left(\frac{\partial u}{\partial x}\right)^2 + 2B_{11}\frac{\partial u}{\partial x}\frac{\partial \gamma_x}{\partial x} + \\
&D_{11}\left(\frac{\partial \gamma_x}{\partial x}\right)^2 + kQ_{55}\left(\gamma_x + \frac{\partial w}{\partial x}\right)^2]dx
\end{aligned} \tag{1.11}$$

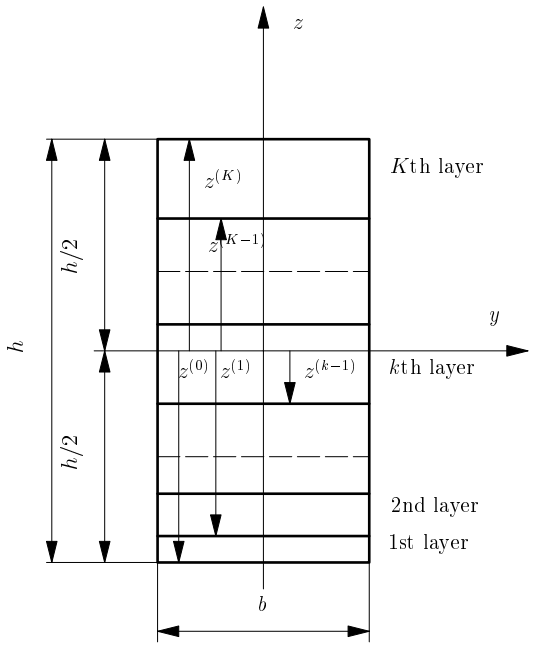

Figure 1.2: Layers of the beam

In the case of bending (without axial loading) of sandwich or laminated composite beam with symmetrical layer stacking sequence the coupling stiffness coefficient $B_{11} = 0$ and the strain energy functional (1.11) of the Timoshenko's beam can be simplified

$$U = \frac{1}{2}\int_0^L \left[D_{11}\left(\frac{\partial \gamma_x}{\partial x}\right)^2 + kQ_{55}\left(\gamma_x + \frac{\partial w}{\partial x}\right)^2 \right] dx \tag{1.12}$$

For the stress analysis of beam using a variational approach the potential energy Π of the structure must be determined

$$\Pi = U - W \tag{1.13}$$

Here W is a work of external loads. Employing a principle of minimum of potential energy the solution of the beam bending problem can be obtained

$$\delta\Pi = \delta(U - W) = 0 \tag{1.14}$$

Here δ denotes variation of the displacements in the functional of the potential energy. In many cases only approximate solution can be obtained. This means that approximate minimum of the potential energy of the structure is determined. Mainly approximate solutions are obtained by using the

Ritz's method (analytical solution) or the finite element method (numerical solution). The background for the finite element and the Ritz's method is similar. Actually, the finite element method is generalization of the Ritz's method for the computers. In the present textbook both the Ritz and the finite element methods in the form of the displacement method are used. For solution of simple examples of the stress and vibration analysis of structures the Ritz's method is used. More complex examples are analysed by using the finite element method. In order to understand principles of the Ritz's and the finite element method further the variation of the potential energy functional of the Timoshenko's beam (1.14) will be performed in the analytical form.

Let us consider the beam under external load $q(x)$ (see Figure 1.3). Stress resultants for the beam element are shown in Figure 1.4. Shorthand expression (1.12) of the Timoshenko's beam strain energy is as follows

$$U = \frac{1}{2}\int_0^L \left[M_x \frac{\partial \gamma_x}{\partial x} + Q_x \left(\gamma_x + \frac{\partial w}{\partial x} \right) \right] dx \tag{1.15}$$

Here the stress resultants for the uncoupled problem are given by

$$M_x = D_{11}\frac{\partial \gamma_x}{\partial x}, \quad Q_x = kQ_{55}\left(\gamma_x + \frac{\partial w}{\partial x} \right) \tag{1.16}$$

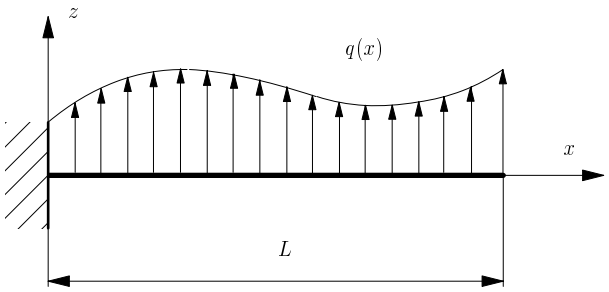

Figure 1.3: Timoshenko's beam in bending

Work of external forces can be expressed as follows

$$W = \int_0^L q(x) w \, dx \tag{1.17}$$

For the beam considered (see Figure 1.3) the kinematic (essential) boundary conditions are given by

$$w \mid_{x=0} = 0, \quad \gamma_x \mid_{x=0} = 0 \tag{1.18}$$

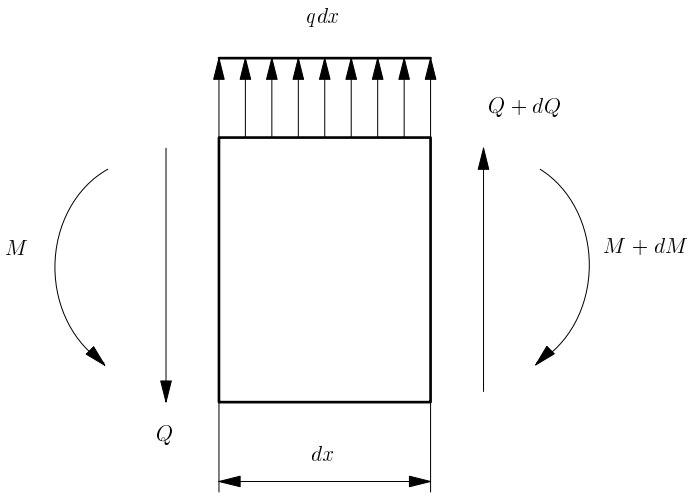

Figure 1.4: Stress resultants of the Timoshenko's beam

Substituting the strain energy functional of the beam (1.15) and the work of external forces (1.17) into (1.14) a variational equation of the problem is obtained

$$\delta\Pi = \int_0^L \left\{ M_x \delta \left(\frac{\partial \gamma_x}{\partial x} \right) + Q_x \left[\delta\gamma_x + \delta \left(\frac{\partial w}{\partial x} \right) \right] \right\} dx - \int_0^L q(x)\delta w dx \tag{1.19}$$

Employing integration by parts the first term of the variational equation can be transformed as follows

$$\int_0^L M_x \delta \left(\frac{\partial \gamma_x}{\partial x} \right) dx = M_x \delta\gamma_x \mid_0^L - \int_0^L \frac{\partial M_x}{\partial x} \delta\gamma_x \, dx \tag{1.20}$$

By using the same procedure the last term of the variational equation can be transformed

$$\int_0^L Q_x \delta \left(\frac{\partial w}{\partial x} \right) dx = Q_x \delta w \mid_0^L - \int_0^L \frac{\partial Q_x}{\partial x} \delta w \, dx \tag{1.21}$$

Variations δw and $\delta\gamma_x$ are to be arbitrary in the whole beam ($\delta w \neq 0, \ \delta\gamma_x \neq 0$) with the exception of the point $x = 0$, where the kinematic (essential) boundary conditions are prescribed. Therefore, taking into account (1.20) and (1.21) from the variational equation (1.19) an equilibrium equations of the beam can be obtained

$$\frac{\partial M_x}{\partial x} - Q_x = 0, \quad \frac{\partial Q_x}{\partial x} - q = 0 \tag{1.22}$$

In the same manner from the variational equation (1.19) the natural boundary conditions at $x = L$ can be obtained since here $\delta w \neq 0$ and $\delta\gamma_x \neq 0$

$$Q_x \mid_{x=L} = 0, \quad M_x \mid_{x=L} = 0 \tag{1.23}$$

This means that by using the variational approach (the Ritz's or the displacement finite element method) it is not necessary to prescribe the naturaly boundary conditions for the stress resultants. The fulfilment of the conditions (1.23) is performed by minimizing the potential energy of the beam. Therefore, in the Ritz's and the displacement finite element method only the essential (kinematic) boundary conditions should be prescribed.

Substituting the expressions (1.16) into (1.22) a differential equations of the Timoshenko's beam can be obtained

$$\begin{aligned} &D_{11}\frac{\partial^2\gamma_x}{\partial x^2} - kQ_{55}\left(\gamma_x + \frac{\partial w}{\partial x}\right) = 0, \\ &kQ_{55}\left(\frac{\partial\gamma_x}{\partial x} + \frac{\partial^2 w}{\partial x^2}\right) - q = 0 \end{aligned} \tag{1.24}$$

In the case of beam made from isotropic homogeneous material the stiffness coefficients in these equations are given by

$$D_{11} = E\frac{bh^3}{12}, \quad Q_{55} = Gbh$$

Here h is thickness of the beam. Eqs (1.24) are the well known differential equations of the sixth order describing the of the Timoshenko's beam. In ordinary cases, for example, for the simply supported beam it is possible to obtain an exact analytical solutions of the differential equations (1.24). However, in the cases of more complex boundary conditions it is rather difficult to obtain the analytical solutions of the eqs (1.24). In this case more convinient is to use the variational methods - the Ritz's or the displacement finite element method.

1.2 Shear Correction Factor

Distribution of trasverse shear stresses in a layered cross section is nonuniform. Therefore, also the trasverse shear strains are distributed nonuniformly. According with Timoshenko's model (1.3) the transverse shear strains are constant over the cross section of the beam. To smooth this contradiction a shear correction factor k is introduced.

The distribution of transvere shear stresses in a layered cross section and a shear correction factor associated with it is a problem widely discussed in the

literature. Several approaches have been proposed for calculating the shear correction factor or coefficient for different composite laminates including sandwich structures. Most of these approaches are based on matching certain characteristics, as predicted by the first order shear deformation theory (FOSDT), with the corresponding characteristics of the theory of elasticity. Among the characteristics used are the tranverse shear strain energy, the velocity of propagation of flexural waves, the complementary energy. However, the values of the shear correction factor obtained by using different approaches are to be about the same.

In the present textbook for evaluation of the shear correction coefficient (factor) two methods are considered. Firstly, the method of evaluation of the shear correction factor based on the complementary energy approach will be outlined. For the isotropic homogeneous structure this method was developed by Reissner in 1945. Later it was generalized for the multilayered structures.

The shear correction factor is calculated by equating the transverse shear micro strain complementary energy Φ_{**} to the transverse shear macro strain complementary energy Φ_{*}. It should be noted that the term macro strains is used to define average strains in the cross section of the beam. The term micro strains is used for the strains defined on the level of the layer.

The transverse shear macro strains γ_{xz} (see formulae (1.3)) can be expressed from the second formula (1.16)

$$\gamma_{xz} = \frac{Q_x}{k\ Q_{55}}$$

Substituting this formula in the transverse macro shear strain complementary energy expression one can obtain

$$\Phi_{*} \equiv \frac{1}{2} Q_x\ \gamma_{xz} = \frac{1}{2} \frac{Q_x^2}{k\ Q_{55}} \tag{1.25}$$

Here the shear force Q_x is obtained by averaging through the cross section of the beam of micro strains σ_{xz} according the third formula of eqs (1.7).

On the other hand the transverse shear micro strain complementary energy Φ_{**} can be calculated from the transverse shear micro stresses σ_{xz} . These stresses in each kth layer of the beam are calculated by using the equilibrium equation of the theory of elasticity

$$\frac{\partial \sigma_x^{(k)}}{\partial x} + \frac{\partial \sigma_{xz}^{(k)}}{\partial z} = 0 \tag{1.26}$$

Here $\sigma_x^{(k)}$ can be determined from the micro strains $\varepsilon_x^{(k)}(z)$ of the kth layer by using the Hooke's law

$$\sigma_x^{(k)} = A_{11}^{(k)} \varepsilon_x^{(k)}(z) \tag{1.27}$$

where the strains $\varepsilon_x^{(k)}(z)$ can be determined employing the first formula of (1.3)

$$\varepsilon_x^{(k)} \equiv z\kappa_x = z\frac{\partial \gamma_x}{\partial x} \tag{1.28}$$

Here only strains due to bending of the beam are taken into account. The first term in the first formula of (1.3) represents the strain due to tension or compression. This term can be omitted since in the integration procedure of the equation (1.26) with respect of boundary conditions at the layer interfaces the constants of integration are to be arbitrary.

Top and bottom surfaces of the beam are supposed to be free of tractions in the tangential direction. Therefore, boundary conditions for the transverse shear stresses for the top and bottom layers are given by

$$\sigma_{xz}^{(1)} \mid_{z=z_0} = 0, \quad \sigma_{xz}^{(K)} \mid_{z=z_K} = 0 \tag{1.29}$$

At the layers interfaces the transverse shear stresses are equal for the adjacent layers

$$\sigma_{xz}^{(k)} \mid_{z=z_k} = \sigma_{xz}^{(k+1)} \mid_{z=z_k}, \quad k = 1, 2, 3, ..., K-1 \tag{1.30}$$

Further derivation of the shear correction coefficient as was mentioned previously is based on the assumption of pure bending of the beam. Then the first term in the second relation (1.8) can be omitted

$$M_x = D_{11}\frac{\partial \gamma_x}{\partial x} \tag{1.31}$$

Employing the expressions (1.28) and (1.31) in the formula (1.27) one can obtain

$$\sigma_x^{(k)} = zA_{11}^{(k)} d_{11} M_x \tag{1.32}$$

Here $d_{11} = 1/D_{11}$ is a compliance of the beam in bending. The derivative of the longitudinal stress in the layer (1.32) can be obtained taking into account the first equilibrium equation (1.22)

$$\frac{\partial \sigma_x^{(k)}}{\partial x} = zA_{11}^{(k)} d_{11} Q_x \tag{1.33}$$

Eq. (1.26) is integrated employing the boundary conditions (1.29), (1.30) and taking into account the expression (1.33). After integration the transverse shear stress in the layer is obtained

$$\sigma_{xz}^{(k)}(z) = g_k(z) Q_x \tag{1.34}$$

Here the function $g_k(z)$ contains the stiffness properties of the laminated beam and elastic properties of each individual layer

$$g_k(z) = d_{11}\left\{-A_{11}^{(k)}\frac{z^2}{2} + \sum_{j=1}^{k}\left[A_{11}^{(j)} - A_{11}^{(j-1)}\right]\frac{z_j^2}{2}\right\} \tag{1.35}$$

It should be noted that calculating this expression the substitution $A_{11}^{(0)} = 0$ must be used.

The transverse shear micro strain in each layer can be calculated by using the Hooke's law

$$\gamma_{xz}^{(k)} = \frac{\sigma_{xz}^{(k)}}{G_{xz}^{(k)}} \tag{1.36}$$

Taking into account eq. (1.34) the transverse shear micro strain complementary energy Φ_{**} can be expressed as a sum of the energy for each layer

$$\Phi_{**} = \frac{1}{2}b\sum_{k=1}^{K}\int_{z_k}^{z_{k+1}}\frac{\sigma_{xz}^{(k)}(z)\sigma_{xz}^{(k)}(z)}{G_{xz}^{(k)}}dz = \frac{1}{2}Q_x^2 b\sum_{k=1}^{K}\int_{z_k}^{z_{k+1}}\frac{1}{G_{xz}^{(k)}}g_k^2(z)dz \tag{1.37}$$

The shear correction coefficient is obtained by equating the transverse shear macro strain complementary energy (1.25) and the transverse shear micro strain complementary energy (1.37)

$$\Phi_* = \Phi_{**} \tag{1.38}$$

Employing this relation one can obtain the expression for the shear correction coefficient

$$k = \frac{1}{k_s}, \quad k_s = Q_{55}b\sum_{k=1}^{K}\int_{z_k}^{z_{k+1}}\frac{g_k^2(z)}{G_{xz}^{(k)}}dz \tag{1.39}$$

As an example the calculations for a homogeneous one layer ($K = 1$) beam of thickness h made from isotropic material are performed. In this case the following quantities are obtained

$$z_1 = -\frac{h}{2}, \quad z_2 = \frac{h}{2}, \quad A_{11}^{(1)} = E, \quad G_{xz}^{(k)} = G, \tag{1.40}$$

$$D_{11} = \frac{1}{12}Ebh^3, \quad d_{11} = \frac{12}{Ebh^3}, \quad Q_{55} = bhG,$$

$$g_1(z) = \frac{3}{2}\frac{1}{bh}\left[1 - 4\frac{z^2}{h^2}\right], \quad \sigma_{xz}(z) = \frac{3}{2}\frac{1}{bh}\left[1 - 4\frac{z^2}{h^2}\right]Q,$$

$$\int_{-h/2}^{h/2} g_1^2(z)dz = \frac{8}{15}h, \quad k = \frac{5}{6}$$

This is a well known result for the shear correction coefficient k of the isotropic beam obtained by the Reissner's method. For the sandwich or multilayered laminated composite beams the shear correction coefficient k can be obtained by using numerical integration of the expression (1.39). The results of such analysis will be shown below.

The second method of evaluation of the shear correction coefficient, which is used in the present textbook, is the Reuss' method. According the Reuss' method the effective transverse shear stiffness G_R can be obtained by averaging of the transverse shear compliances

$$\frac{1}{G_R} = \sum_{k=1}^{K} \frac{1}{G_{xz}^{(k)}} \frac{h_k}{h} \tag{1.41}$$

Here $h_k = z_k - z_{k-1}$ is thickness of the kth layer and h is total thickness of the beam. Actually, the second formula of eq. (1.9) is averaging of the transverse shear modulus by using the Voigt's method

$$G_V = \sum_{k=1}^{K} G_{xz}^{(k)} \frac{h_k}{h} \tag{1.42}$$

Here $G_V = Q_{55}/bh$ is the effective transverse shear stiffness of the beam according Voigt's method. So, in this case the shear correction coefficient according the Reuss's method can be defined as follows

$$k = \frac{G_R}{G_V} \tag{1.43}$$

Let us consider a symmetric sandwich beam (see Figure 1.5) with a soft core of thickness h_2, the Young's modulus E_2 and the shear modulus G_2. The core of the sandwich beam is covered with a thin face sheets. Materials of the core and face sheets are isotropic. In this case parameters of the beam are given by

$$h_1 = h_3, \quad h = 2h_1 + h_2, \quad G_1 = G_3, \quad E_1 = E_3 \tag{1.44}$$

According the Reuss' formula (1.43) for sandwich beam the shear correction coefficient can be calculated by the expression

$$k = \frac{1}{k_s}, \quad k_s = \left(2\frac{h_1}{h}\frac{1}{G_1} + \frac{h_2}{h}\frac{1}{G_2}\right)\left(2\frac{h_1}{h}G_1 + \frac{h_2}{h}G_2\right) \tag{1.45}$$

The results for the shear correction coefficient of the sandwich beam obtained by the Reissner's and the Reuss' methods as function of core stiffness are presented in Figure 1.6. Analysis was carried out for the thin face sheets

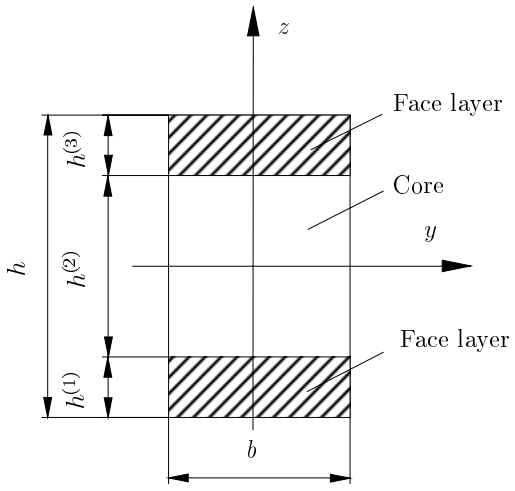

Figure 1.5: Cross section of the sandwich beam

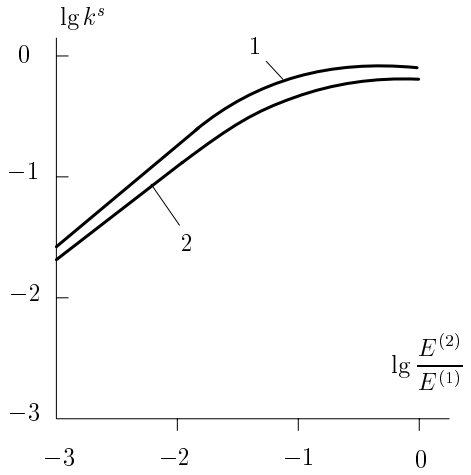

Figure 1.6: Shear correction coefficient calculated by the Reuss' (curve 1) and by the Reissner's method (curve 2) for $h^{(2)}/h = 0.95$

($h_2/h_1 = 0.95$) and for more thick face sheets ($h_2/h_1 = 0.75$). It is seen that in the case of thin face sheets results obtained by both methods are in good agreement. In the case of more thick face sheets there are differences between the results. So, in the case of thin face sheets for the analysis of sandwich beams the shear correction coefficient can be calculated by using the simple Reuss' formula (1.45). In other cases more accurate Reissner's formula (1.39) should be used.

1.3 Timoshenko's Beam Finite Element SI8

Let us consider the bending of sandwich or laminated composite beam with symmetric layer stacking sequence. In this case the beam stiffness coupling coefficient according (1.9) $B_{11} = 0$ and the strain energy functional is defined by expression (1.12)

$$U = \frac{1}{2}\int_0^L (D_{11}k_x^2 + kQ_{55}\gamma_{xz}^2)\, dx \tag{1.46}$$

Here strains are defined by relations (1.3) and (1.4). The functional can be written in the matrix form

$$U = \frac{1}{2}\int_0^L \boldsymbol{\varepsilon}^T \boldsymbol{D}\boldsymbol{\varepsilon} dx \tag{1.47}$$

Here the matrices $\boldsymbol{\varepsilon}$ and $\boldsymbol{D}$ are defined as follows

$$\boldsymbol{\varepsilon} = \begin{bmatrix} k_x \\ \gamma_{xz} \end{bmatrix}, \quad \boldsymbol{D} = \begin{bmatrix} D_{11} & 0 \\ 0 & kQ_{55} \end{bmatrix} \tag{1.48}$$

The corresponding strain-displacement relations also can be written in the matrix form

$$\boldsymbol{\varepsilon} = \boldsymbol{L}\boldsymbol{u} \tag{1.49}$$

Here the matrices $\boldsymbol{u}$ and $\boldsymbol{L}$ are given by

$$\boldsymbol{u} = \begin{bmatrix} w \\ \gamma_x \end{bmatrix}, \quad \boldsymbol{L} = \begin{bmatrix} 0 & \dfrac{\partial}{\partial x} \\ \dfrac{\partial}{\partial x} & 1 \end{bmatrix} \tag{1.50}$$

Solution of bending problem of the beam (see Figure 1.4) can be obtained by using a displacement approach of the finite element method (FEM). In the FEM the continuous beam is represented by assembly of the finite elements. The unknown functions are deflection of the beam $w(x)$ and rotation $\gamma_x(x)$. In the variational problem (1.19) these functions represent an essential boundary conditions. So, if we set these functions as nodal displacements for the finite element, the kinematic (essential) boundary conditions for the adjacent finite elements are satisfied.

Both unknown functions $w(x)$ and $\gamma_x(x)$ within the finite element can be approximated by using the third order polynomial shape functions. The finite element of Timoshenko's beam with the third order polynomial shape

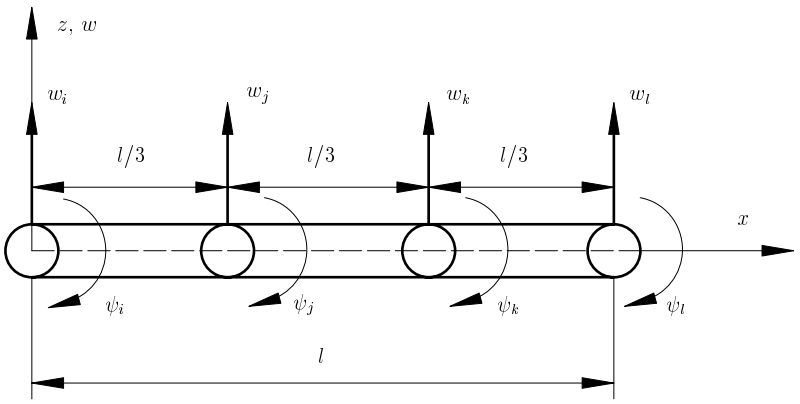

Figure 1.7: Finite element of Timoshenko's beam

functions is presented in Figure 1.7. For the present finite element the nodal displacements $\boldsymbol{v}_i$ are the deflection w_i and the rotation γ_x^i

$$\boldsymbol{v}_i = \begin{bmatrix} w_i \\ \gamma_x^i \end{bmatrix} \tag{1.51}$$

Approximation of the displacements within this finite element is assumed as follows

$$\boldsymbol{u} = \boldsymbol{N}\boldsymbol{v}_e \tag{1.52}$$

Here $\boldsymbol{v}_e$ is displacement vector for the finite element

$$\boldsymbol{v}_e^T = \{\boldsymbol{v}_i^T, \boldsymbol{v}_j^T, \boldsymbol{v}_k^T, \boldsymbol{v}_l^T\} \tag{1.53}$$

The matrix of shape functions $\boldsymbol{N}$ is given by

$$\boldsymbol{N} = [N_i\boldsymbol{I}_2, N_j\boldsymbol{I}_2, N_k\boldsymbol{I}_2, N_l\boldsymbol{I}_2] \tag{1.54}$$

Here $\boldsymbol{I}_2$ is a 2×2 unity matrix

$$\boldsymbol{I}_2 = \begin{bmatrix} 1 & 0 \\ 0 & 1 \end{bmatrix} \tag{1.55}$$

and N_i, N_j, N_k, N_l are the well known third order polynomial shape functions

$$\begin{aligned} N_i &= 1 - \frac{11}{2}\frac{x}{l} + 9(\frac{x}{l})^2 - \frac{9}{2}(\frac{x}{l})^3, \\ N_j &= 9\frac{x}{l} - \frac{45}{2}(\frac{x}{l})^2 + \frac{27}{2}(\frac{x}{l})^3, \\ N_k &= -\frac{9}{2}\frac{x}{l} + 18(\frac{x}{l})^2 - \frac{27}{2}(\frac{x}{l})^3, \\ N_l &= \frac{x}{l} - \frac{9}{2}(\frac{x}{l})^2 + \frac{9}{2}(\frac{x}{l})^3 \end{aligned} \tag{1.56}$$

The shape function N_i in the node i has the value 1 and in all other nodes (j, k, l) the value is zero. The shape functions (1.56) are shown in Figure 1.8.

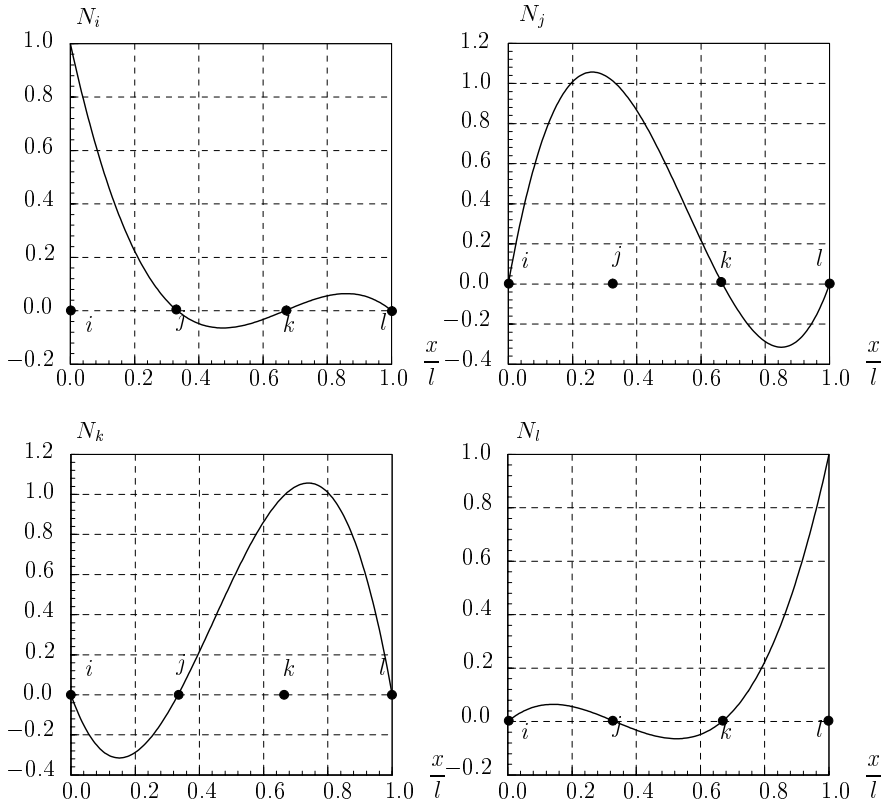

Figure 1.8: Shape functions of the finite element

Substituting the approximation(1.52) into the strain displacement relations (1.49) one obtains

$$\boldsymbol{\varepsilon} = \boldsymbol{B}\boldsymbol{v}_e \tag{1.57}$$

Here the matrix $\boldsymbol{B}$ is introduced

$$\boldsymbol{B} = \boldsymbol{L}\boldsymbol{N} \tag{1.58}$$

Substituting the relations (1.57) into the strain energy functional (1.47) for the finite element of length l (see Figure 1.7) one can obtain a discretised form of the functional

$$U_e = \frac{1}{2}\int_0^l \boldsymbol{\varepsilon}^T \boldsymbol{D}\boldsymbol{\varepsilon}\, dx = \frac{1}{2}\boldsymbol{v}_e^T \boldsymbol{K}_e \boldsymbol{v}_e \tag{1.59}$$

Here $\boldsymbol{K}_e$ is the finite element stiffness matrix

$$\boldsymbol{K}_e = \frac{1}{2}\int_0^l \boldsymbol{B}^T \boldsymbol{D}\boldsymbol{B} dx \tag{1.60}$$

To solve the bending problem of the beam the work of external forces W_e acting on the finite element must be defined. In the case of distributed load $q(x)$ the work of external forces of the finite element can be given by

$$W_e = \int_0^l qw\ dx = \int_0^l q\boldsymbol{u}^T \boldsymbol{R}\ dx \tag{1.61}$$

Here the matrix $\boldsymbol{R}^T = [1 \quad 0]$ is introduced and the first relation (1.50) is taken into account. The discretised form of the functional can be obtained by substituting the approximation (1.52) in the eq. (1.61)

$$W_e = \int_0^l q\boldsymbol{u}^T \boldsymbol{R}\ dx = \boldsymbol{v}_e^T \boldsymbol{F}_e \tag{1.62}$$

Here the finite element nodal forces $\boldsymbol{F}_e$ are defined as follows

$$\boldsymbol{F}_e = \int_0^l q\boldsymbol{N}^T \boldsymbol{R}\ dx \tag{1.63}$$

In the case when concentrated forces and moments are acting on the beam these forces must be added to the nodal forces $\boldsymbol{F}_e$.

Further the standard procedure of finite element method is applied for solution of the beam bending problem. At first the continuous beam is discretised by finite elements. Using the finite element properties, i.e. the element stiffness matrix $\boldsymbol{K}_e$ (1.60) and the element nodal forces $\boldsymbol{F}_e$ on the basis of the principle of minimum of potential energy the assembly of linear equations is obtained

$$\boldsymbol{K}\boldsymbol{v} = \boldsymbol{F} \tag{1.64}$$

Here $\boldsymbol{K}$ is a global stiffness matrix, $\boldsymbol{v}$ is a displacement vector of the beam and $\boldsymbol{F}$ is the vector of the nodal forces (external forces) acting on the beam. Taking into account the boundary conditions the system of linear equations (1.64) can be solved

$$\boldsymbol{v} = \boldsymbol{K}^{-1}\boldsymbol{F} \tag{1.65}$$

Further by using the displacements $\boldsymbol{v}$ the stresses in each finite element can be calculated. For Timoshenko's beam the stress-strain relations are defined by (1.31) and by the last formula of (1.8)

$$M_x = D_{11}k_x, \quad Q_x = kQ_{55}\gamma_{xz} \tag{1.66}$$

Note that $2\epsilon_{xz} = \gamma_{xz}$. Thus, the relations (1.66) can be written in the matrix form

$$\boldsymbol{\sigma} = \boldsymbol{D}\boldsymbol{\varepsilon} \tag{1.67}$$

Here $\boldsymbol{\sigma}^T = [M_x,\ Q_x]$ is vector of the stress resultants, $\boldsymbol{\varepsilon}^T = [k_x\ \gamma_{xz}]$ is vector of deformations and matrix $\boldsymbol{D}$ represents the stiffness of beam

$$\boldsymbol{D} = \begin{bmatrix} D_{11} & 0 \\ 0 & kQ_{55} \end{bmatrix} \tag{1.68}$$

Substituting the relations (1.56) in eq. (1.67) the stress resultants in each finite element can be calculated through displacements

$$\boldsymbol{\sigma} = \boldsymbol{D}\boldsymbol{B}\boldsymbol{v}_e \tag{1.69}$$

Here the nodal displacements $\boldsymbol{v}_e$ were obtained from the solution of the linear equations (1.65). Using the values of the bending moment M_x and the shear force Q_x the longitudinal σ_x and shear σ_{xz} stresses in all layers of the beam can be calculated. In detail this procedure will be outlined in chapter 2.

For dynamic analysis of the beam, for example, in the case of vibration analysis the finite element mass matrix is necessary to use. This matrix can be obtained from the kinetic energy of the structure. Kinetic energy depends on density of the material ρ and velocity of the displacements $\dot{u}_i$. For the Timohenko's hypothesis (1.1) in the case of bending of the beam in one plane ($u_2 = 0$) the functional of kinetic energy T_e for the finite element is given by

$$\begin{aligned} T_e &= \frac{1}{2}\int_{V_e} \rho \dot{u}_i^2\ dV = \frac{1}{2}\int_0^l \int_{-b/2}^{b/2} \int_{z_0}^{z_K} \rho(\dot{u}_1^2 + \dot{u}_3^2)\ dxdydz = \\ &= \frac{1}{2}\int_0^l \int_{z_0}^{z_K} \rho(\dot{u}^2 + 2z\dot{u}\dot{\gamma}_x + z^2\dot{\gamma}_x^2)\ dxdz = \\ &= \frac{1}{2}\int_0^l [\rho_0(\dot{u}^2 + \dot{w}^2) + 2\rho_1\dot{u}\dot{\gamma}_x + \rho_2\dot{\gamma}_x^2]dx \end{aligned} \tag{1.70}$$

Here a generalised densities ρ_0, ρ_1 and ρ_2 of the beam are introduced

$$\begin{aligned} \rho_o &= b\sum_{k=1}^{K} \rho_k[z_k - z_{k-1}], \\ \rho_1 &= b\frac{1}{2}\sum_{k=1}^{K} \rho_k[z_k^2 - z_{k-1}^2], \\ \rho_2 &= b\frac{1}{3}\sum_{k=1}^{K} \rho_k[z_k^3 - z_{k-1}^3] \end{aligned} \tag{1.71}$$

Here ρ_k is density of the kth layer.

Further let us consider a sandwich or laminated composite beam with symmetric layer stacking sequence. Only flexural motions of the beam is considered. In this case $\rho_1 = 0$ and $u = 0$. The functional of kinetic energy (1.70) is simplified and can be written in the matrix form

$$T_e = \frac{1}{2}\int_0^l [\rho_0 \dot{w}^2 + \rho_2 \dot{\gamma}_x^2]\, dx = \frac{1}{2}\int_0^l \dot{\boldsymbol{u}}^T \boldsymbol{R}_0 \dot{\boldsymbol{u}}\, dx \tag{1.72}$$

Here the displacement matrix $\boldsymbol{u}$ is defined by the first relation (1.50) and the matrix $\boldsymbol{R}_0$ is given by

$$\boldsymbol{R}_o = \begin{bmatrix} \rho_0 & 0 \\ 0 & \rho_2 \end{bmatrix} \tag{1.73}$$

Substituting the approximation (1.52) in the functional (1.72) a mass matrix of the finite element is obtained

$$T_e = \frac{1}{2}\dot{\boldsymbol{v}}_e^T \boldsymbol{M}_e \dot{\boldsymbol{v}}_e \tag{1.74}$$

Here $\boldsymbol{M}_e$ is the mass matrix of the finite element of Timoshenko's beam

$$\boldsymbol{M}_e = \int_0^l \boldsymbol{N}^T \boldsymbol{R}_0 \boldsymbol{N} dx \tag{1.75}$$

All elements of the stiffness matrix $\boldsymbol{K}_e$ (1.60) and the mass matrix $\boldsymbol{M}_e$ (1.75) can be obtained performing the analytical integration. However, it is rather difficult procedure and instead of analytical integration the numerical integration can be performed. For numerical integration the Gauss' formula and selective integration technique is used.

Selective integration means that the strain energy of the finite element (1.59) is separated in two parts - the bending energy and the transverse shear strain energy. In this case the stiffness matrix $\boldsymbol{K}_e$ (1.60) can be represented by

$$\boldsymbol{K}_e = \boldsymbol{K}_e^B + \boldsymbol{K}_e^Q = \frac{1}{2}\int_0^l \boldsymbol{B}^T \begin{bmatrix} D_{11} & 0 \\ 0 & 0 \end{bmatrix} \boldsymbol{B} dx + \frac{1}{2}\int_0^l \boldsymbol{B}^T \begin{bmatrix} 0 & 0 \\ 0 & kQ_{55} \end{bmatrix} \boldsymbol{B} dx \tag{1.76}$$

The part of stiffness matrix $\boldsymbol{K}_e^Q$ associated with the transverse shear strain energy is integrated by the reduced number of integration points in the Gauss' integration formula.

The Timoshenko's beam finite element considered above is specified as $SI8$. Here SI denotes that this is a beam element and 8 denotes the number

of degrees of freedom (DOF) of the finite element. Note that the present finite element $SI8$ is based on the single layer theory. However, this element can be used for the analysis of homogeneous beams as well as for the multilayered beams. In the last case the shear correction coefficient should be used in order to calculate the reduced transverse shear stiffness.

1.4 Sandwich Beam Finite Element SI20

Let us consider a beam with three layers (see Figure 1.9). Each of the three layers can be represented as a simple beam finite element $SI12$. The finite element $SI12$ is generalization of the finite element $SI8$, which was delivered in the previous section. In the present model displacements in each layer are represented by the single layer approximation (1.1). Thus, the rotations γ_x are different in each layer. This is the broken line or the so-called zig-zag model. Note that for the single layer theory outlined above there is only one function characterizing the rotation of the cross section of beam. Using the single layer theory for laminated beams there is also only one rotation function γ_x for the whole stack of layers. In this case non-uniform distribution of the transverse shear strains is corrected by the shear correction coefficient. In the zig-zag model it is not necessary to correct the shear strains since this model gives a non-uniform distribution of the transverse shear strains.

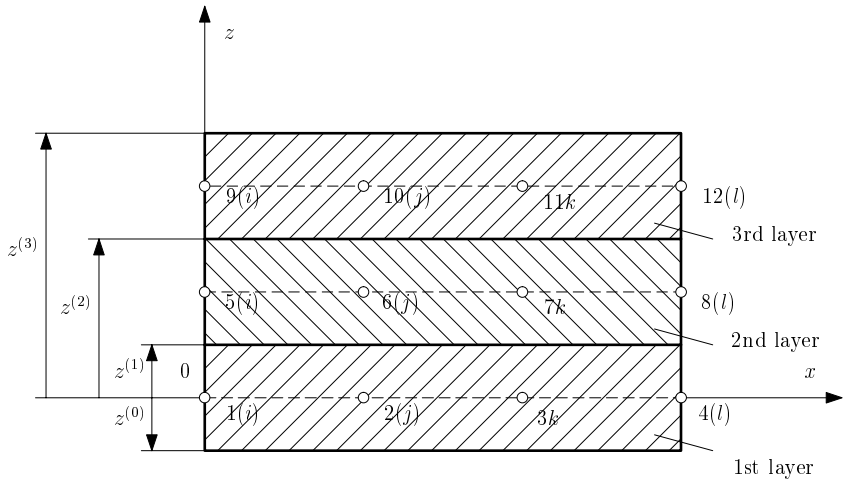

Figure 1.9: Sandwich beam finite element composed from the simple beam finite elements $SI12$.

In the finite element $SI12$ four additional degrees of freedom (DOF) are

related with the longitudinal displacement u. In this case instead of expression (1.46) the strain energy functional for the finite element has the form

$$U = \frac{1}{2}\int_0^l (Q_{11}\epsilon_x^2 + D_{11}k_x^2 + kQ_{55}\gamma_{xz}^2)\, dx = \frac{1}{2}\int_0^l \boldsymbol{\varepsilon}^T \boldsymbol{D}\boldsymbol{\varepsilon}\, dx \tag{1.77}$$

Here $\epsilon_x,\ k_x$ were defined by the formulae (1.4) and γ_{xz} by formula (1.3). In functional (1.77) the matrices $\boldsymbol{\varepsilon}$ and $\boldsymbol{D}$ are defined as follows

$$\boldsymbol{\varepsilon} = \begin{bmatrix} \epsilon_x \\ k_x \\ \gamma_{xz} \end{bmatrix}, \quad \boldsymbol{D} = \begin{bmatrix} Q_{11} & 0 & 0 \\ 0 & D_{11} & 0 \\ 0 & 0 & kQ_{55} \end{bmatrix} \tag{1.78}$$

In the strain-displacement relations (1.49) the matrices $\boldsymbol{u}$ and $\boldsymbol{L}$ are given by

$$\boldsymbol{u} = \begin{bmatrix} u \\ w \\ \gamma_x \end{bmatrix}, \quad \boldsymbol{L} = \begin{bmatrix} \dfrac{\partial}{\partial x} & 0 & 0 \\ 0 & 0 & \dfrac{\partial}{\partial x} \\ 0 & \dfrac{\partial}{\partial x} & 1 \end{bmatrix} \tag{1.79}$$

For the finite $SI12$ at the node there are three displacements. The nodal displacements $\boldsymbol{v}_i$ are represented by the longitudinal displacement u_i, the deflection w_i and the rotation γ_x^i

$$\boldsymbol{v}_i = \begin{bmatrix} u_i \\ w_i \\ \gamma_x^i \end{bmatrix} \tag{1.80}$$

For this finite element instead of eq. (1.54) the matrix of shape functions $\boldsymbol{N}$ is defined as follows

$$\boldsymbol{N} = [N_i\boldsymbol{I}_3, N_j\boldsymbol{I}_3, N_k\boldsymbol{I}_3, N_l\boldsymbol{I}_3] \tag{1.81}$$

Here $\boldsymbol{I}_3$ is a 3×3 unity matrix

$$\boldsymbol{I}_3 = \begin{bmatrix} 1 & 0 & 0 \\ 0 & 1 & 0 \\ 0 & 0 & 1 \end{bmatrix}$$

The shape functions N_i, N_j, N_k, N_l are the same (see eq. (1.56)) as for the finite element $SI8$. The stiffness matrix $\boldsymbol{K}_e$ of the finite element $SI12$ is determined by using the same formula (1.60) as for the finite element $SI8$.

The mass matrix for the finite element $SI12$ is obtained by using the functional (1.70)

$$T_e = \frac{1}{2}\int_0^l [\rho_0(\dot{u}^2 + \dot{w}^2) + 2\rho_1 \dot{u}\dot{\gamma}_x + \rho_2 \dot{\gamma}_x^2]\, dx = \frac{1}{2}\int_0^l \dot{\boldsymbol{u}}^T \boldsymbol{R}_0 \dot{\boldsymbol{u}}\, dx \qquad (1.82)$$

The displacement matrix $\boldsymbol{u}$ is defined by the first relation (1.79) and the matrix $\boldsymbol{R}_0$ is given by

$$\boldsymbol{R}_0 = \begin{bmatrix} \rho_0 & 0 & \rho_1 \\ 0 & \rho_0 & 0 \\ \rho_1 & 0 & \rho_2 \end{bmatrix} \qquad (1.83)$$

The mass matrix $\boldsymbol{M}_e$ of the finite element $SI12$ is determined by using the formula (1.75), where the matrices $\boldsymbol{N}$ and $\boldsymbol{R}_0$ are defined by the formulae (1.81) and (1.83), respectively.

In the capacity of reference axis of the sandwich beam composed by the three simple finite elements $SI12$ the axis of the first (bottom) layer (see Figure 1.9) is considered. In this case the Timoshenko's hypothesis (1.1) for each layer (simple beam) must be defined in the reference axis xz of the bottom layer

$$u_1^{(k)}(x,z) = u_{(k)}(x) + z\gamma_x^{(k)}(x), \quad u_3^{(k)}(x,z) = w(x), \quad k = 1,2,3 \qquad (1.84)$$

Here for the first (bottom) layer $-h_1/2 \le z \le h_1/2$, for the second layer (core) $h_1/2 \le z \le h_1/2 + h_2$ and for the third (top) layer $h_1/2 + h_2 \le z \le h_1/2 + h_2 + h_3$ (see Figures 1.9 and 1.10).

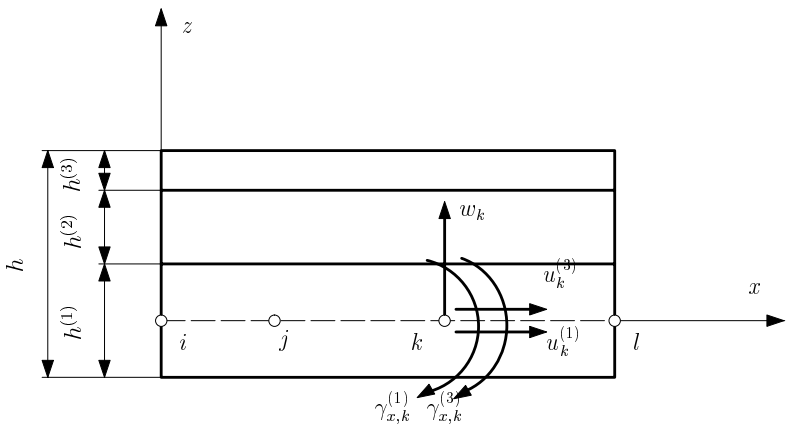

Figure 1.10: Sandwich beam finite element (superelement) $SI20$ with 4 nodes and 20 degrees of freedom

Taking into account eq. (1.84) for the bottom (first) layer the displacements can be represented by

$$u_1^{(1)}(x,z) = u_{(1)}(x) + z\gamma_x^{(1)}(x), \quad u_3^{(1)}(x,z) = w(x) \tag{1.85}$$

Here $u_{(1)}, w$ are the displacements at the reference axis and $\gamma_x^{(1)}$ is rotation of the cross section of the first (bottom) layer (see Figure 1.11).

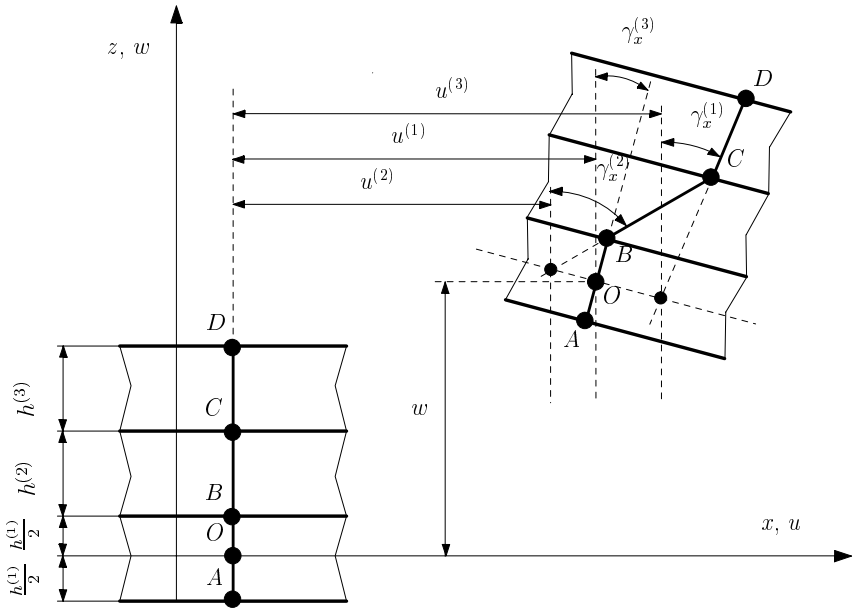

Figure 1.11: Initial and deformed shape of the sandwich beam cross section

For the top (third) layer of the sandwich beam (see Figure 1.11) the displacements according (1.84) can be represented by

$$u_1^{(3)}(x,z) = u_{(3)}(x) + z\gamma_x^{(3)}(x), \quad u_3^{(3)}(x,z) = w(x) \tag{1.86}$$

Here again $u_{(3)}, w$ are displacements at the reference axis and $\gamma_x^{(3)}$ is rotation of the cross section of the third (top) layer (see Figure 1.11).

The displacement continuity conditions between the layers can be written as follows

$$\begin{aligned} u_1^{(1)}(x,z) &= u_1^{(2)}(x,z)\mid_{z=z_1}, \quad u_1^{(2)}(x,z) = u_1^{(3)}(x,z)\mid_{z=z_2}, \\ u_3^{(1)}(x,z) &= u_3^{(2)}(x,z)\mid_{z=z_1}, \quad u_3^{(2)}(x,z) = u_3^{(3)}(x,z)\mid_{z=z_2} \end{aligned} \tag{1.87}$$

Taking into account these continuity conditions the displacement representation for the core can be given by

$$u_1^{(2)}(x,z) = u_{(2)}(x) + z\gamma_x^{(2)}(x), \quad u_3^{(2)}(x,z) = w(x) \tag{1.88}$$

Here $u_{(2)}(x)$ and $\gamma_x^{(2)}(x)$ are defined as dependent variables

$$u_{(2)} = F_1 u_{(1)} + F_2 u_{(3)} + F_3 \gamma_x^{(1)} - F_3 \gamma_x^{(3)}, \qquad (1.89)$$
$$\gamma_x^{(2)} = -F_4 u_{(1)} + F_4 u_{(3)} + F_2 \gamma_x^{(1)} + F_1 \gamma_x^{(3)}$$

where

$$F_1 = 1 + F_2, \quad F_2 = -\frac{h_1}{2h_2}, \quad F_3 = F_1 \frac{h_1}{2}, \quad F_4 = \frac{1}{h_2} \qquad (1.90)$$

The superelement composed in such way (see Figure 1.9) has 36 nodal displacements, i.e. for each of three layers (simple beams) there are 12 nodal displacements. Therefore, for the superelement we have 16 relations (1.87) linking the 36 nodal displacements. It brings to 20 independent unknown nodal displacements. For the sandwich beam considered the following five displacements are selected as independent basic variables

$$\boldsymbol{u}^T = [u_{(1)}, w, \gamma_x^{(1)}, u_{(3)}, \gamma_x^{(3)}] \qquad (1.91)$$

Here $\boldsymbol{u}$ is the basic displacement vector. Approximation of the displacements within the finite element $SI20$ is performed by using the same shape functions (1.56) as for the simple beam finite elements $SI8$ and $SI12$

$$\boldsymbol{u} = \boldsymbol{N}\boldsymbol{v}_e \qquad (1.92)$$

Here $\boldsymbol{v}_e$ is the displacement vector of the finite element $SI20$

$$\boldsymbol{v}_e^T = [\boldsymbol{v}_i^T, \boldsymbol{v}_j^T, \boldsymbol{v}_k^T, \boldsymbol{v}_l^T] \qquad (1.93)$$

Here $\boldsymbol{v}_m^T$ are displacements in the mth node ($m = i, j, k, l$)

$$\boldsymbol{v}_m^T = [u_m^{(1)}, w_m, \gamma_x^{(1)m}, u_m^{(3)}, \gamma_x^{(3)m}] \qquad (1.94)$$

Matrix of the shape functions $\boldsymbol{N}$ is defined by

$$\boldsymbol{N} = [N_i \boldsymbol{I}_5, N_j \boldsymbol{I}_5, N_k \boldsymbol{I}_5, N_l \boldsymbol{I}_5]$$

Here $\boldsymbol{I}_5$ is a 5×5 unity matrix. For each of three layers the displacements and rotations can be obtained from the basic displacement vector $\boldsymbol{u}$, which was defined by the expression (1.91)

$$\boldsymbol{u}^{(k)} = \begin{bmatrix} u_{(k)} \\ w \\ \gamma_x^{(k)} \end{bmatrix} = \boldsymbol{H}^{(k)} \boldsymbol{u} \qquad (1.95)$$

Here matrices $\boldsymbol{H}^{(k)}$ are given by

$$\boldsymbol{H}^{(1)} = \begin{bmatrix} 1 & 0 & 0 & 0 & 0 \\ 0 & 1 & 0 & 0 & 0 \\ 0 & 0 & 1 & 0 & 0 \end{bmatrix}, \tag{1.96}$$

$$\boldsymbol{H}^{(2)} = \begin{bmatrix} F_1 & 0 & F_3 & F_2 & -F_3 \\ 0 & 1 & 0 & 0 & 0 \\ -F_4 & 0 & F_2 & F_4 & F_1 \end{bmatrix},$$

$$\boldsymbol{H}^{(3)} = \begin{bmatrix} 0 & 0 & 0 & 1 & 0 \\ 0 & 1 & 0 & 0 & 0 \\ 0 & 0 & 0 & 0 & 1 \end{bmatrix}$$

The strain energy U_e of the sandwich finite element can be obtained as a sum of the strain energies $U_e^{(k)}$ of all three layers

$$U_e = \sum_{k=1}^{3} U_e^{(k)} = \sum_{k=1}^{3} \frac{1}{2} \int_0^l \boldsymbol{\varepsilon}^{(k)T} \boldsymbol{D}^{(k)} \boldsymbol{\varepsilon}_{(k)} \, dx \tag{1.97}$$

Here the matrices $\boldsymbol{\varepsilon}^{(k)}$ and $\boldsymbol{D}^{(k)}$ are defined for each layer according formulae (1.78). It should be noted that elasticity matrix $\boldsymbol{D}^{(k)}$ must be calculated for each layer by using formulae (1.9) and taking into account that the reference axis is selected the axis of the first (bottom) layer. The strains $\boldsymbol{\varepsilon}^{(k)}$, which were defined by the first formula (1.78), in each layer can be calculated by the relations (1.49)

$$\boldsymbol{\varepsilon}^{(k)} = \boldsymbol{L}\boldsymbol{u}^{(k)} \tag{1.98}$$

Here the matrix $\boldsymbol{L}$ is defined by the second formula (1.79) and vector $\boldsymbol{u}^{(k)}$ is defined by the expression (1.95). Substituting the expressions (1.95) and (1.92) into (1.98) one obtains

$$\boldsymbol{\varepsilon}^{(k)} = \boldsymbol{L}\boldsymbol{u}^{(k)} = \boldsymbol{L}\ \boldsymbol{H}^{(k)}\boldsymbol{u} = \boldsymbol{L}\boldsymbol{H}^{(k)}\boldsymbol{N}\boldsymbol{v}_e = \boldsymbol{B}^{(k)}\boldsymbol{v}_e \tag{1.99}$$

Substituting this relation into the strain energy expression of the sandwich beam finite element (1.97) one can obtain the discretised form of the strain energy

$$U_e = \frac{1}{2}\boldsymbol{v}_e^T \boldsymbol{K}_e \boldsymbol{v}_e \tag{1.100}$$

Here the sandwich beam finite element $SI20$ stiffness matrix is given by

$$\boldsymbol{K}_e = \sum_{k=1}^{3} \int_0^l \boldsymbol{B}^{(k)T} \boldsymbol{D}^{(k)} \boldsymbol{B}^{(k)} dx \tag{1.101}$$

The mass matrix of the sandwich beam finite element $SI20$ can be obtained in the similar way. The functional of the kinetic energy of the sandwich beam finite element according the expression (1.82) is given by

$$T_e = \sum_{k=1}^{3} T_e^{(k)} = \sum_{i=1}^{3} \frac{1}{2} \int_0^l \dot{\boldsymbol{u}}^{(k)T} \boldsymbol{R}_0^{(k)} \dot{\boldsymbol{u}}^{(k)} dx \tag{1.102}$$

Here $\boldsymbol{u}^{(k)}$ is defined by the formula (1.95) and $\boldsymbol{R}_o$ by the formula (1.83), where the generalised densities $\rho_o^{(k)}, \rho_1^{(k)}$ and $\rho_2^{(k)}$ of the layers are used. These densities are calculated for each layer by using the formulae (1.71). In these calculations as reference axis the axis of the first (bottom) layer is used (see Figure 1.9).

Substituting the expressions (1.95) in the functional (1.102) the mass matrix of the sandwich beam finite element can be obtained

$$T_e = \dot{\boldsymbol{v}}_e^T \boldsymbol{M}_e \dot{\boldsymbol{v}}_e \tag{1.103}$$

Here $\boldsymbol{M}_e$ is the mass matrix of the sandwich beam finite element $SI20$

$$\boldsymbol{M}_e = \sum_{k=1}^{3} \int_0^l \boldsymbol{N}^T \boldsymbol{H}^{(k)T} \boldsymbol{R}_0^{(k)} \boldsymbol{H}^{(k)} \boldsymbol{N} dx \tag{1.104}$$

Integration of the stiffness matrix (1.101) and the mass matrix (1.104) of the finite element is performed by numerical integration using the Gauss' formula.

1.5 Sandwich Beam Finite Element SIM12

For the sandwich beams with very thin face sheets and with very soft core it can be assummed that in the face sheets there is no bending, but only membrane stress state (see Figure 1.12). Further it is assumed that in the core there are no axial streses but only the transverse shear stresses. In this case more simple finite element than the sandwich beam finite element $SI20$ based on the zig-zag model can be developed.

Let us consider the sandwich beam (see Figure 1.5) with very thin face sheets of thickness $h_b = h_1, h_t = h_3$ and with very soft coft core of thickness $h_c = h_2$. Here it is assummed that botom face sheet may have different thickness h_b than the top face sheet thickness h_t. Both face sheets can also be assumed with the same thickness $h_f = h_b = h_t$. In sandwich beams this case with symmetric layers take place more often than the case with non-symmetric face sheets.

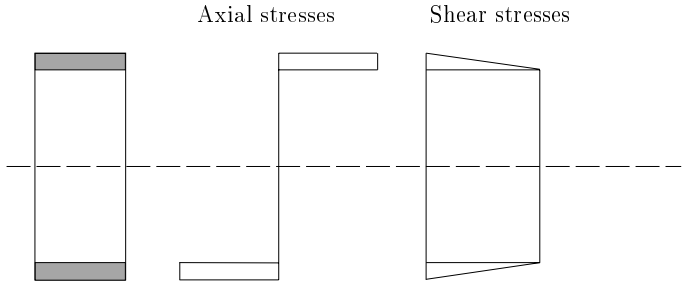

Figure 1.12: Stress distribution in sandwich beam with very thin faces and soft core

Let us consider the sandwich beam finite element of length l. In this case also the Timoshenko's hypothesis (1.1) can be used

$$u_1(x,z) = u(x) + z\gamma_x(x), \quad u_3(x,z) = w(x) \tag{1.105}$$

In the core the axial strain (see (1.3)) is assumed to be zero and only the transverse shear strains are acting

$$\varepsilon_x = \epsilon_x + z\kappa_x = 0, \quad \gamma_{xz} = \gamma_x + \frac{\partial w}{\partial x} \tag{1.106}$$

In this case the strain energy functional (1.6) for the core U_e^c is given by

$$U_e^c = \frac{1}{2}\int_0^l Q_x \gamma_{xz} dx \tag{1.107}$$

Here the shear force Q_x can be expressed through strains by the last relation (1.8) without shear correction ($k = 1$)

$$Q_x = Q_{55}^{(2)}\gamma_{xz} \tag{1.108}$$

Here the transverse shear stiffness $Q_{55}^{(2)}$ according (1.9) is calculated through the shear modulus G_c of the core

$$Q_{55}^{(2)} = Q_{55}^c = bh_c A_{55}^{(2)} = bh_c G_c$$

In eq. (1.108) the shear correction coefficient is not used because in the model outlined here it is assumed that transverse shear strains and stresses are constant through the core thickness (see Figure 1.12).

Substituting eq. (1.108) into the strain energy expression for the core (1.107) one can obtain

$$U_e^c = \frac{1}{2}\int_0^l \gamma_{xz} Q_{55}^c \gamma_{xz} dx \tag{1.109}$$

The nodal displacements of the finite element must be selected taking into account that in the face sheets there are also axial displacements u. So, the displacement vector for the sandwich beam is taken as follows

$$\boldsymbol{u}^T = [u, w, \gamma_x] \tag{1.110}$$

Similarly as for the finite element $SI2$ (see formula (1.80)) it is assumed that for the ith node there are three nodal displacements - the axial displacement u_i, the deflection w_i and the rotation γ_x^i

$$\boldsymbol{v}_i^T = [u_i, w_i, \gamma_x^i] \tag{1.111}$$

Thus, the finite element displacement vector is given by

$$\boldsymbol{v}_e^T = [\boldsymbol{v}_i^T, \boldsymbol{v}_j^T, \boldsymbol{v}_k^T, \boldsymbol{v}_l^T] \tag{1.112}$$

Now eq. (1.106) in the matrix notation can be written as

$$\gamma_{xz} = \boldsymbol{L}_c \boldsymbol{u} \tag{1.113}$$

where

$$\boldsymbol{L}_c = \begin{bmatrix} 0 & \dfrac{\partial w}{\partial x} & 1 \end{bmatrix}$$

Approximation of displacements within the finite element is assumed the same as for the finite elements $SI8$ and $SI12$

$$\boldsymbol{u} = \boldsymbol{N} \boldsymbol{v}_e \tag{1.114}$$

Here $\boldsymbol{N}$ was defined by eq. (1.81) in which the shape functions was defined by expressions (1.56).

Substituting the approximation (1.114) into formula (1.113) one can obtain

$$\gamma_{xz} = \boldsymbol{L}^c \boldsymbol{u} = \boldsymbol{B}^c \boldsymbol{v}_e \tag{1.115}$$

Here the matrix $\boldsymbol{B}^c$ is introduced

$$\boldsymbol{B}^c = \boldsymbol{L}^c \boldsymbol{N} \tag{1.116}$$

Substituting the relation (1.115) into the strain energy functional of the core (1.109) the discretized form of the functional is obtained

$$U_e^c = \frac{1}{2} \boldsymbol{v}_e^T \boldsymbol{K}_e^c \boldsymbol{v}_e \tag{1.117}$$

Here $\boldsymbol{K}_e^c$ is a stiffness matrix of the core

$$\boldsymbol{K}_e^c = \int_0^l \boldsymbol{B}^{cT} Q_{55}^c \boldsymbol{B}^c dx \tag{1.118}$$

Stifness matrix of the core characterizes the strain energy stored only in the core U_e^c. To obtain the total strain energy of the sandwich beam finite element the strain energy of the face sheets should be added. The strain energy of the top U_e^t and the bottom U_e^b face sheets for the membrane stress state can be expressed as follows

$$U_e^t = \frac{1}{2} b h_t \int_0^l \sigma_x^f \varepsilon_x^f dx, \quad U_e^b = \frac{1}{2} b h_b \int_0^l \sigma_x^f \varepsilon_x^f dx \tag{1.119}$$

Here $\sigma_x^f, \varepsilon_x^f$ are axial stresses and strains in the face sheets. It should be noted that in the expression (1.119) an explicit integration was performed over the volume V_e of the sandwich finite element, since for the membrane stress state in faces the coordinate z for faces is fixed at

$$\bar{h}^t = \frac{1}{2}(h^c + h^t), \qquad -\bar{h}^b = -\frac{1}{2}(h^c + h^b)$$

Here $z = \bar{h}^t$ for the top face and $z = -\bar{h}^b$ for the bottom face sheet. Substituting the Hooke's law for the face sheets $\sigma_x^f = E_f \varepsilon_x^f$ into (1.119) one can obtain the strain energy functional for the face sheets

$$U_e^t = \frac{1}{2} b h_t \int_0^l \varepsilon_x^f E_f \varepsilon_x^f dx, \quad U_e^b = \frac{1}{2} b h_b \int_0^l \varepsilon_x^f E_f \varepsilon_x^f dx \tag{1.120}$$

For the face sheets of equal thickness the notation $f = t = b$ is used. So, the index f is used for the top as well as for the bottom layer. The axial strains in the face sheets in the formulae (1.119) and (1.120) can be expressed as follows

$$\varepsilon_x^f = \frac{\partial u}{\partial x} + \bar{h}^f \frac{\partial \gamma_x}{\partial x} = \boldsymbol{L}^f \boldsymbol{u} \tag{1.121}$$

Here

$$\boldsymbol{L}^f = \begin{bmatrix} \dfrac{\partial}{\partial x} & 0 & \bar{h}^f \dfrac{\partial}{\partial x} \end{bmatrix}$$

where $\bar{h}^f = -\bar{h}^b$ for the bottom face sheet and $\bar{h}^f = \bar{h}^t$ for the top face sheet. Substituting the approximation (1.114) into eq. (1.121) one can obtain

$$\varepsilon_x^f = \boldsymbol{B}^f \boldsymbol{v}_e = [\boldsymbol{B}_i^f, \boldsymbol{B}_j^f, \boldsymbol{B}_k^f, \boldsymbol{B}_l^f] \boldsymbol{v}_e \tag{1.122}$$

where

$$\boldsymbol{B}_i^f = \begin{bmatrix} \dfrac{\partial N_i}{\partial x} & 0 & \bar{h}^f \dfrac{\partial N_i}{\partial x} \end{bmatrix} \tag{1.123}$$

Expression for strains in the face sheets (1.122) now is substituted into the strain energy functional (1.120). After the explicit integration over the width b of the beam, over the top face thickness h_f and over the bottom face thickness h_b one can obtain

$$U_e^{t+b} = \frac{1}{2}\boldsymbol{v}_e^T(\boldsymbol{K}_e^t + \boldsymbol{K}_e^b)\boldsymbol{v}_e \tag{1.124}$$

Here the stiffness matrices for the top face and for the bottom face are given by

$$\boldsymbol{K}_e^t = bh_t \int_0^l \boldsymbol{B}^{tT} E^t \boldsymbol{B}^t dx, \quad \boldsymbol{K}_e^b = bh_b \int_0^l \boldsymbol{B}^{bT} E^b \boldsymbol{B}^b dx$$

The strain energy of the sandwich beam is a sum of the strain energies of the face sheets U_e^t, U_e^b and the core U_e^c. The stiffness matrix of the sandwich beam finite element also is the sum of the stiffness matrices of the core and the face sheets

$$\boldsymbol{K}_e = \boldsymbol{K}_e^c + \boldsymbol{K}_e^t + \boldsymbol{K}_e^b$$

The mass matrix of the finite element can be obtained similarly calculating seperately the mass matrices for the core and face sheets. For the core the functional of kinetic energy (1.72) with displacements defined by (1.110) in the matrix form can be written as follows

$$T_e^c = \frac{1}{2}\int_0^l (\rho_0 \dot{w}^2 + \rho_2 \dot{\gamma}_x^2) dx = \frac{1}{2}\int_0^l \dot{\boldsymbol{u}}^T \boldsymbol{R}^c \dot{\boldsymbol{u}} dx \tag{1.125}$$

where the matrix $\boldsymbol{R}^c$ is given by

$$\boldsymbol{R}^c = \begin{bmatrix} 0 & 0 & 0 \\ 0 & \rho_0 & 0 \\ 0 & 0 & \rho_2 \end{bmatrix}$$

Here according (1.72) for the core with density ρ_c the generalised densities ρ_0^c and ρ_2^c are calculated by

$$\rho_0^c = bh^c\rho^c, \quad \rho_2^c = \frac{1}{12}b(h^c)^3$$

Substituting the approximation (1.114) into the functional (1.125) one can obtain

$$T_e^c = \frac{1}{2}\dot{\boldsymbol{v}}_e^T \boldsymbol{M}_e^c \dot{\boldsymbol{v}}_e$$

Here $\boldsymbol{M}_e^c$ is mass matrix of the core

$$\boldsymbol{M}_e^c = \int_0^l \boldsymbol{N}^T \boldsymbol{R}_c \boldsymbol{N} dx \tag{1.126}$$

For the face sheets the functional of kinetic energy in the form (1.70) is employed

$$T_e^f = \frac{1}{2} \int_{V_e} \rho_f (\dot{u}_1^2 + \dot{u}_3^2) dV \tag{1.127}$$

Here ρ_f is the density of the face sheets. It is assumed that densities for the top ρ_t and the bottom ρ_b face sheets are equal $\rho_f = \rho_t = \rho_b$. Taking into account (1.105), (1.110) and assumption about membrane stress state in the face sheets after explicit integration over the width b of the beam, over the top face thickness h_t and over the bottom face thickness h_b the kinetic energy (1.127) may now be written as a sum of kinetic energies in the top T_e^t and the bottom T_e^t face sheets

$$\begin{aligned} T_e^f = T_e^t + T_e^b, \quad T_e^t = \frac{1}{2} b h_t \rho^f \int_0^l \dot{\boldsymbol{u}}^T \boldsymbol{R}^f \dot{\boldsymbol{u}} dx, \\ T_e^b = \frac{1}{2} b h_b \rho_f \int_0^l \dot{\boldsymbol{u}}^T \boldsymbol{R}^f \dot{\boldsymbol{u}} dx \end{aligned} \tag{1.128}$$

where

$$\boldsymbol{R}^f = \begin{bmatrix} 1 & 0 & \bar{h}^f \\ 0 & 1 & 0 \\ \bar{h}^f & 0 & (\bar{h}^f)^2 \end{bmatrix}$$

Here again for the top face sheet the following notation is used

$$\bar{h}^f = \bar{h}^t = \frac{1}{2}(h^c + h^t)$$

Similarly for the bottom face sheet

$$\bar{h}^f = -\bar{h}^b = -\frac{1}{2}(h^c + h^b)$$

Substituting the approximation (1.114) into functional (1.128) one can obtain

$$T_e^{t+b} = \frac{1}{2} \dot{\boldsymbol{v}}_e^T (\boldsymbol{M}_e^t + \boldsymbol{M}_e^b) \dot{\boldsymbol{v}}_e \tag{1.129}$$

Here the mass matrices for the top and bottom faces are given by

$$\boldsymbol{M}_e^t = \rho_t b \int_0^l \boldsymbol{N}^T \boldsymbol{R}^t \boldsymbol{N} dx, \quad \boldsymbol{M}_e^b = \rho_b b \int_0^l \boldsymbol{N}^T \boldsymbol{R}^b \boldsymbol{N} dx \tag{1.130}$$

where the matrices $\boldsymbol{R}^t$ and $\boldsymbol{R}^b$ are defined by

$$\boldsymbol{R}^t = \begin{bmatrix} R_1^t & 0 & R_2^t \\ 0 & R_1^t & 0 \\ R_2^t & 0 & R_3^t \end{bmatrix}, \quad \boldsymbol{R}^b = \begin{bmatrix} R_1^b & 0 & R_2^b \\ 0 & R_1^b & 0 \\ R_2^b & 0 & R_3^b \end{bmatrix} \tag{1.131}$$

Here for the top face sheet we have

$$R_1^t = h_t, \quad R_2^t = h_t \frac{h_t + h_c}{2}, \quad R_3^t = h_t \frac{(h_t + h_c)^2}{4}$$

Similarly for the bottom face sheet we have

$$R_1^b = h_b, \quad R_2^b = -h_b \frac{h_b + h_c}{2}, \quad R_3^b = h_b \frac{(h_b + h_c)^2}{4}$$

The kinetic energy of sandwich beam is a sum of energies of the core T_e^c, the top T_e^t and the bottom T_e^b face sheets. Therefore, the mass matrix of the sandwich beam $\boldsymbol{M}_e$ is a sum of the mass matrices of the separate layers

$$\boldsymbol{M}_e = \boldsymbol{M}_e^c + \boldsymbol{M}_e^t + \boldsymbol{M}_e^b \tag{1.132}$$

The sandwich beam finite element considered above is specified as $SIM12$. Here SI denotes that this is a beam finite element, M denotes that assumption of membrane stress state in the face sheets is used and 12 denotes the number of degrees of freedom (DOF) of the finite element. The finite element $SIM12$ can be used for static and dynamic analysis of sandwich beams with very thin face sheets and with very soft core.

Chapter 2

Stress and Failure Analysis

2.1 Calculation of Stresses

In order to estimate the failure loads of the sandwich or laminated composite beams as first step the stresses in the layers must be determined. Stress analysis in sandwich and laminated composite beams is similar. Symmetric sandwich or laminated composite beams with symmetric layer stacking sequence can be analysed on the basis of the finite element $SI8$, which was delivered in the section 1.3. Laminated composite beams with general layer stacking sequence can be analysed by the finite element $SI12$, which was delivered in the section 1.4.

The final result of the finite element solution, which was outlined in the sections 1.3 and 1.4, is displacements and the stress resultants N_x, M_x, Q_x. From this data the stresses in the layers can be calculated. The stress-strain relations (1.8) can be represented in matrix form

$$\begin{bmatrix} N_x \\ M_x \end{bmatrix} = \begin{bmatrix} Q_{11} & B_{11} \\ B_{11} & D_{11} \end{bmatrix} \begin{bmatrix} \epsilon_x \\ k_x \end{bmatrix} \tag{2.1}$$

$$Q_x = kQ_{55}\gamma_{xz} \tag{2.2}$$

Note that $\gamma_{xz} = 2\epsilon_{xz}$. Firstly, let us consider the algorithm of calculation of the longitudinal stresses in the beam. The stress-strain relations (2.1) and (2.2) in the matrix form are similar to (1.67)

$$\boldsymbol{\sigma} = \boldsymbol{D}\boldsymbol{\varepsilon} \tag{2.3}$$

Here $\boldsymbol{\sigma}^T = [N_x, M_x, Q_x]$, $\boldsymbol{\varepsilon}^T = [\epsilon_x, k_x, \gamma_{xz}]$ and $\boldsymbol{D}$ is elasticity matrix

$$\boldsymbol{D} = \begin{bmatrix} Q_{11} & B_{11} & 0 \\ B_{11} & D_{11} & 0 \\ 0 & 0 & kQ_{55} \end{bmatrix} \tag{2.4}$$

Substituting the expression (1.57) (for the finite element $SI12$ this expression is similar as for the finite element $SI8$) into eq. (2.3) the stress resultants in the each finite element can be calculated similarly as by eq. (1.69)

$$\boldsymbol{\sigma} = \boldsymbol{D}\boldsymbol{B}\boldsymbol{v}_e \tag{2.5}$$

Here the element nodal displacements $\boldsymbol{v}_e$ is obtained from the finite element solution (1.65), where the stiffness matrix $\boldsymbol{K}_e$ of the finite element $SI12$ is used.

The inverse stress-strain relations (2.1) can be obtained in the analytical form

$$\begin{bmatrix} \epsilon_x \\ k_x \end{bmatrix} = \begin{bmatrix} q_* & b_* \\ b_* & d_* \end{bmatrix} \begin{bmatrix} N_x \\ M_x \end{bmatrix} \tag{2.6}$$

Here

$$q_* = \frac{D_{11}}{\Delta}, \quad b_* = -\frac{B_{11}}{\Delta}, \quad d_* = \frac{Q_{11}}{\Delta}, \quad \Delta = Q_{11}D_{11} - B_{11}^2 \tag{2.7}$$

For the sandwich and laminated composite beams with symmetric layer stacking sequence $B_{11} = 0$ and

$$q_* = \frac{1}{Q_{11}}, \quad b_* = 0, \quad d_* = \frac{1}{D_{11}} \tag{2.8}$$

Taking into account these expressions from (2.6) one can obtain

$$\epsilon_x = \frac{N_x}{Q_{11}}, \quad k_x = \frac{M_x}{D_{11}} \tag{2.9}$$

Using the strains ϵ_x and k_x obtained according formulae (2.6) or (2.9) the longitudinal strains $\varepsilon_x^{(k)}$ in each layer can be calculated by the first formula (1.3)

$$\varepsilon_x^{(k)}(x,z) = \epsilon_x(x) + zk_x(x) \tag{2.10}$$

Here for the kth layer $z_{(k-1)} \le z \le z_{(k)}$.

The normal stresses $\sigma_x^{(k)}$ in each layer can be calculated by using Hooke's law according formula (1.27)

$$\sigma_x^{(k)}(x,z) = A_{11}^{(k)}\varepsilon_x^{(k)}(x,z) \tag{2.11}$$

The transverse shear stresses $\sigma_{xz}^{(k)}$ in each layer can be calculated by formula (1.34)

$$\sigma_{xz}^{(k)}(x,z) = g_k(z)Q_x(x) \tag{2.12}$$

Here for the kth layer ($z_{(k-1)} \leq z \leq z_{(k)}$) the function $g_k(z)$ is calculated by using the formula (1.35). The shear force Q_x in the formula (2.12) is calculated by using the formula (2.5), where nodal displacements are obtained by the finite element solution (1.65).

The algorithm of the stress analysis in the sandwich or laminated composite beams contains the following steps.

1. The finite element solution (1.65) is obtained with given loads and boundary conditions. The result of the finite element solution is the nodal displacement vector $\boldsymbol{v}$.

2. For each finite element by using the element nodal displacements $\boldsymbol{v}_e$ the stress resultants $\boldsymbol{\sigma^T} = [N_x, M_x, Q_x]$ are calculated by formula (2.5). The stress resultants are calculated in the middle of each finite element or in the Gauss' integration points.

3. In each finite element in the points, where stress resultants were calculated, the longitudinal stresses $\sigma_x^{(k)}$ in each layer according formula (2.11) and the shear stresses $\sigma_{xz}^{(k)}$ in each layer according formula(2.12) is calculated.

The algorithm of the stress analysis outlined above is based on using the finite element method. The same algorithm of the stress analysis of sandwich or laminated composite beams can be used also in the case of analytical solution by using the Ritz's method. The only difference is that in the first step of algorithm the displacements of the beam is obtained by using the Ritz's procedure. The remaining steps are the same, i.e. from displacements obtained in the first step the stress resultants are calculated and then from the stress resultants the longitudinal (axial) and the transverse shear stresses in each layer are calculated.

2.2 Failure Analysis of Sandwich Beams

Let us consider a symmetric sandwich beam with core made from isotropic material. In the case of isotropic face sheets the layer parameters are as follows

$$E^{(1)} = E^{(3)} = E^f, \quad E^{(2)} = E^c, \quad G^{(1)} = G^{(3)} = G^f, \quad G^{(2)} = G^c,$$
$$h^{(1)} = h^{(3)} = h^f, \quad h^{(2)} = h^c \tag{2.13}$$

Here E^f and E^c are Young's modulus of the face sheets and core, respectively, G^f and G^c are shear modulus of the face sheets and core, respectively, and

h^f and h^c are thickness of the face sheets and core, respectively. Note that the shear and the Young's modulus are coupled with the relation

$$G^f = \frac{E^f}{2(1+\nu^f)}, \quad G^c = \frac{E^c}{2(1+\nu^c)} \tag{2.14}$$

Here ν^f and ν^c are Poisson's ratio of the face sheets and core, respectively.

The face shhets can be made also from laminated composite material, which is represented as an orthotropic layer characterised by two independent parameters of material

$$E^f = E_x, \quad G^f = G_{xz} \tag{2.15}$$

There is no difference in the algorithm of the stress analysis in the sandwich beams whether the face sheets are made from isotropic material or from the orthotropic material.

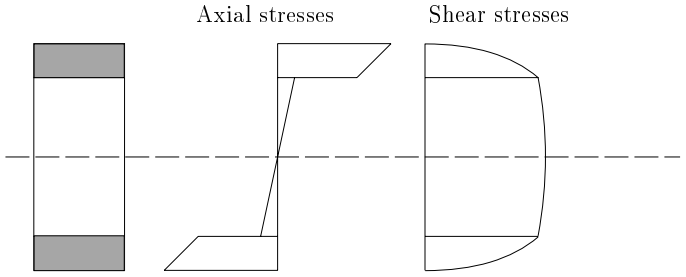

Figure 2.1: Stress distribution in sandwich beam

Formulae, which were delivered in the section 2.1, can be used for analysis of sandwich beams with different parameters. In the case $E^c < E^f$ distribution of the axial stress $\sigma_x^{(k)}$ according formula (2.11) and the shear stress $\sigma_{xz}^{(k)}$ according formula (2.12) is shown schematically in Figure 2.1. The axial (longitudinal) strains due to bending vary linearly through the thickness of the beam (see formula (2.10)) such that the stiff faces will experience much higher axial stresses than the softer core material. The core shear stress is parabolically distributed. Its value at the interface due to the soft core is approximately equal to the maximum value which appear at the beam's neutral axis. The shear stress is continuous at the interface between layers (see formula (1.30)) and diminish rapidly towards the outer fibres of the face layers.

The core material in the sandwich beam is usually much softer than the face material ($E^c << E^f$). This means that axial stresses in the core are very small and practically can be neglected. This also implies that the shear

stress is constant through the thickness of the core layer. Stress distributions in the case of very soft core ($E^c << E^f$) are shown in Figure 2.2.

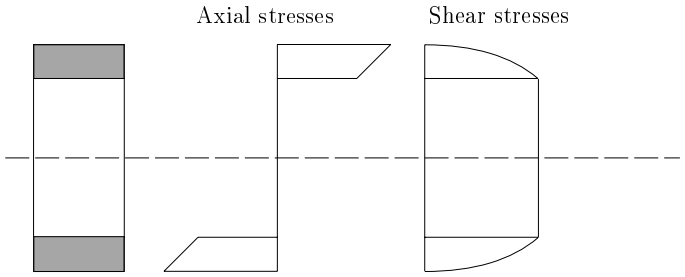

Figure 2.2: Stress distribution in sandwich beam for the case $E_c << E_f$

An efficient sandwich configuration normally has a core which is rigid enough in shear. It allows to use the faces which are much thinner than overall height of the beam ($h^f << h^c$). In this case the bending stresses in the faces can be neglected and in face sheets there are the membrane stress state. The distribution of stresses in the case of soft core and very thin face sheets are shown in the Figure 1.12.

A theory developed on the basis of assumption of membrane stress state in the face sheets and with zero axial stresses in the core is the so called engineering theory of sandwich beams. This theory was used in the section 1.5 to deliver the sandwich beam finite element $SIM8$.

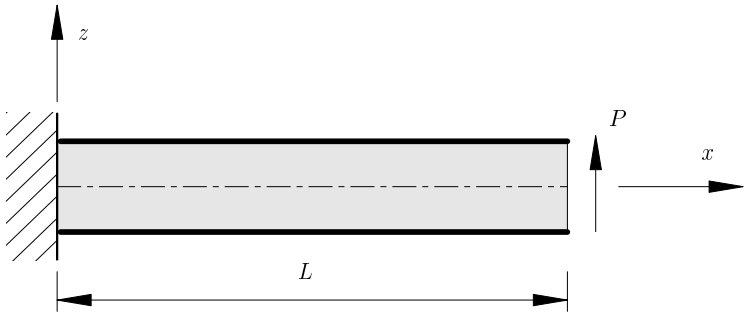

Figure 2.3: Shear loaded cantilever beam

The sandwich cantilever beam shown in Figure 2.3 is used to ilustrate the stress and failure analysis described above. The concentrated tip load P gives a uniformly distributed shear force such that $Q_x(x) = P$. The data for the parameters of material and geometry of this cantilever are given by

$$E^f = 16000 \text{ MPa} = 1.6 * 10^4 \text{ N/mm}^2, \quad G^f = 1400 \text{ MPa},$$

$$E^c = 210 \text{ MPa}, \quad G^c = 85 \text{ MPa},$$
$$h^c = 50 \text{ mm}, \quad h^f = 7.5 \text{ mm}, \quad h = 2h^f + h^c = 65 \text{ mm},$$
$$b = 80 \text{ mm}, \quad L = 150 \text{ mm},$$
$$P = 10^4 \text{ N}, \quad k = 0.279 \tag{2.16}$$

Here the shear correction coefficient is calculated by using the Reuss's formula (1.45). The materials of cantilever are glass fibre reinforced polyester face sheets and expanded PVC core layer. Expanded PVC is a foam material. Face sheets are represented by the orthotropic layers and core is isotropic material. It is evident that in this very short cantilever dominant are the shear deformations.

For the present example as the first approximation the solution on the basis of engineering theory of sandwich beams (see Ref. [3]) is given. For cantilever it is easy to obtain the analytical solution by using this simplified engineering theory. The analytical solution is as follows

$$w_{\text{eng}} = \frac{PL^3}{6D}\left[3\left(\frac{x}{L}\right)^2 - \left(\frac{x}{L}\right)^3\right] + \frac{PL}{G^c A^s}\frac{x}{L}, \tag{2.17}$$
$$M_x^{\text{eng}} = -PL\left(1 - \frac{x}{L}\right), \quad Q_x^{\text{eng}} = P,$$
$$\sigma^{f,\text{eng}} = \frac{PL}{bh_f h}\left(1 - \frac{x}{L}\right), \quad \sigma_{xz,c}^{\text{eng}} = \frac{P}{bh}$$

Here the axial stress $\sigma^{f,\text{eng}}$ is calculated for the bottom face sheet. The bending stiffness D and the transverse shear stiffness $G^c A^s$ of the sandwich beam for the engineering theory is calculated by the simplified expressions (see Ref. [3])

$$D = E^f \frac{bh^f h^2}{2}, \quad G^c A^s = G^c \frac{bh^2}{h^c}, \quad A^s = A\frac{h}{h^c} \tag{2.18}$$

In our theory of sandwich beams based on the Timoshenko's theory the bending stiffness is noted as D_{11} and the transverse shear stiffness is noted as kQ_{55}. The solution (2.17) obtained on the basis of engineering theory of sandwich beams is used only as reference solution for comparison with more acurate theory outlined in the present textbook.

Solution of the present example can be obtained by using the finite element method. For better understanding of the algorithm let us solve this example by using the Ritz's method.

Total potential energy Π of the beam is a sum of the stain energy U (1.12) and the work W of external force P

$$\Pi = U - W = \frac{1}{2}\int_0^L \left[D_{11}\left(\frac{\partial \gamma_x}{\partial x}\right)^2 + kQ_{55}\left(\gamma_x + \frac{\partial w}{\partial x}\right)^2\right] dx -$$

$$-P\ w\Big|_{x=L} \tag{2.19}$$

Essential boundary conditions are given by

$$w\Big|_{x=0} = 0, \quad \gamma_x\Big|_{x=0} = 0 \tag{2.20}$$

The two unknown functions w and γ_x can be approximated as follows

$$w = a_1\frac{x}{L} + a_2\left[3\left(\frac{x}{L}\right)^2 - \left(\frac{x}{L}\right)^3\right], \quad \gamma_x = b_1\left[2\left(\frac{x}{L}\right) - \left(\frac{x}{L}\right)^2\right] \tag{2.21}$$

For the Ritz's approximation the essential boundary conditions (2.20) must be satisfied. It is evident from the expressions (2.21) that the essential boundary conditions (2.20) is satisfied. It is seen that for the deflection w the approximation is taken in the form of analytical solution (2.17) obtained on the basis of engineering theory. The first derivative of the rotation γ_x is given by

$$\frac{\partial\gamma_x}{\partial x} = b_1\frac{2}{L}\left(1 - \frac{x}{L}\right) \tag{2.22}$$

It is seen that for analytical solution the bending moment at the tip of cantilever (see Figure 2.3) must be zero

$$M_x\Big|_{z=L} = 0$$

For the Ritz's method this is a natural boundary condition and preliminary it is not necessary to satisfy this boundary condition. In the Ritz's method the natural boundary conditions are satisfied approximately by minimizing the functional of the total potential energy. Taking into account the formulae (1.16) and (2.22) it is seen that by using the approximation (2.21) for the rotation γ_x the bending moment M_x at the tip of cantilever is zero. Such an approximation for γ_x can improve the accuracy of the solution.

Substituting the approximation (2.21) into the functional (2.19) after integration over the length of the cantilever one obtains the total potential energy of the beam as function of the unknown Ritz's coefficients

$$\Pi = \Pi(a_1, a_2, b_1)$$

Minimum of the potential energy gives the state of equilibrium

$$\frac{\partial\Pi}{\partial a_1} = 0, \quad \frac{\partial\Pi}{\partial a_2} = 0, \quad \frac{\partial\Pi}{\partial b_1} = 0 \tag{2.23}$$

Using these formulae the system of linear equations for the unknown Ritz's coefficients is obtained

$$\begin{array}{rcrcrcl} \left(\dfrac{D_{11}}{kQ_{55}}\dfrac{4}{3L^2}+\dfrac{8}{5}\right)b_1 & + & \dfrac{2}{3}\dfrac{a_1}{L} & + & \dfrac{8}{5}\dfrac{a_2}{L} & = & 0 \\ \dfrac{2}{3}b_1 & + & \dfrac{a_1}{L} & + & \dfrac{a_2}{L} & = & \dfrac{P}{kQ_{55}} \\ \dfrac{8}{5}b_1 & + & \dfrac{a_1}{L} & + & \dfrac{24}{5}\dfrac{a_1}{L} & = & \dfrac{2P}{kQ_{55}} \end{array} \tag{2.24}$$

Solution of these equations with the data (2.16) is as follows

$$b_1 = -1.048 * 10^{-2}, \quad a_1 = 2.64 \text{ mm}, \quad a_2 = 1.09 \text{ mm} \tag{2.25}$$

According to the first expression (2.21) the tip deflection of the cantilever can be calculated

$$w\Big|_{x=L} = a_1 + 2a_2 = 4.82 \text{ mm}$$

By using the same data for the reference solution (2.17) the deflection is given by

$$w_{\text{eng}}\Big|_{x=L} = 3.16 \text{ mm}$$

Bending moment M_x at the clamped end of cantilever is as follows

$$M_x\Big|_{x=0} = D_{11}\frac{\partial \gamma_x}{\partial x}\Big|_{x=0} = D_{11}\frac{2}{L}b_1 = -2.24 * 10^6 \text{ Nmm}$$

The reference solution (2.17) gives

$$M_x^{\text{eng}}\Big|_{x=0} = -PL = -1.5 * 10^6 \text{ Nmm}$$

The shear force at the clamped end of the cantilever is given by

$$Q_x\Big|_{x=0} = kQ_{55}\left(\gamma_x + \frac{\partial w}{\partial x}\right)\Big|_{x=0} = kQ_{55}\frac{a_1}{L} = 8800 \text{ N}$$

The reference solution (2.17) gives

$$Q_x^{\text{eng}}\Big|_{x=0} = P = 10^4 \text{ N}$$

The axial stresses are calculated in each layer at the clamped end of the cantilever by using the formulae (2.9)-(2.11). Results are presented in Figure 2.4.

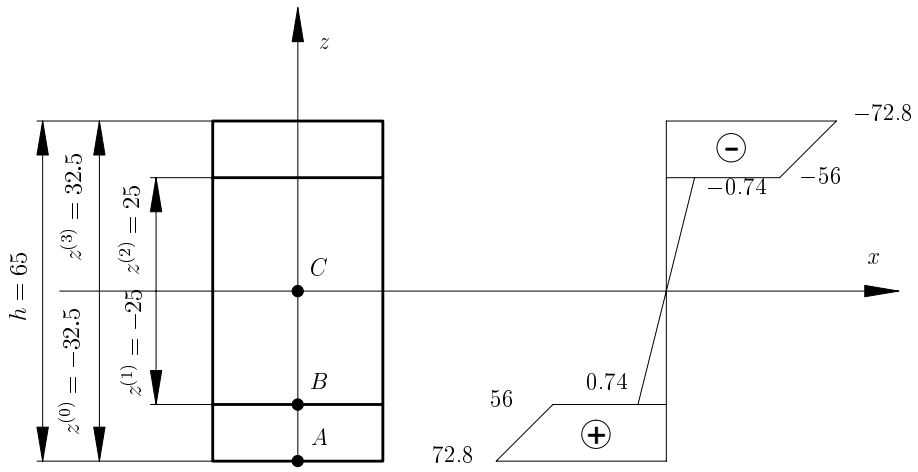

Figure 2.4: Axial stresses $\sigma_x(z)$ in [N/mm^2] at the clamped end of the cantilever

The reference solution (2.17) for axial stress in the bottom face sheet is as follows

$$\sigma_f^{\text{eng}}\Big|_{x=0} = \frac{PL}{bh_f h} = 36 \text{ N/mm}^2$$

The transverse shear stresses in each layer are calculated by using the formula (2.12). Results are presented in Figure 2.5.

The reference solution (2.17) for the transverse shear stress in the core is given by

$$\sigma_{xz,c}^{\text{eng}} = \frac{P}{bh} = 1.92 \text{ N/mm}^2$$

It is seen that for the transverse shear stress there is exelent agreement of the results obtained by using the formula (2.12) and the engineering theory of sandwich beams. Significantly larger is difference for the deflection and axial stresses. It is because in this example there is relatively high E^c/E^f ratio and relatively thick faces. In this case engineering theory gives only a rough estimate of the solution. Engineering theory can be used only for the sandwich beams with very thin faces and very soft core. Solution by Ritz's method with only three independent variables also can be evaluated as first rough approximation, especially for the stresses. More accurate results can be obtained only by the finite element method.

The second step after stress analysis is failure analysis of the sandwich beam. For this example it is evident that failure may occur in the cross

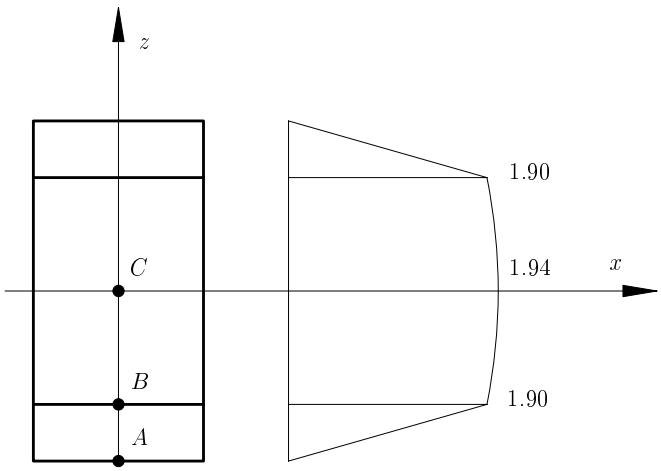

Figure 2.5: Transverse shear stresses $\sigma_{xz}(z)$ in [N/mm^2] at the clamped end of the cantilever

section at the clamped end. In this cross section there are three points throughout the height of the beam, where the critical stress state can be achieved. These are: point A at the outer fibre in the bottom (or top) layer, point B at the interface between the face layer and the core and point C on the neutral axis of the beam.

In the point A the failure (strength) criterion is as follows

$$\sigma_x^A \leq [\sigma_A] \tag{2.26}$$

Here $[\sigma_A]$ is allowable axial stress in tension or compression for the orthotropic face sheet.

In the point B as failure criterion at the interface the Misses criterion can be used

$$\sigma_M^B = \sqrt{(\sigma_x^B)^2 + 3(\sigma_{xz}^B)^2} \leq [\sigma_B] \tag{2.27}$$

Here σ_M^B is Misses equivalent stress in the point B, $[\sigma_B]$ is allowable Misses equivalent stress at the interface.

In the point C there is pure shear stress state and as failure criterion also the Misses criterion can be used

$$\tau^C \leq [\tau_C] \quad \text{or} \quad \sigma_M^C = \sqrt{3(\sigma_{xz}^C)^2} \leq [\sigma_C] \tag{2.28}$$

Here σ_M^C is Misses equivalent stress in the point C, $[\sigma_C]$ is allowable Misses equivalent stress in the core and $[\tau_C]$ is allowable shear stress in the core.

Let us assume the following strength parameters for the core, face sheets and the interface

$$[\sigma_A] = 100 \text{ N/mm}^2, \quad [\sigma_B] = 2 \text{ N/mm}^2, \quad [\sigma_C] = 2 \text{ N/mm}^2 \tag{2.29}$$

The stresses at the clamped end of cantilever in the cross section for the tip load $P = 10^4\ N$ is given by (see the solution above)

$$\begin{aligned} &\sigma_x^A = 72.8 \text{ N/mm}^2, \quad \sigma_x^B = 0.74 \text{ N/mm}^2, \\ &\sigma_{xz}^B = 1.90 \text{ N/mm}^2, \quad \sigma_{xz}^C = 1.94 \text{ N/mm}^2 \end{aligned} \tag{2.30}$$

Since the solution of this example is geometrically (small deflections) and physically (Hooke's law) linear solution the stresses are linear functions of the applied load P, i.e. for the limit load P_{limit} the stresses $\sigma_{\text{limit}}^{A,B,C}$ in the points A, B, C can be calculated from the stresses $\sigma_{A,B,C}$ in the same points under load $P = 10^4\ N$

$$\sigma_{\text{limit}}^{A,B,C} = \frac{P_{\text{limit}}}{P}\sigma_{A,B,C} \leq [\sigma_{A,B,C}] \tag{2.31}$$

The limit load can be calculated for the failure in the points A, B, C, recpectively

$$P_{\text{limit}} = \frac{[\sigma_{A,B,C}]}{\sigma_{A,B,C}}P \tag{2.32}$$

By using the formulae (2.31) and (2.32) the limit loads are calculated

$$P_{\text{limit}}^A = 1.37 * 10^4\ N, \quad P_{\text{limit}}^B = 0.593 * 10^4\ N, \quad P_{\text{limit}}^C = 0.595 * 10^4\ N$$

So, the weakest point for the sandwich cantilever to be designed is the interface point B and thus the limit (allowable) load is 5930 N. In the point C on the neutral axis of the beam stresses at the limit load also are rather high and very close to the failure stresses.

The stress and failure analysis examined above is only the first step of the full failure analysis of the sandwich beam or so called first crack analysis. The second step of the full failure analysis of the beam is crack propagation analysis on the basis of linear fracture mechanics. It should be noted that for sandwich and laminated composite structures it is not sufficient to carry out analysis only on the basis of failure criterion. For correct estimation of the failure loads the analysis of cracking of the structure on the basis of methods of fracture mechanics must be carried out. So, there is significant difference from the failure analysis of the standard steel or aluminium beams, where in most cases the strength analysis on the basis of strength (failure) criteria is sufficient to estimate the limit (allowable) loads or to calculate the dimensions of the structure.

2.3 Failure Analysis of Laminated Composite Beams

A laminated composite or laminate consists of a bonded stack of plies, which usually in the calculations are asummed as unidirectionally reinforced single layers. Individual layers are aligned at specific angle to the global reference direction. If the angles of the layers are arbitrary these are the so called angle-ply laminates. If the angles of the layers are 0^0 and 90^0 these are the so called cross-ply laminates.

For the laminates to be designed the material is chosen and the stiffness properties are known. With the given stiffness properties of the layers for laminate the stresses in each layer can be calculated by using the theory outlined in the section 2.1 of the present chapter. Using the failure (strength) criterion each play can be tested to establish the load factor by which the ply must be scaled up to achieve the failure. This set of calculations is repeated for each ply, to find in which ply the lovest load factor occurs and in which, under the given applied load ratios, first ply failure is predicted.

Even though one ply has failed, in most cases the laminate may still be capable of sustaining additional loads. There are continuous discusions about the best way to calculate the behaviour of the laminate after the first play has failed. In most cases the intralamina (in the play) or interlaminar (at the interface between two plies) cracks may initiate further delamination cracking. This crack propagation can be analysed only by using the methods of fracture mechanics. Special case of fracture is delamination buckling of plies [19]. In the present section only the first ply failure analysis of the laminates is performed.

The strength properties of the laminates depend not only on the properties of each ply in the stack and its relation to the directions of the applied stresses but also on the proportions of plies in the laminate and the bonding of the plies. The discussion which follows releates only to the symmetric cross-ply laminates.

Let us consider an example of stress and failure analysis of a cross-ply $[0^0/90^0/0^0]$ laminated composite beam with the simply supported boundary conditions (see Figure 2.6).

A top and bottom layers of the angle 0^0 are aligned in the direction of the beam axis x. A middle layer of the angle 90^0 is aligned in the transverse direction. This three layered beam is made from carbon fibre reinforced plastic (CFRP). The present example was studied by Pagano [4] using the equations of theory of elasticity. We are using the Pagano's exact solution as reference solution. Each layer of the beam is unidirectionally reinforced

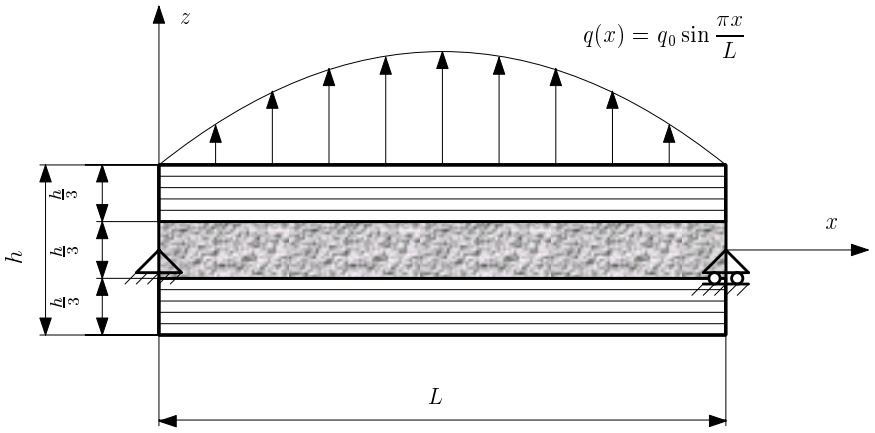

Figure 2.6: Cross-ply $[0^0/90^0/0^0]$ simply supported laminated composite beam

layer having the stiffness properties as follows

$$E_1 = 1.724 * 10^5 \text{ MPa} = 1.724 * 10^5 \text{ N/mm}^2, \quad E_2 = 6895 \text{ MPa},$$
$$G_{12} = 3448 \text{ MPa}, \quad G_{23} = 1379 \text{ MPa}, \quad \nu_{12} = 0.25 \quad (2.33)$$

Here the axis 1 is in the fibre direction and the axes 2, 3 are transverse to the fibre direction. For the cross-ply $[0^0/90^0/0^0]$ laminate the layer properties are noted as follows

$$E_x^{(1)} = E_x^{(3)} = E_1, \quad E_x^{(2)} = E_2, \quad G_{xz}^{(1)} = G_{xz}^{(3)} = G_{12}, \quad G_{xz}^{(2)} = G_{23}$$

Geometric properties of the beam and the amplitude q_0 of the sinusoidal load $q(x) = q_0 sin(\pi x/L)$ are given by $(h/L = 1/10)$

$$L = 240 \text{ mm}, \quad b = 1, \quad h_1 = h_2 = h_3 = 8 \text{ mm}, \quad h = 24 \text{ mm},$$
$$z_0 = -12 \text{ mm}, \quad z_1 = -4 \text{ mm}, \quad z_2 = 4 \text{ mm}, \quad z_3 = 12 \text{ mm},$$
$$q_0 = 0.6895 \text{ N/mm} \quad (2.34)$$

In order to calculate the transverse shear stiffness of the beam the shear correction coefficient must be calculated. By using the Reuss' formula (1.45) the shear correction coefficient of this cross-ply $[0^0/90^0/0^0]$ laminate was calculated and the value $k = 0.833$ was obtained. By using the more accurate Reissner's formula (1.39) the value of the shear correction coefficient $k = 0.569$ was obtained. Further for solution the value $k = 0.569$ is employed, since the Reissner's formula is more accurate as Reuss' formula.

The bending D_{11} and the transverse shear stiffness kQ_{55} for this cross-ply $[0^0/90^0/0^0]$ laminate is calculated by using the formulae (1.9)

$$kQ_{55} = k\ b\sum_{k=1}^{3} G_{xz}^{(k)} h_k = 3.76 * 10^4 \text{ N}, \tag{2.35}$$

$$D_{11} = b\frac{1}{3}\sum_{k=1}^{3} E_x^{(k)}[z_k^3 - z_{k-1}^3] = 1.92 * 10^8 \text{ Nmm}^2$$

Solution of the present example can be obtained by using the finite element method. For better understanding of algorithm of analysis the example is solved by using the Ritz's method.

Total potential energy Π of the beam is a sum of the strain energy U and the work W of the external sinusoidally distributed load $q(x)$

$$\Pi = U - W = \frac{1}{2}\int_0^L \left[D_{11}(\frac{\partial\gamma_x}{\partial x})^2 + kQ_{55}(\gamma_x + \frac{\partial w}{\partial x})^2\right] dx$$
$$- \int_0^L q_0 sin\left(\frac{\pi x}{L}\right) w\ dx \tag{2.36}$$

The essential (kinematic) boundary conditions are given by

$$w\Big|_{x=0} = 0, \quad w\Big|_{x=L} = 0 \tag{2.37}$$

The two unknown functions w and γ_x can be approximated by trigonometric functions

$$w(x) = a_1 \sin\left(\frac{\pi x}{L}\right), \tag{2.38}$$

$$\gamma_x(x) = b_1 \cos\left(\frac{\pi x}{L}\right) \tag{2.39}$$

It is evident that approximation for the deflection is such that essential boundary conditions (2.37) are satisfied. For this example rotation γ_x is not presented in the essential boundary conditions. The approximation for rotation γ_x is taken in such form (see the second expression (2.39)) because for this function (cosine) the first derivative is a sine function. According the first formula (1.16) the bending moment also is the sine function, for which the value on the supports of the beam is zero. The bending moment is a natural boundary condition for the functional of Timoshenko's beam (see (1.23)). For the Ritz's method it is not necessary preliminary to satisfy the natural boundary conditions. If the natural boundary conditions are also preliminary satisfied by Ritz's approximation the accuracy of the solution can be improved.

Substituting the approximation (2.39) in functional (2.36), after integration over the length of the beam one can obtain the total potential energy of the structure as function of unknown coefficients a_1 and b_1

$$\Pi = \Pi(a_1, b_1)$$

Minimum of the potential energy gives the state of equilibrium

$$\frac{\partial \Pi}{\partial b_1} = 0, \quad \frac{\partial \Pi}{\partial a_1} = 0 \tag{2.40}$$

Using these formulae the system of linear equations for the unknown Ritz's coefficients is obtained

$$\begin{array}{rcrcc} (\dfrac{D_{11}}{kQ_{55}}\dfrac{\pi}{L} + \dfrac{L}{\pi})b_1 & + & a_1 & = & 0 \\ b_1 & + & \dfrac{\pi}{L}a_1 & = & \dfrac{q_0}{kQ_{55}}\dfrac{L}{\pi} \end{array} \tag{2.41}$$

Solution of these equations can be obtained in the analytical form

$$b_1 = -\frac{q_0 L^3}{D_{11}\pi^3}, \tag{2.42}$$

$$a_1 = \frac{q_0 L^4}{D_{11}\pi^4}\left[1 + \frac{D_{11}}{kQ_{55}}\frac{\pi^2}{L^2}\right] \tag{2.43}$$

By using these formulae and approximation (2.39) the deflection in the midspan of beam can be calculated

$$w = \Big|_{x=L/2} \equiv a_1 = 0.23 \text{ mm}$$

It should be noted that in the case of classical Bernoulli-Euler's beam theory the transfer shear stiffness is infinity $kQ_{55} \to \infty$. In this case the deflection w_{cl} (classical theory without shear deformations) in the midspan of beam is given by

$$w_{\text{cl}}\Big|_{x=L/2} = \frac{q_o L^4}{D_{11}\pi^4}$$

The deflection of beam w_{T} calculated by the Timoshenko's beam theory can be represented by

$$w_{\text{T}} = w_{\text{cl}} k_1$$

Here the coefficient k_1 in our example is given by

$$k_1 = \left[1 + \frac{D_{11}}{kQ_{55}}\frac{\pi^2}{L^2}\right] = 1.875$$

	Pagano [4]	Timoshenko	Bernouli-Euler
	$\bar{w}_{\text{exact}}$	$\bar{w}_{\text{T}}$	$\bar{w}_{\text{cl}}$
Deflection $\bar{w}$	0.9316	0.9591	0.5115
Relative error [%]	-	+2.95	−45.1

Table 2.1: Maximum deflection $\bar{w}$ of the cross-ply $[0^0/90^0/0^0]$ laminated composite beam

So, for this example the deflection of the beam calculated by the Timoshenko's theory is 87.5 % higher that deflection obtained by using the classical beam theory.

It is of interest to compare the present solution with the reference solution of Pagano [4]. Here the results were presented in the dimensionless form

$$\bar{w} = cw$$

where coefficient c for our example is given by

$$c = \frac{100E_2h^3}{q_0L^4} = 4.17$$

The results of analysis for the midspan deflection obtained by using different theories are presented in Table 2.1.

In Table 2.1 relative error was calculated by formula

$$\varepsilon = \frac{w - w_{\text{exact}}}{w_{\text{exact}}} * 100\%$$

It is seen that the Timoshenko's theory for moderately thick CFRP beam ($h/L = 1/10$) gives a good estimation of the deflection in comparison with the exact solution obtained by theory of elasticity. In the same time the result obtained by using the classical theory is not correct even for the moderate beam height to length ratio.

Stresses in the beam can be calculated from the bending moment M_x and the shear force Q_x. The maximum moment is in the midspan of the beam

$$M_x\Big|_{x=L/2} = D_{11}\frac{\partial\gamma_x}{\partial x}\Big|_{x=L/2} = \frac{q_0L^2}{\pi^2}$$

Here

$$\frac{\partial\gamma_x}{\partial x}\Big|_{x=\frac{L}{2}} = -b_1\frac{\pi}{L} = \frac{q_0L^2}{D_{11}\pi^2} \tag{2.44}$$

It can be showed that the expression for maximum bending moment obtained by using the Ritz's method is equal to the maximum bending moment obtained by the analytical solution. Actually, the reaction force R at the supports is given by

$$R = \frac{1}{2}\int_0^L q_0 \sin\left(\frac{\pi x}{L}\right)\ dx = \frac{q_0 L}{\pi}$$

Bending moment in the midspan of beam is given by

$$M_x\Big|_{x=L/2} = \frac{q_0 L^2}{2\pi} - \int_0^{L/2} q_0 \sin\left(\frac{\pi x}{L}\right)\left[\frac{L}{2} - x\right]\ dx = \frac{q_0 L^2}{\pi^2}$$

This analytical result for the bending moment is the same as was obtained by using the Ritz's method.

Maximum of the shear force is on the supports

$$Q_x\Big|_{x=0} = kQ_{55}\left(\gamma_x + \frac{\partial w}{\partial x}\right)\Big|_{x=0} = kQ_{55}\left(b_1 + a_1\frac{\pi}{L}\right) = 52.64\ N$$

This result for the shear force obtained by the Ritz's method is very close to the analytical solution

$$Q_x\Big|_{x=0} = R = \frac{q_0 L}{\pi} = 52.74\ N$$

The highest axial stresses occur in the cross section with maximum bending moment M_x, i.e. in the midspan of the beam. The stresses in the layers are calculated from the strains

$$\varepsilon_x^{(k)}(z) = z\frac{\partial \gamma_x}{\partial x}$$

Using this expression the strains in each point of the cross section of the beam can be calculated. For example, in the point A of the outer fibre $z_3 = 12$ mm of the top layer (see Figure 2.7) the axial strain is given by

$$\varepsilon_x^A = \varepsilon_x^{(3)}(z_3) = z_4\frac{\partial \gamma_x}{\partial x}\Big|_{x=L/2} = 2.52 * 10^{-4}$$

The axial stress in this point is calculated by using the Hooke's law

$$\sigma_x^A = E_1\varepsilon_x^A = 43.3\ \mathrm{N/mm^2}$$

In the point D at the outer fibre of the bottom layer $z_0 = -12$ mm there is axial compression stress of the same value

$$\sigma_x^D = E_1\varepsilon_x^D = -43.3\ \mathrm{N/mm^2}$$

In the same manner the axial stresses in other points of the cross section are evaluated

$$\sigma_x^{B,3} = E_1 \varepsilon_x^B = 14.43 \text{ N/mm}^2, \quad \sigma_x^{B,2} = E_2 \varepsilon_x^B = 0.58 \text{ N/mm}^2$$

Here $\sigma_x^{B,3}$ is the axial stress in the top layer (layer 3) at $z_2 = 4$ mm and $\sigma_x^{B,2}$ is the axial stress in the middle layer (layer 2) at $z_2 = 4$ mm.

Results for stresses in the Pagano's reference solution [4] were presented in the dimensionless form

$$\bar{\sigma}_x = \frac{\sigma_x}{q_0}, \quad \bar{\sigma}_{xz} = \frac{\sigma_{xz}}{q_0} \tag{2.45}$$

Using these expressions the stresses presented in [4] can be recalculated. Results for axial stresses in the cross section at the midspan of beam are presented in Figure 2.7.

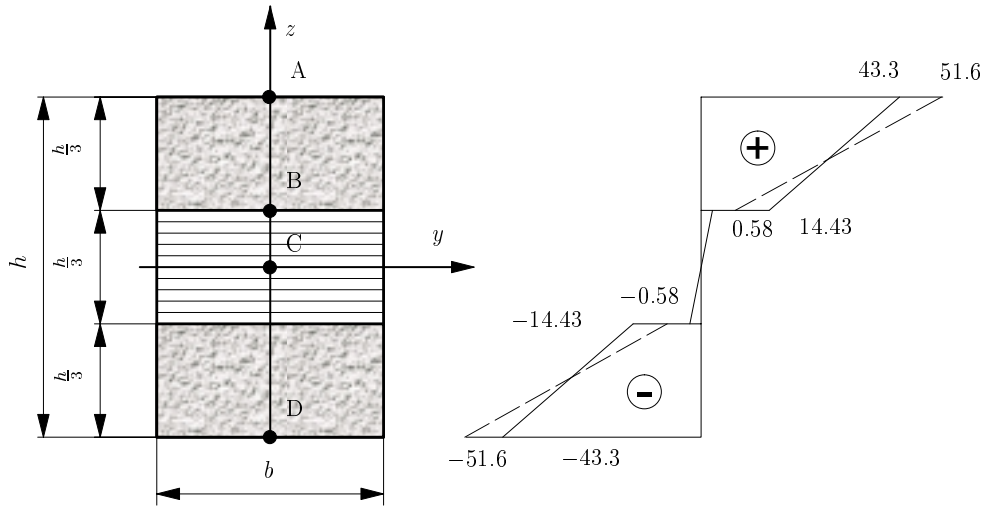

Figure 2.7: Axial stresses in the cross section at the midspan of beam ($h/L = 1/10$): — Timoshenko's theory, - - - Pagano [4]

For the maximum bending stress our result $\sigma_x^A = 43.3$ N/mm^2 is about 16% lower that the value $\sigma_x^A = 51.6$ N/mm^2 obtained by the exact solution of Pagano [4].

Maximum of the transverse shear stress is observed in the cross section at the supports of beam. Transverse shear stresses in each layer can be calculated by using the formula (2.12)

$$\sigma_{xz}^{(k)}(z) = g_k(z) Q_x, \quad k = 1, 2, 3$$

Maximum of the transverse shear stress is at the neutral axis of beam (point C)

$$\sigma_{xz}^{C} = \sigma_{xz}^{(2)}\Big|_{z=0} = g_2(0)Q_x$$

Here $g_2(0)$ at $z = 0$ is calculated by the formula (1.35)

$$g_2(0) = \frac{1}{D_{11}}\left[-E_2\frac{z^2}{2} + E_1\frac{(z^{(0)})^2}{2} + (E_2 - E_1)\frac{(z^{(1)})^2}{2}\right] = 5.76 * 10^{-2}$$

Thus the maximum of the transverse shear stress is given by

$$\sigma_{xz}^{C} = g_2(z = 0)Q_x(x = 0) = 3.03 \text{ N/mm}^2$$

The transverse shear stress distribution in the cross section at $x = 0$ is presented in Figure 2.8.

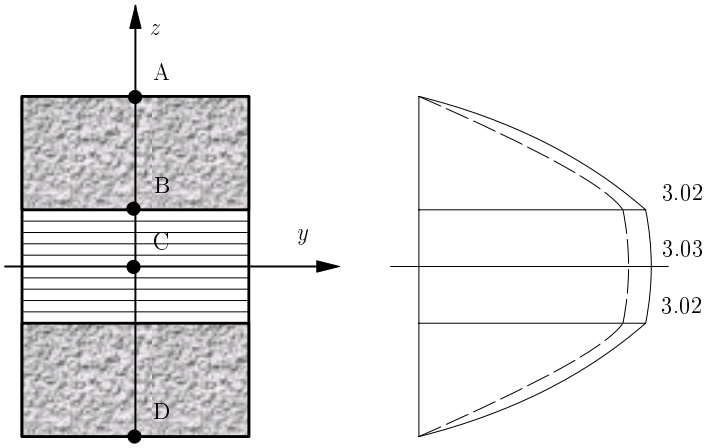

Figure 2.8: Transverse shear stresses in the cross section at $x = 0$ of the beam ($h/L = 1/10$): —- Timoshenko's theory, - - - - Pagano [4]

It is seen that the transverse shear stress distribution obtained by the Timoshenko's theory is very close to the solution obtained by the theory of elasticity [4]. From the stress analysis presented above it can be concluded that for thin beams and beams of moderate thickness ($h/L \leq 1/10$) the stresses in composite laminates can be calculated by the beam theory. However, for the thick beams ($h/L = 1/4$) correct results for stresses can be obtained only by using the theory of elasticity.

The second step after the calculation of stresses is the failure analysis. The failure analysis can be performed using the transverse shear and axial stresses

and the failure criterion of the orthotropic material. Four points of the cross section of the beam for possible failure must be analysed (see Figure 2.8). The first is point A at the outer fiber of the top layer. Here only axial tension stresses are acting. The second is point D, where only compression stresses are acting. Note that for the carbon fiber reinforced plastics (CFRP) the strength in tension and compression is different. The compression strength is about 30% lower. The third is point B at the interface of layers, where failure can occur. The fourth is point C at the neutral axis, where pure shear stress is acting.

In all four points the failure conditions can be written

$$\begin{aligned} \sigma_x^A &\le [\sigma_{L+}], \\ |\sigma_x^D| &\le [\sigma_{L-}], \\ \sigma_x^B &\le [\sigma_{T+}], \\ \sigma_{xz}^B &\le [\sigma_{xz}^{TT}], \\ \sigma_{xz}^C &\le [\sigma_{xz}^{TT}] \end{aligned} \tag{2.46}$$

Here $[\sigma_{L+}]$ is allowable stress in tension in the fiber (longitudinal) direction, $[\sigma_{L-}]$ is allowable stress in compression in the fiber direction, $[\sigma_{T+}]$ is allowable stress in tension transverse (T) to the fibers, $[\sigma_{xz}^{TT}]$ is allowable stress in the transverse shear of the layer. For present CFRP composite the following allowable stresses are assumed

$$\begin{aligned} [\sigma_{L+}] = 600 \text{ N/mm}^2, \quad [\sigma_{L-}] = 400 \text{ N/mm}^2, \\ [\sigma_{T+}] = 20 \text{ N/mm}^2, \quad [\sigma_{xz}^{TT}] = 20 \text{ N/mm}^2 \end{aligned} \tag{2.47}$$

Note that evaluation of stresses was performed under acting load $q_0 = 0.6895$ N/mm. Since the relation between external loads and stresses in the structure is linear, the limit loads for each point can be calculated

$$q_{0,\text{limit}} = \frac{[\sigma_{A,B,D,C}]}{\sigma_{A,B,D,C}} \tag{2.48}$$

The values of the limit loads are as follows

$$\begin{aligned} q_{0,\text{limit}}^A &= \frac{[\sigma_{L+}]}{\sigma_A} = 9.5 \text{ N/mm}, \\ q_{0,\text{limit}}^B &= \frac{[\sigma_{T+}]}{\sigma_B} = 23.8 \text{ N/mm}, \\ q_{0,\text{limit}}^D &= \frac{[\sigma_{L-}]}{\sigma_D} = 6.4 \text{ N/mm}, \\ q_{0,\text{limit}}^C &= \frac{[\sigma_{TT}]}{\sigma_{xz}^C} = 4.5 \text{ N/mm}, \end{aligned}$$

$$q^B_{0,\text{limit}} = \frac{[\sigma_{TT}]}{\sigma^B_{xz}} = 4.6 \text{ N/mm} \tag{2.49}$$

It is seen that the weekest point of this cross-ply laminate is point C and the limit load of the present structure is 4.5 N/mm. Verification of the present failure analysis can be performed only experimentally through measurements of the first ply cracking and the failure loads.

Chapter 3

Vibrations of Composite Beams

The first step in a general dynamic analysis of the structures is the free vibration analysis, i.e. calculation of the natural frequencies and corresponding free vibration modes. In detail the dynamic analysis of structures was outlined in the textbook [5]. In the present chapter the vibrations of sandwich and laminated composite beams are investigated.

The wide use of laminated composite beams in industry, for example, as rotating blades of turbines or robot arms requires in-deep study the vibration characteristics of these beams. The classical lamination theory, which neglects the shear deformations and rotatory inertia, fail to predict a correct natural frequencies of laminated beams. It will be shown below by analysing the vibrations of laminated composite beams. In the classical lamination theory (see, for example, the textbook [6]) the transverse shear deformations are ignored. Since transverse shear deformations are more important for composites, due to the relatively high ratio of extensional modulus in the fibre direction to the transverse shear modulus, the Timoshenko's beam theory should be used for the vibration analysis of composite structures.

Timoshenko's beam theory was outlined in section 1.1. The stiffness $\boldsymbol{K}_e$ and the mass $\boldsymbol{M}_e$ matrices for the four different finite elements were delivered. These are the finite element $SI8$ for analysis of symmetric laminates or sandwich beams with flexural deformations only, the finite element $SI12$ for analysis of non-symmetric laminates, where both flexural and stretching deformations are taken into account, and the finite element $SI20$, which was delivered on the basis of the broken line or the so called zig-zag model. The fourth finite element $SIM8$ was delivered for analysis of sandwich beams with very thin faces and soft core. All these finite elements depending on beam geometry and material properties can be used for the vibration analysis of sandwich and laminated composite beams.

The simplest case is analysis of symmetric laminates or symmetric sand-

wich beams. Such analysis can be performed by using the finite element *SI*8 or obtainig solution by using the analytical methods.

Further for better understanding the symmetric laminated beams is analysed by using the Rayleigh-Ritz's energy approach. The terminology Rayleigh-Ritz's method is used only for the vibration analysis of structures, because Rayleigh in 1870 was the first, who used the energy approach in the vibration analysis. In 1908 a German scientist W. Ritz proposed more general variational method to obtain the approximate solution of partial differential equations. Today this general method is called the Ritz's method. Since some basic ideas of the method was proposed earlier by Rayleigh, in the case of using the Ritz's method in the vibration analysis, the method is called Rayleigh-Ritz's method. The history of investigations of variational principles and methods was outlined in the textbook [7].

3.1 Solution by Rayleigh-Ritz's Method

Let us consider the vibration analysis of the simply supported beam of length L (see Figure 3.1).

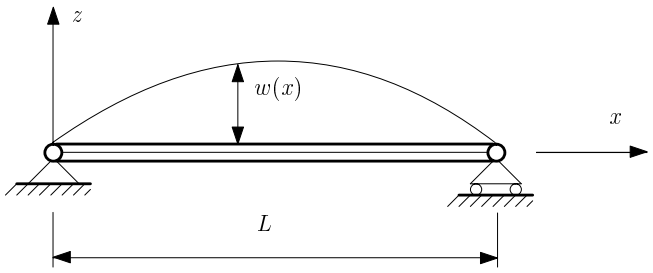

Figure 3.1: Vibrations of simply supported beam

Symmetric laminated composite or sandwich beams are considered. The parameters of material for the beams to be calculated will be given later in numerical examples.

Essential boundary conditions for the simply supported beam are given by

$$w = \Big|_{x=0} = 0, \quad w = \Big|_{x=L} = 0 \tag{3.1}$$

In the case of symmetric laminates or sandwich beams the functional of the strain energy is given by the expression (2.19) excluding the external load

$(P = 0)$

$$U = \frac{1}{2}\int_0^L \left[D_{11}\left(\frac{\partial \gamma_x}{\partial x}\right)^2 + kQ_{55}\left(\gamma_x + \frac{\partial w}{\partial x}\right)^2 \right] dx \tag{3.2}$$

The functional of kinetic energy of the beam in general case of non-symmetric laminates and including rotatory inertia is given by the expression (1.70). For the symmetric laminates or sandwich beams the generalized density $\rho_1 = 0$. To obtain a simplified solution the effect of rotatory inertia is neglected, i.e. it is assumed that generalized density $\rho_2 = 0$. In general the rotatory inertia must be taken into account. For example, in some cases of analysis of the sandwich beams it is neccesary to perform the vibration analysis taking into account rotatory inertia. In this case not only the flexural modes, but also the tranverse shear vibration modes are obtained. For the sandwich beams with very soft core the frequencies corresponding to the tranverse shear vibration modes follows just after the first three or four frequencies, which correspond to the flexural vibration modes.

The simplified ($\rho_2 = 0$) functional of kinetic energy of the Timoshenko's beam is given by the expression

$$T = \frac{1}{2}\int_0^L (\rho_0 \dot{w}^2)\, dx \tag{3.3}$$

In the free vibrations the beam may be assumed to behave sinusoidally with respect to time. In order to describe the motions of the beam in the one period of vibrations between the time 0 and $T = 2\pi/\omega$ (T is the period of vibrations with frequency ω) the Hamiltonian variational principle (see the textbook [7]) can be used. The procedure of solution is in minimizing the functional Φ, which is defined as follows

$$\Phi = \int_0^{2\pi/\omega} L dt = \int_0^{2\pi/\omega} (T - U) dt \tag{3.4}$$

The quantity $L = T - U$ is the so called Lagrangian function.

Minimization of the functional (3.4) is performed by using the Rayleigh-Ritz's method. For this the unknown functions w and γ_x are approximated by

$$\begin{aligned} w(x,t) &= a_1 \sin\left(\frac{n\pi x}{L}\right) \sin(\omega t), \\ \gamma_x(x,t) &= b_1 \cos\left(\frac{n\pi x}{L}\right) \sin(\omega t) \end{aligned} \tag{3.5}$$

It is seen that for this approximation the essential boundary conditions (3.1) are satisfied. Substituting the approximation (3.5) into functional (3.4) after integration over the time period and over the length of the beam the energy Φ is obtained as function of the unknown Ritz's coefficients

$$\Phi = \Phi(a_1, b_1) \tag{3.6}$$

Minimum of this function can be obtained

$$\frac{\partial \Phi}{\partial b_1} = 0, \quad \frac{\partial \Phi}{\partial a_1} = 0 \tag{3.7}$$

Using these expressions the eigenvalue problem is formulated in order to calculate natural frequencies ω_n of the beam

$$\begin{array}{rcrcl} (D_{11}\left(\frac{n\pi}{L}\right)^2 + kQ_{55})b_1 & + & kQ_{55}\frac{n\pi}{L}a_1 & = & 0 \\ kQ_{55}\frac{n\pi}{L}b_1 & + & \left[kQ_{55}\left(\frac{n\pi}{L}\right)^2 - \omega_n^2\rho_0\right]a_1 & = & 0 \end{array} \tag{3.8}$$

This is a set of linear homogeneous equations. For the non-trivial solution ($a_1 \neq 0, b_1 \neq 0$) the determinant D of the system of linear equations (3.8) must be zero

$$D = 0 \tag{3.9}$$

Under this condition the free vibration frequencies of the Timoshenko's beam ω_n^{T} can be found

$$(\omega_n^{\mathrm{T}})^2 = \frac{\frac{D_{11}}{\rho_0}\left(\frac{n\pi}{L}\right)^4}{\left[1 + \left(\frac{n\pi}{L}\right)^2 \frac{D_{11}}{kQ_{55}}\right]} \tag{3.10}$$

In classical Bernoulli-Euler's beam theory the transverse shear deformations are neglected and transverse shear stiffness of the beam is assumed to be infinity $kQ_{55} \to \infty$. In this case the eigenfrequencies ω_n^{cl} (classical theory without shear deformations) of the beam are calculated by the formula

$$(\omega_n^{\mathrm{cl}})^2 = \frac{D_{11}}{\rho_0}\left(\frac{n\pi}{L}\right)^4 \tag{3.11}$$

This expression is easly recognized to be the well known solution for the natural flexural frequencies of the classical beam theory for a simply supported

beam. The frequencies calculated by the Timoshenko's beam theory and by the classical theory are related by

$$\omega_n^{\mathrm{T}} = \frac{\omega_n^{\mathrm{cl}}}{k_2} \tag{3.12}$$

Here the coefficient k_2 is given by

$$k_2 = 1 + \left(\frac{n\pi}{L}\right)^2 \frac{D_{11}}{kQ_{55}}$$

It is seen that for higher (n is higher) frequencies the influence of the transverse shear deformations is higher. A significant influence of the transverse shear deformations is for the thick beams and for the beams with a low transverse shear stiffness.

Similarly as outlined above by using the Rayleigh-Ritz's method a solution of the vibration problem can also be obtained for the Timoshenko's beam with other boundary conditions, for example, for the cantilever or for the beams with clamped-clamped boundary conditions.

More complex structures can be analysed by using the finite element method. The theoretical background of the finite element method is the same as for the Ritz's method. Both methods are based on minimization of functional by using the same variational principle. The only difference is that approximation of the unknown functions in the Ritz's method is taken for the whole structure, but in the finite element method the approximation is carried out within the finite element by using the so called shape functions. Minimization procedure in the Ritz's method is carried out after inegration of the functional by "hand". Also all other mathematical treatment is performed in the analytical form. In the finite element method minimization procedure is carried out by using numerical methods and computer. It can be said that the finite element method is the Ritz's method for the computers. The details of the finite element method one can find in the textbooks (see, for example, Bathe [5] and others).

3.2 Solution by Finite Element Method

In finite element method the beam can be represented as assembly of finite elements. For example, the beam of length L can be discretized by N finite elements of length $l = L/N$. For each finite element the strain energy is represented in the form (1.59)

$$U_e = \frac{1}{2}\boldsymbol{v}_e^T \boldsymbol{K}_e \boldsymbol{v}_e \tag{3.13}$$

Similarly for each finite element the functional of kinetic energy (1.70) or (1.72) is represented in the discrete form (1.74)

$$T_e = \frac{1}{2}\dot{\boldsymbol{v}}_e^T \boldsymbol{M}_e \dot{\boldsymbol{v}}_e \tag{3.14}$$

The whole structure is represented as assembly of N finite elements and the strain energy of the structure U is a sum of the strain energies of the elements

$$U = \sum_{i=1}^{N} U_{i,e} = \frac{1}{2}\boldsymbol{v}^T \boldsymbol{K} \boldsymbol{v} \tag{3.15}$$

Here $\boldsymbol{v}$ is a vector of nodal displacements of the whole structure and $\boldsymbol{K}$ is a stiffness matrix of the structure

$$\boldsymbol{K} = \sum_{i=1}^{N} \boldsymbol{K}_{i,e} \tag{3.16}$$

Similarly the kinetic energy of the whole structure T is a sum of the kinetic energies of elements

$$T = \sum_{i=1}^{N} T_{i,e} = \frac{1}{2}\dot{\boldsymbol{v}}^T \boldsymbol{M} \dot{\boldsymbol{v}} \tag{3.17}$$

Here $\boldsymbol{M}$ is a mass matrix of the structure

$$\boldsymbol{M} = \sum_{i=1}^{N} \boldsymbol{M}_{i,e} \tag{3.18}$$

The equation of motion of the structure can be found by using a stationarity condition of the Lagrange functional L

$$\delta L = \delta(T - U) = 0 \tag{3.19}$$

Here δ means variations of displacements for the space coordinate. Taking into account the discretized form of the kinetic (3.17) and the strain energy (3.15) in absence of external loads the stationarity condition (3.19) gives the equation of motion

$$\frac{d}{dt}\left(\frac{\partial T}{\partial \dot{\boldsymbol{v}}^T}\right) + \frac{\partial U}{\partial \boldsymbol{v}^T} = 0 \tag{3.20}$$

Substituting here the expressions (3.15) and (3.16) one can obtain the equation of motion of the structure in absence of the external loads

$$\boldsymbol{M}\ddot{\boldsymbol{v}}(t) + \boldsymbol{K}\boldsymbol{v}(t) = 0 \tag{3.21}$$

For the harmonic oscillations all nodal points perform a sinusoidal periodic motions

$$\boldsymbol{v}(t) = \boldsymbol{v}_0 \sin(\omega t) \tag{3.22}$$

Here $\boldsymbol{v}_0$ is the amplitude of harmonic oscilations and ω is a frequency of oscilations. Substituting the expression (3.22) into equation of motion (3.21) the frequency equation can be obtained

$$\boldsymbol{K}\boldsymbol{v}_0 - \omega^2 \boldsymbol{M}\boldsymbol{v}_0 = 0 \tag{3.23}$$

Solution of this equation is solution of the eigenvalue problem

$$\boldsymbol{K}\boldsymbol{v}_0 = \lambda \boldsymbol{M}\boldsymbol{v}_0 \tag{3.24}$$

Here $\lambda = \omega^2$. Solution of this equation gives the eigenvalues λ_n, natural frequencies $\omega_n = \sqrt{\lambda_n}$ and corresponding eigenmodes Φ_n. Eigenvalues and eigenmodes must satisfy the equation (3.24)

$$\boldsymbol{K}\boldsymbol{\Phi}_n = \lambda_n \boldsymbol{M}\boldsymbol{\Phi}_n \tag{3.25}$$

The eigenvalue problem (3.24) can be solved by various numerical methods, for example, by the Jacobi, by the Lanczos' or by the subspace iteration method. In the vibration analysis of structures by the finite element method mainly the Lanczos' or the subspace iteration methods are used. In this section an examples of frequency analysis for the beams are solved by using the subspace iteration method. This effective iteration method gives the first n_f frequencies $\omega_n (n = 1, 2, ..., n_f)$, where n_f is chosen number of frequencies to be calculated. Details of the subspace iteration method was outlined in textbook [5].

3.3 Numerical Examples

Three groups of laminated composite or sandwich beams can be analysed. The first group is a short beams. For this group by convention the beam length L to height h ratio is $L/h \leq 10$. The second group by convention is beams of moderate thickness $100 \leq L/h \leq 10$, and the third group is the thin beams $L/h \geq 100$. In order to evaluate the limits of the models (Timoshenko's beam or classical Bernoulli- Euler's beam model) to be used in the frequency analysis numerical examples of laminated composite and sandwich beams are considered.

Further the following notations are used to characterize the boundary conditions of the beam. Notation S means a simple support with the boundary condition

$$w = 0$$

Notation C means clamped end with the boundary conditions

$$w = 0, \quad \gamma_x = 0$$

Notation F means free end of the beam, where the bending moment and the shear force is zero

$$M_x = 0, \quad Q_x = 0$$

So, the notation SS means a simply supported beam, the notation CC means a clamped-clamped beam, the notation CS is used for the clamped- simply supported beam, and the notation CF is used for the cantilever beam with one clamped and one free end.

3.3.1 Vibrations of simply-supported unidirectionally reinforced graphite-epoxy beam

Let us consider a simply-supported unidirectionally reinforced graphite-epoxy beam, for which the material properties are given by

$$\begin{aligned} E_1 = 14.48 * 10^{10} \text{ Pa}, \quad E_2 = 0.965 * 10^{10} \text{ Pa}, \\ G_{23} = 0.345 * 10^{10} \text{ Pa}, \quad G_{12} = G_{13} = 0.414 * 10^{10} \text{ Pa}, \\ \nu_{12} = 0.25, \quad \rho = 1390 \text{ kg/m}^3 \end{aligned} \tag{3.26}$$

Here the axis 1 is in the fibre direction and axes 2, 3 are in the transverse direction.

The beam is considered of unit width ($b = 1$ m). Two beams are considered. The first is relatively short beam ($L/h = 15, h = 1$ m$, L = 15$ m) and the second is thin beam ($L/h = 120, h = 0.125$ m$, L = 15$ m). Since the beams to be calculated are macro homogeneous (there is only one layer) the shear correction coefficient is the same as for isotropic beam, i.e. $k = 5/6$ (see formula (1.40)).

Natural frequencies for this numerical example are calculated in three different ways. Firstly, the analytical formula (3.10) obtained on the basis of Timoshenko's beam theory is used. Note that in this formula the rotatory inertia was neglected. Secondly, the frequencies are calculated by using the formula (3.11), which represents the classical Bernoulli-Euler's beam theory.

n	Analytical solution $f^{\mathrm{T}}_{\mathrm{anal}}$, Hz	$f^{\mathrm{cl}}_{\mathrm{anal}}$, Hz	Finite element $SI12$ $f^{\mathrm{T}}_{\mathrm{FEM}}$, Hz
1	19.2	20.6	18.8
2	64.8	82.4	62.0
3	120.0	185.3	112.8
4	177.1	329.4	164.7
*	-	-	170.1
5	233.9	514.7	216.3

Table 3.1: Natural frequencies f [Hz] of simply-supported unidirectional $[0^0]$ graphite-epoxy beam with $L/h = 15$

n	Analytical solution $f^{\mathrm{T}}_{\mathrm{anal}}$, Hz	$f^{\mathrm{cl}}_{\mathrm{anal}}$, Hz	Finite element $SI12$ $f^{\mathrm{T}}_{\mathrm{FEM}}$, Hz
1	2.57	2.57	2.57
2	10.23	10.28	10.22
3	22.88	23.13	22.82
4	40.35	41.11	40.17
5	62.40	64.24	61.98

Table 3.2: Natural frequencies f [Hz] of simply-supported unidirectional $[0^0]$ graphyte-epoxy beam with $L/h = 120$

Finally, the vibrations of the beam is analysed by the finite element method using the finite element $SI12$. The frequency equation (3.23) was solved by using the subspace iteration method. Results of the frequency analysis for $L/h = 15$ are presented in Table 3.1.

In Table 3.1 the notation (*) means that the fifth frequency corresponds to the extensional mode. Other frequencies presented in Table 3.1 correspond to the flexural modes with the wavenumber n. It is seen that the frequencies obtained by the finite element method are lower than analytical, because in the finite element solution rotatory inertia is taken into account. In the analytical solution $f^{\mathrm{T}}_{\mathrm{anal}}$ rotatory inertia was neglected. The classical Bernoulli-Euler's beam theory gives satisfactory estimation only for the first frequency. For the higher frequencies the differences of the results obtained by Timoshenko's and classical theories are significant.

Results of the frequency analysis for thin beam ($L/h = 120$) are presented in Table 3.2.

From analysis of the results presented in Table 3.2 it is seen that for thin

beams the classical theory gives good results even for the higher frequencies.

3.3.2 Vibrations of cross-ply graphite-epoxy beam

Let us consider the symmetric cross-ply $[0^0/90^0/90^0/0^0]$ laminated graphite-epoxy beam. Material properties are the same as in the previous example (see (3.26)). Relatively short beam is considered ($L/h = 15,\ h = 1\ m,\ b = 1\ m$). Cross section of this beam with symmetric layer stacking sequence is presented in Figure 3.2.

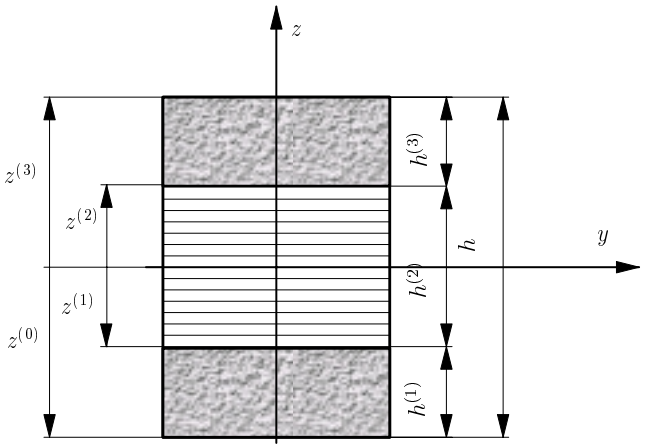

Figure 3.2: Cross section of the cross-ply $[0^0/90^0/90^0/0^0]$ graphite-epoxy beam

Solution for the simply-supported (SS) beam is obtained by two methods - anlytical and FEM. For analytical solution the formula (3.10) is used. A shear correction coefficient was calculated by the Reissner's method (see formula (1.39)) and the value $k = 0.825$ was obtained. This value of the shear correction coefficient is used in the analtical formula (3.10) for calculation of the effective transverse shear stiffness kQ_{55}.

The second solution is obtained by using the finite element $SI20$ based on the broken line (zig-zag) model. In this case the shear correction coefficient is not necessary to use, since the broken line model represents a non-homogeneous transverse shear deformations over the height of cross section of the beam.

Results of the frequency analysis for this cross-ply simply supported beam ($L/h = 15$) are presented in Table 3.3.

From analysis of the results presented in Table 3.3 it is seen that the model based on Timoshenko's hypothesis for the whole stack of layers with

n	Analytical solution $f^{\mathrm{T}}_{\mathrm{anal}}$, Hz	Finite element $SI12$ $f^{\mathrm{T}}_{\mathrm{FEM}}$, Hz
1	18.07	17.73
2	61.31	58.53
3	113.85	101.20
4	168.30	144.50
5	222.51	160.75

Table 3.3: Natural frequencies f [Hz] of simply-supported cross-ply $[0^0/90^0/90^0/0^0]$ graphite-epoxy beam $(L/h = 15)$

	1	2	3	Extensional mode	4	5
SS	17.73	58.53	101.2	-	114.5	160.8
CC	32.18	71.30	117.1	-	165.4	215.8
CS	24.84	65.62	112.9	121.6	162.7	213.3
CF	6.61	34.3	79.1	120.2	130.6	179.5

Table 3.4: Natural frequencies f [Hz] of cross-ply $[0^0/90^0/90^0/0^0]$ graphite-epoxy beam $(L/h = 15)$ under various boundary conditions

additional shear correction (the so called single layer theory) gives a good estimation for the first two frequencies. For higher frequencies a more accurate broken line model must be used.

It is of interest to estimate the influence of boundary conditions on natural frequencies of the beam. In Table 3.4 the first five frequencies of the cross-ply laminated beams with four different boundary conditions are presented. Results was obtained by using the finite element $SI20$.

From analysis of the results presented in Table 3.4 it is seen that for the lower frequencies there are significant influence of boundary conditions. For higher frequencies the influence of boundary conditions is smaller. For thin beams in the higher frequency range the influence of boundary conditions is insignificant.

3.3.3 Vibrations of simply-supported sandwich beam

Let us consider the frequency analysis of simply-supported symmetric sandwich beam. Two beams are considered. The first beam is with thin faces and with very soft core. Face sheets are made from aluminium alloy and the core is made from polymer foam material. The properties of materials and

geometry of this beam ($L/h = 11.83$) are as follows (see [8])

$$\begin{aligned} L = 1.08 \text{ m}, \quad b = 0.1 \text{ m}, \quad h = 8.45 * 10^{-2} \text{ m}, \\ h_2 = 8.02 * 10^{-2} \text{ m}, \quad h_1 = h_3 = 0.215 * 10^{-2} \text{ m}, \\ E_1 = E_3 = 7.1 * 10^4 \text{ MPa}, \quad E_2 = 22 \text{ MPa}, \\ \nu_1 = \nu_2 = \nu_3 = 0.315, \\ \rho_1 = \rho_3 = 2700 \text{ kg/m}^3, \ \rho_2 = 40 \text{ kg/m}^3, \\ k_{\text{Reuss}} = 0.637 * 10^{-2}, \quad k_{\text{Reissner}} = 0.602 * 10^{-2} \end{aligned} \tag{3.27}$$

Here the shear correction coefficient for the Reuss's method k_{Reuss} was calculated by the formula (1.45) and for the Reissner's method k_{Reissner} by the formula (1.39).

The second beam is considered with thicker face sheets and with stiffer core. The input data for this beam ($L/h = 16.1$) are given by (see ref. [8])

$$\begin{aligned} L = 0.633 \text{ m}, \quad b = 0.1 \text{ m}, \quad h = 3.93 * 10^{-2} \text{ m}, \\ h_2 = 1.89 * 10^{-2} \text{ m}, \quad h_1 = h_3 = 1.02 * 10^{-2} \text{ m}, \\ E_1 = E_3 = 7.1 * 10^4 \text{ MPa}, \quad E_2 = 3900 \text{ MPa}, \\ \nu_1 = \nu_2 = \nu_3 = 0.315, \\ \rho_1 = \rho_3 = 2700 \text{ kg/m}^3, \quad \rho_2 = 1250 \text{ kg/m}^3, \\ k_{\text{Reuss}} = 0.197, \quad k_{\text{Reissner}} = 0.120 \end{aligned} \tag{3.28}$$

Both beams were calculated by two methods - the analytical and the FEM. The first is Ritz's method. For the simply-supported beam the analytical solution (3.10) was obtained. In this formula the shear correction coefficient was used to take into account a non-homogeneous distribution of the transverse shear strains. It should be noted that in sandwich beam the transverse shear strain and stress distribution is strongly non-homogeneous.

The same analytical formula (3.10) can be used to calculate the frequencies based on the theory of sandwich beams with very thin faces and with very soft core. This theory was outlined in the section 1.5. According this theory in the formula (3.10) the bending stiffness of the sandwich beam D_{11}, the transverse shear stiffness of the beam kQ_{55} and the density ρ_0 of the beam are given by

$$\begin{aligned} kQ_{55} = bh_cG_c, \quad \rho_0 = b(\rho_c h_c + 2\rho_f h_f), \\ D_{11} = 2bh_f h_0^2 E_f, \quad h_0^2 = \frac{1}{4}(h_c + h_f)^2 \end{aligned} \tag{3.29}$$

Substituting these expressions into formula (3.10) the formula to calculate the natural frequencies ω_n^{s} of the simply supported sandwich beams with thin

faces can be written as follows

$$(\omega_n^{\rm s})^2 = \frac{\dfrac{2h_f h_0^2 E_f}{\rho_c h_c + 2\rho_f h_f}\left(\dfrac{n\pi}{L}\right)^4}{\left[1+\left(\dfrac{n\pi}{L}\right)^2 \dfrac{2h_f h_0^2 E_f}{h_c G_c}\right]} \tag{3.30}$$

This formula can be used only for the first sandwich beam with very thin faces ($h/h_f = 39.3$). The parameters of this beam was given by the formulae (3.27). According notations of the formula (3.30) for the sandwich beams with very thin faces the parameters of the first beam are given by

$$\begin{aligned} L = 1.08 \text{ m}, \quad b = 0.1 \text{ m}, \quad h_f = 0.215 * 10^{-2} \text{ m}, \\ h_c = 8.02 * 10^{-2} \text{ m}, E_f = 7.1 * 10^4 \text{ MPa}, \\ E_c = 22 \text{ MPa}, \quad \nu_c = 0.315, \\ G_c = \frac{E_c}{2(1+\nu_c)} = 8.4 \text{ MPa}, \\ \rho_f = 2700 \text{ kg/m}^3, \quad \rho_c = 40 \text{ kg/m}^3, \\ h_0^2 = \frac{1}{4}(h_c + h_f)^2 = 17 * 10^{-4} \text{ m}^2 \end{aligned} \tag{3.31}$$

The results of calculations by the formula (3.30) for the first sandwich beam are presented in the fourth column of Table 3.4. The frequencies of the second sandwich beam (3.28) can not be calculated by the formula (3.30) since the faces of this beam are too thick ($h/h_f = 3.85$) to use the assumption of the membrane stress state in the faces.

The second method for the frequency analysis of the sandwich beam is the finite element method. For the sandwich beams appropriate is the finite element $SI20$ based on broken line model. In the present example beam is divided by $N = 15$ finite elements. Frequency equation (3.23) is solved by the subspace iteration method.

In the analytical solution simply-supported SS beam means that on the supports the boundary conditions are given by

$$w\Big|_{x=0} = 0, \quad w\Big|_{x=L} = 0 \tag{3.32}$$

In the finite element solution by using the finite element $SI20$ there are two possibilities to represent the boundary conditions, which are close to the simply-supported beam boundary conditions. The first possibility is the so called $S1S1$ boundary conditions

$$w\Big|_{x=0} = 0, \quad w\Big|_{x=L} = 0, \tag{3.33}$$

Mode n	Reuss(SS) Anal.	Reissner(SS) Anal.	Thin f. (SS) Anal.	S1S2 SI20	S1S1 SI20	Class.(SS) Anal.
1	96.0	93.9	92.1	87.5	90.8	252
2	203	198	194.3	184	186	1008
3	308	301	294	278	283	2268
4	413	402	393	376	380	4032
5	517	504	493	444	481	6301

Table 3.5: Natural frequencies f [Hz] of simply-supported sandwich beam with very soft core (3.27)

$$u_{(1)}\Big|_{x=0} = 0, \quad u_{(1)}\Big|_{x=L} = 0,$$
$$u_{(3)}\Big|_{x=0} = 0, \quad u_{(3)}\Big|_{x=L} = 0$$

In this case on both supports the axial displacements u are restricted in the bottom (layer 1) and top (layer 3) layers. The second type of boundary conditions is the so called $S1S2$ boundary conditions

$$w\Big|_{x=0} = 0, \quad w\Big|_{x=L} = 0, \tag{3.34}$$
$$u_{(1)}\Big|_{x=0} = 0, \quad u_{(3)}\Big|_{x=0} = 0$$

In this case the axial displacements u for the both face sheets are restricted only on the left support.

In all three cases of boundary conditions (3.32)-(3.35) the rotations γ_x in all three layers are free. The difference of the single beam boundary conditions (3.32) and the compound beam boundary conditions (3.34) and (3.35) is in the fact that axial displacemnts in the case of single beam are restricted only at the beam axis, while for the compound beam the axial displacements are constrained at the top and bottom layers.

Results of frequency analysis of the first sandwich beam with very soft core (3.27) are presented in Table 3.5. Results also are presented in the Figure 3.3, where the experimental frequencies were obtained in [8].

For comparison in Table 3.5 the frequencies calculated by formula (3.11) obtained by the classical (Class.) Bernoulli-Euler's beam theory also are presented.

Results of the frequency analysis for the second sandwich beam with more stiff core (3.28) are presented in Table 3.6. Results also are presented in Figure 3.4, where the experimental frequencies were obtained in [8].

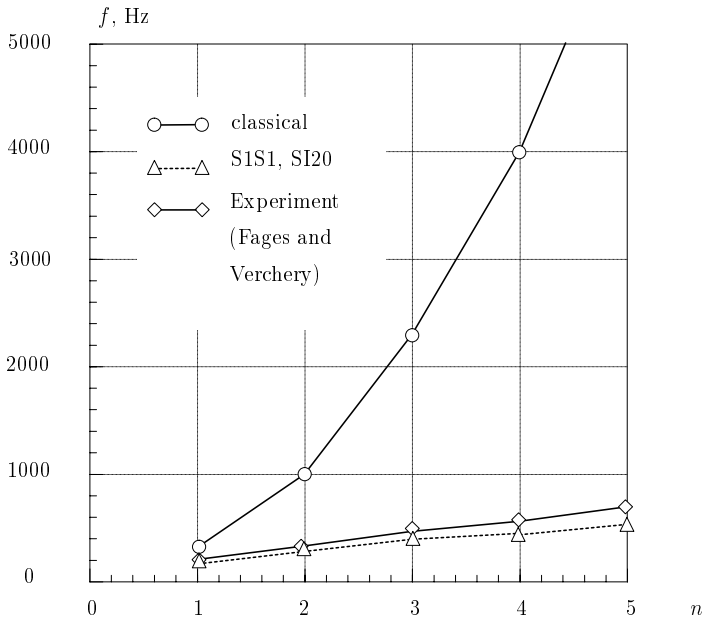

Figure 3.3: Experimental and theoretical frequencies for the first sandwich beam with very soft core (3.27)

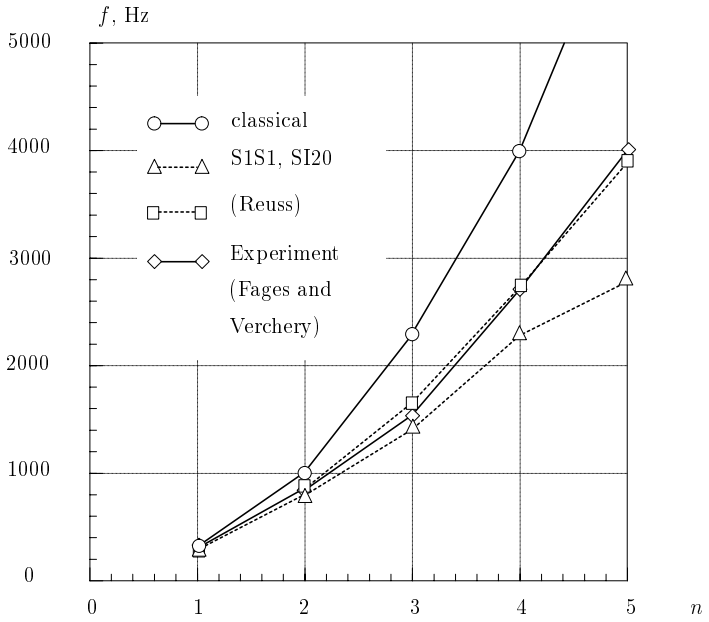

Figure 3.4: Experimental and theoretical frequencies for the second sandwich beam with more stiff core (3.28)

Mode n	Reuss(SS) Anal.	Reissner(SS) Anal.	S1S2 SI20	S1S1 SI20	Class. (SS) Anal.
1	242	237	233	292	250
2	886	830	794	800	1002
3	1768	1584	1425	1551	2254
4	2758	2385	2297	2223	4008
5	3786	3193	-	2795	6262

Table 3.6: Natural frequencies f [Hz] of simply-supported sandwich beam with more stiff core (3.28)

From the results presented in Tables 3.4 and 3.6 it is seen that frequencies calculated by the single layer Timoshenko's beam theory by using the Reuss or the Reissner's method for estimation of the shear correction coefficient for the first three frequencies are in good agreement with the results obtained by more complex broken line (zig-zag) model. However, for the higher frequencies there are some differences. For the sandwich beams with very soft core the classical Bernoulli-Euler's beam theory can not be used. For the sandwich beams with relatively stiff core with $(L/h \geq 15)$ the classical beam theory can be used only to estimate the first frequency. For calculations of higher frequencies of sandwich beams the classical theory can not be used.

Chapter 4

Damping the vibrations

Damping is a significant dynamic parameter for the noise and vibration control as well as the impact resistance for the structures. Composites with polymer matrix have more high damping properties than metal alloys, for example, steel or aluminium alloys. It is due to fact that constituents of the composites, fibres and matrix, offer higher damping properties than metals. In the glass or carbon (graphite) fibres the damping is relatively small. More high damping is observed for aramid (Kevlar) fibres. Polymer resins (matrix), for example, epoxy or polyester, offer more high damping than fibres.

For the noise and vibration control it is necessary to have more high damping of the structures as those, which offer polymer composites. For this special damping layers made from various viscoelastic materials are widely applied for structures subjected to dynamic loading, especially those used in the ship-building or in aerospace technology.

In Figure 4.1 there are presented some possible designs of structures with special damping layers. The first design (Figure 4.1, structure 1) is the structure, for example, steel structure, covered with the viscoelastic layer made from material having high damping properties. Such design often is used in automotive industry to reduce vibrations of structural members of cars in order to protect the car drivers and passengers against noise. Similar design often is used also in the ship-building.

The second design (see Figure 4.1, structure 2) is when the basic structure (basic layer) is covered with a viscoelastic damping layer and further this damping layer is covered with a thin constraining layer. Such design is a typical non-symmetric sandwich structure, which mainly is used in aerospace technology.

The third design (see Figure 4.1, structure 3) is when the basic structure (basic layer) is covered with a honeycomb core and at the top with more stiff damping layer from the viscoelastic polymer material. Such design also is

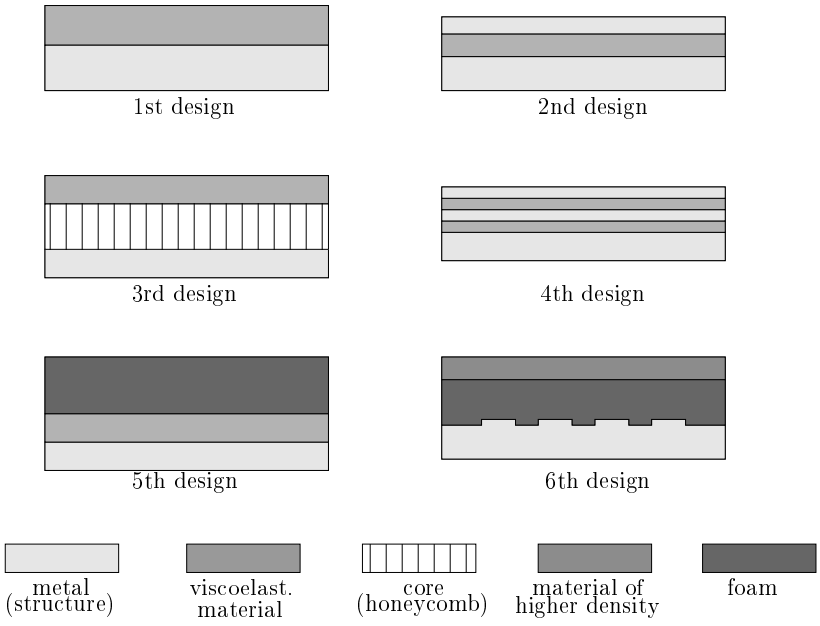

Figure 4.1: Structures with damping layers

used in aerospace technology.

The fourth design (see Figure 4.1, structure 4) is when the basic structure (basic layer) is covered with several viscoelastic layers. Between these damping layers are included thin layers of stiff material. Such design can be used, for example, in the vibration control devices.

The fifth design (see Figure 4.1, structure 5) is when then basic structure (basic layer) is covered with more stiff viscoelastic polymer layer and at the top this layer is covered with very soft foam material. Such design can be used, for example, in the noise control.

The sixth design (see Figure 4.1, structure 6) is when the basic structure (basic layer) is covered with the soft core made from the foam material and then this core is covered with more stiff laminated composite material. Such design can be used, for example, in the civil engineering.

All structures with the damping layers presented in Figure 4.1 can be used in the design of beams, plates and shells. In the present chapter beams with damping layers are analysed. Beams having the structure presented in Figure 4.1 can be analysed by using the Timoshenko's beam theory and the broken line (zig-zag) model, which were outlined in the chapter 1. The only difference is that in the chapter 1 the Hooke's law was used in order to describe the linear elastic behaviour of the material. However, the damp-

ing layers have viscoelastic properties and in order to describe the material behaviour another constitutive law must be used. TMaterial models for the damping layers will be outlined in the next section.

4.1 Models of Materials with Damping

Damping is one of the most difficult issues to deal with in the structural dynamics. Introducing the damping data into the finite element model described in chapter 1 is rather easy. The real problem is how to determine a reasonable values for the damping data.

In order to explain the damping in structures let us consider a simply supported beam under steady-state sinusoidal exitation force $P(t) = P_0 \sin \Omega t$ (see Figure 4.2).

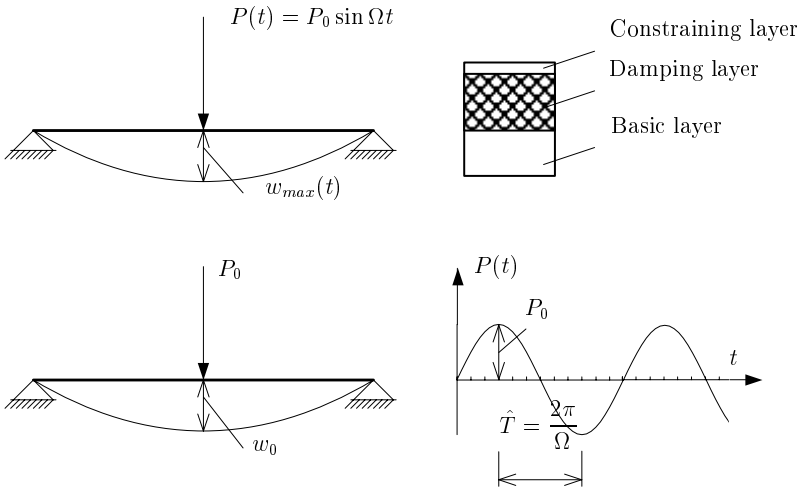

Figure 4.2: Simply-supported beam under steady-state exitation

A cross-section of the beam consists of elastic basic layer, viscoelastic damping layer, and a thin elastic constraining layer. If the amplitude P_0 of the dynamic load is applied as static load then the deflection of the beam is w_0. Under dynamic loading the beam offer harmonic oscilations with the frequency Ω of the exitation force. If $\Omega = \omega_n$, where $\omega_n (n = 1, 2, ...)$ is natural frequencies of the beam, there is a resonanse. If the maximum deflection at the resonant frequency is $w_{\max}$, the resonant magnification factor (RMF) can be defined as

$$RMF = \frac{w_{\max}}{w_0} \tag{4.1}$$

The quantities to measure RMF can be not only displacement, but also velocity, acceleration, stress, or strain. These quantities are named as response. The higher is damping the smaller is RMF of the response characteristics (see Figure 4.3). Note that in the literature about dynamics of structures RMF also is called Q-factor.

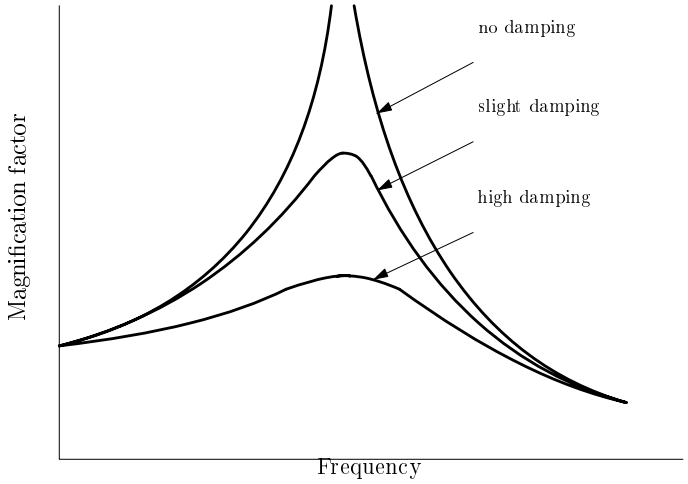

Figure 4.3: Effects of damping on resonant magnification factor

If the exitation force $P(t)$ is canceled then the beam some period of time can continue to vibrate. This is the so called free vibrations. Elastic systems (without damping) after exitation can vibrate without the time limit. Actually, all structures and materials more or less have some damping and the structures after exitation is canceled can vibrate only limited time period, i.e. the motions of the structure are damped out. Elastic free vibrations (without damping) of sandwich and laminated composite beams was analysed in chapter 3.

In linear systems with damping the free vibrations decay exponentially (see Figure 4.4). The higher is damping, the faster is the decay.

The decay can be measured with logarithmic decrement δ, which is defined as follows

$$\delta = \ln\left(\frac{a_i}{a_{i+1}}\right) \tag{4.2}$$

Here a_i and a_{i+1} are the amplitudes of displacements (or stresses, strains e.t.c) in the ith and $(i+1)$th cycles, respectively.

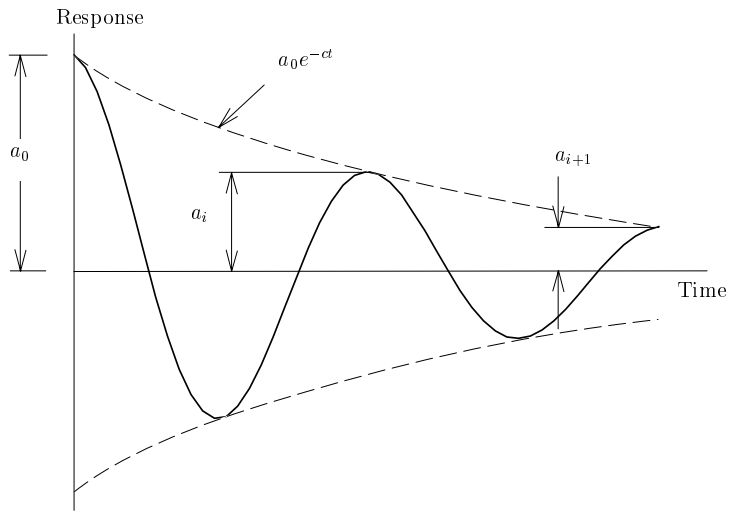

Figure 4.4: Exponential decay

The logarithmic decrement δ and the resonant magnification factor (RMF) are dependent not only on the damping properties of the material, but also on the structural system configuration. For example, for the structure presented in Figure 4.2 the decay (damping of structure) can be increased when constraining layer is taken more thin and other parameters of the beam remain the same. So, damping of the structure and damping in the material is not the same. For the given damping of material the damping of structure can be designed, for example, by changing the layer stacking sequence or thickness of the layers.

There are some kinds of damping that occur in the structures. Following is a brief classification of the kinds of damping in the structures.

The first kind of damping is material damping or internal damping. Internal damping refers to various microscopic phenomena including magnetic effects (magnetoelastic hysteresis), thermal effects (thermoelastic phenomena), and atomic reconstruction (dislocations, stress relaxation at grain boundaries e.t.c). More information about the damping can be found in the literature (see refs [9, 10]).

Energy dissipation in the case of internal damping occurs in the material, therefore this kind of damping is called internal. Typical internal damping is viscoelastic damping of the polymer materials. Briefly this kind of damping will be discussed below. Note that material damping or internal damping also is called structural damping or hysteretic damping.

The second kind of damping is external damping, which represents a

various energy dissipation mechanisms that are external to the structural material itself. In this group mostly used is concept of viscous damping in which damping force P_d are proportional to velocity $\dot{x}$

$$P_d = -C\dot{x}$$

To illustrate the viscous damping often a dashpot is used (see Figure 4.5).

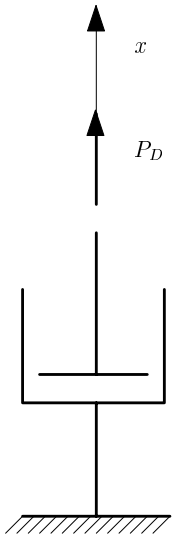

Figure 4.5: Viscous damping

The viscous damping model with one degree of freedom often is used in the textbooks of dynamics of structure to illustrate the damping phenomena. This simple model is often used because it leads to relatively simple mathematics. Aerodinamic damping or damping due to the fluid-structure interaction also falls under the kind of viscous damping. However, in some cases the viscous damping model is not an accurate model of many real-world devices.

The other kind of external damping is frictional damping or the so called Coulomb's damping. The frictional damping is due to the motion of two contacting surfaces. The friction forces appear from the motion and may be idealised by a shear force T which is proportional to the normal force P and opposite in direction to the velocity $\dot{x}$

$$T = -\mu P \tag{4.3}$$

Here μ is coefficient of friction. Below a certain level, friction forces do not cause slip and the contacting surfaces act as single body. When the slip

occurs, a different friction coefficient is observed. In most cases the dynamic coefficient of friction is smaller than the static one. This frictional damping model is used in the solution of dynamic contact problems.

Among the all models discussed above the simplest is viscous damping model. This model is used in the finite element codes to characterise integrally the damping of structure. By using this model the first estimation of the damping in the material or structure can be obtained. Damping in the supports and conections of the structure e.t.c. also can be estimated through the viscous damping model. Parameters for the viscous damping model mostly are obtained from the experiment using the models of structure (beams, plates, shells e.t.c). Details of using the model of viscous damping in the structural analysis were outlined in the textbooks (see, for example, ref. [5]).

Let us consider the model of internal damping which is used for the polymer materials or polymer composites. This is well known model applied for the linear viscoelastic materials. This model is based on the Boltzmann's superposition principle (see ref. [11]).

For simplicity let us consider the one-dimensional case. In this case for the input stress $\sigma(t)$ having arbitrary time history the strain $\varepsilon(t)$ can be calculated by the Boltzmann's superposition integral

$$\varepsilon(t) = \int_{-\infty}^{t} S(t-\tau)\frac{d\sigma(\tau)}{d\tau}\, d\tau \tag{4.4}$$

Here $S(t)$ is the creep compliance. Note that for $t < 0,\ S(t) = 0$. Alternatively, the stress resulting from arbitrary strain input can be calculated by

$$\sigma(t) = \int_{-\infty}^{t} C(t-\tau)\frac{d\varepsilon(\tau)}{d\tau}\, d\tau \tag{4.5}$$

Here $C(t)$ is a relaxation modulus. Note that for $t < 0,\ C(t) = 0$. It should be noted that equations (4.4) and (4.5) for the linear viscoelastic materials are analogous to the Hooke's law for the linear elastic materials.

Further let us consider the vibration of material, i.e. the case of stresses which vary sinusoidally with time by frequency ω

$$\tilde{\sigma}(t) = \sigma_0 e^{i\omega t} \tag{4.6}$$

Here σ_0 is a complex stress amplitude and the suprscript tilde ($\sim$) refers to a sinusoidally varying quantity. Substituting eq. (4.6) into (4.4) one can obtain that the resulting sinusoidally varying strains are given by

$$\tilde{\varepsilon}(t) = \int_{-\infty}^{t} S(t-\tau) i\omega\sigma_0 e^{i\omega t}\, d\tau \tag{4.7}$$

It is convenient to define a new variable $\xi = t - \tau$, so that

$$\tilde{\varepsilon}(t) = \int_{-\infty}^{t} S(\xi) e^{-i\omega\xi} i\omega\sigma_0 e^{i\omega t}\, d\xi \tag{4.8}$$

Terms not involving the functions of ξ may be moved outside the integral, and since $S(t) = 0$ for $t < 0$, the lower limit of the integral can be changed to $-\infty$, so that

$$\tilde{\varepsilon}(t) = i\omega\sigma_0 e^{i\omega t} \int_{-\infty}^{\infty} S(\xi) e^{-i\omega\xi}\, d\xi \tag{4.9}$$

The integral of this equation is just the Fourier transform of the creep compliance, $F[S(\xi)]$, or $S(\omega)$, which can be written as

$$F[S(\xi)] \equiv S(\omega) = \int_{-\infty}^{\infty} S(\xi) e^{-i\omega\xi}\, d\xi \tag{4.10}$$

Thus, the stress-strain relationship reduces to

$$\tilde{\varepsilon}(t) = i\omega\sigma_0 e^{i\omega t} S(\omega) = i\omega S(\omega)\tilde{\sigma}(t) \tag{4.11}$$

In order to obtain this equation in the form close to the Hooke's law, we simply define the frequency domain compliances as follows

$$S^*(\omega) = i\omega S(\omega) \tag{4.12}$$

So, the equation (4.11) becomes

$$\tilde{\varepsilon}(t) = S^*(\omega)\tilde{\sigma}(t) \tag{4.13}$$

Thus, in linear viscoelastic materials the sinusoidally varying stresses are related to the sinusoidally varying strains by the complex compliances in the same way that static stresses and strains are releated by elastic compliances in the linear elastic material. In addition, the time domain compliance $S(t)$ is releated to frequency domain complex compliance $S^*(\omega)$ by the Fourier transform (4.10) and the relation (4.12).

Alternatively, if we substitute sinusoidally varying strain in the equation (4.5), we can obtain that the sinusoidally varying stress are given by

$$\tilde{\sigma}(t) = C^*(\omega)\tilde{\varepsilon}(t) \tag{4.14}$$

where the complex modulus is defined by

$$C^*(\omega) = i\omega C(\omega) \tag{4.15}$$

and $C(\omega)$ is the Fourier transform of the relaxation modulus $C(t)$. Comparison of eqs (4.13) and (4.14) leads that the complex compliance and the complex modulus must be related by $S^*(\omega) = C^*(\omega)^{-1}$.

For the isotropic material as complex modulus, which is used to characterise the material damping properties in tension-compression the complex Young's modulus $E^*(\omega)$ is employed

$$E^*(\omega) = E'(\omega) + iE''(\omega) \tag{4.16}$$

Here $E'(\omega)$ is the storage modulus and $E''(\omega)$ is the loss modulus (or dissipation modulus). In the same manner the damping properties in shear are characterized by the complex shear modulus $G^*(\omega)$

$$G^*(\omega) = G'(\omega) + iG''(\omega) \tag{4.17}$$

For anisotropic materials a stiffness matrix of complex moduli $C^*_{ij}(\omega)$ can be used to characterise the damping properties in various directions

$$C^*_{ij}(\omega) = C'_{ij}(\omega) + iC''_{ij}(\omega) \tag{4.18}$$

Relation (4.16) can be changed in the following manner

$$E^*(\omega) = E'(\omega) + iE''(\omega) = E'(\omega)[1 + i\eta(\omega)] = |E^*(\omega)|e^{-i\gamma(\omega)} \tag{4.19}$$

Here $|E^*(\omega)|$ is modulus of the complex number and $\eta(\omega)$ is the loss factor (also called loss coefficient or damping factor)

$$\eta(\omega) = \frac{E''(\omega)}{E'(\omega)} = \tan[\gamma(\omega)] \tag{4.20}$$

The quantity $\gamma(\omega)$ is called loss angle and characterise the phase lag between $\tilde{\sigma}(t)$ and $\tilde{\varepsilon}(t)$.

Thus, the real part $E'(\omega)$ of the complex modulus is associated with elastic energy storage, whereas the imaginary part $E''(\omega)$ is associated with the energy dissipation, or damping. The concept of the complex modulus and loss angle is presented in Figure 4.6. For larger loss angles the imaginary part of the complex modulus is larger, i.e. the damping of material is higher.

The physical interpretation of the equation (4.20) may be given with the aid of the rotating vector diagram in Figure 4.7.

The stress and strain vectors are both assumed to be rotating with angular velocity ω, and the physical oscilation is generated by either the horizontal or vertical projection of the vectors. The complex exponential representations of the rotating stress and strain vectors in the diagram (see Figure 4.7) are given by

$$\tilde{\sigma}(t) = \sigma_0 e^{i(\omega t+\gamma)}, \quad \tilde{\varepsilon}(t) = \varepsilon_0 e^{i\omega t} \tag{4.21}$$

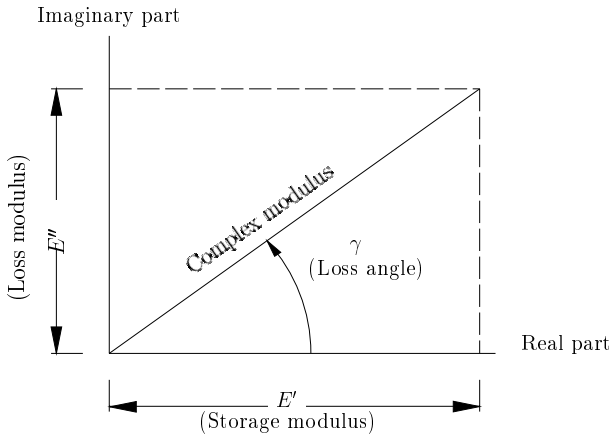

Figure 4.6: Concept of complex modulus and loss angle

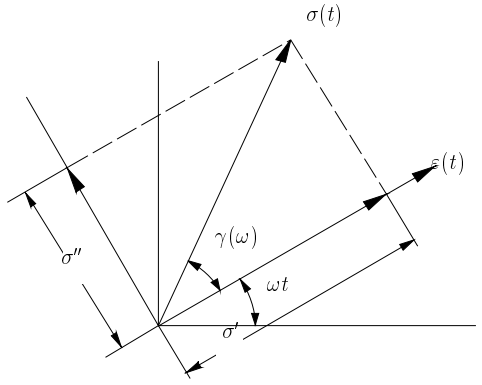

Figure 4.7: Rotating vector diagram for physical interpretation of complex modulus

In this case the one-dimensional complex modulus $E^*(\omega)$ is defined by

$$E^*(\omega) = \frac{\tilde{\sigma}(t)}{\tilde{\varepsilon}(t)} = \frac{\sigma_0 e^{i\gamma}}{\varepsilon_0} = \frac{\sigma_0}{\varepsilon_0}(\cos\gamma + i\sin\gamma) = \tag{4.22}$$
$$= \frac{\sigma_0'}{\varepsilon_0} + i\frac{\sigma_0''}{\varepsilon_0} = E'(\omega) + iE''(\omega) = E'(\omega)[1 + i\eta(\omega)]$$

It is seen that the strain lags the stress by the phase angle γ. The storage modulus $E'(\omega)$ is the in-phase component of the stress σ_0' divided by the strain ε_0. The loss modulus $E''(\omega)$ is the out-of-phase component of stress σ_0'' divided by the strain ε_0. The loss factor $\eta(\omega)$ is the tangent of the phase angle γ. Experimental determination of the complex modulus involves the

measurment of the storage modulus $E'(\omega)$ and the loss factor $\eta(\omega)$ as a function of frequency ω. Several techniques for doing this were described in ref. [12].

The inverse Fourier transform of the parameter $S(\omega)$ defined by the equation (4.10) is the creep compliance $S(t)$ as given by

$$F^{-1}[S(\omega)] \equiv S(t) = \frac{1}{2\pi}\int_{-\infty}^{\infty} S(\omega)e^{i\omega t}\, d\omega \tag{4.23}$$

where $F^{-1}[\ ]$ is the operator of inverse Fourier transform. Equations (4.10) and (4.23) form the so called Fourier transform pair, which make it possible to transform back and forth between the time domain and frequency domain. Inverse Fourier transforms have been used to estimate the time domain creep behaviour of the polymer and polymer composite materials from frequency domain complex modulus data obtained from vibration tests.

Damping properties of the material can be characterized in the terms of dissipated energy per one cycle of vibrations. To illustrate this for simplicity we assume frequency independent complex modulus $E^* = E' + iE''$. In this case constitutive equation (4.14) can be written as

$$\tilde{\sigma}(t) = (E^* \equiv E' + iE'')\tilde{\varepsilon}(t) \tag{4.24}$$

Taking into account that strains are varying sinusoidally

$$\tilde{\varepsilon}(t) = \varepsilon_0 e^{i\omega t} \tag{4.25}$$

the equation (4.24) can be written as follows

$$\tilde{\sigma}(t) = E'\tilde{\varepsilon}(t) + \frac{E''}{\omega}\frac{d\tilde{\varepsilon}(t)}{dt} \tag{4.26}$$

For further rearrangig of the constitutive equation the following formulae are employed

$$\frac{1}{\cos\gamma} = \sqrt{1+\tan^2\gamma} = \sqrt{1+\eta^2}, \tag{4.27}$$
$$\sin(\omega t+\gamma) = \sin\omega t\cos\gamma + \cos\omega t\sin\gamma$$

Sinusoidally varying strains can be represented not only in the complex form (4.25), but also in the following form

$$\tilde{\varepsilon}(t) = \varepsilon_0 \sin\omega t \tag{4.28}$$

Taking into account this and previous expression as well as eq. (4.20) the eq. (4.26) can be written as

$$\begin{aligned}\tilde{\sigma}(t) &= E'\varepsilon_0\sin\omega t + E''\varepsilon_0\cos\omega t = \\ &= E'\varepsilon_0\sin(\omega t+\gamma)\sqrt{1+\eta^2}\end{aligned} \tag{4.29}$$

This equation can be plotted in the coordinates $\tilde{\sigma}(t)$ against $\tilde{\varepsilon}(t)$. The graph $\tilde{\sigma}(t)$ versus $\tilde{\varepsilon}(t)$ is a closed loop called a hysteresis loop. It is illustrated in Figure 4.8.

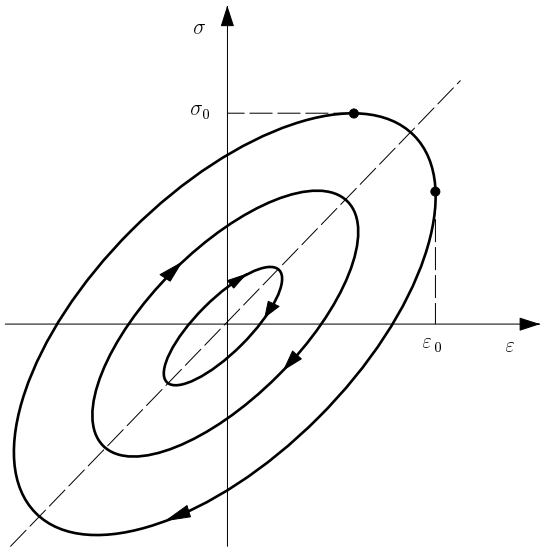

Figure 4.8: Hysteretic damping

The loop is of elliptical shape. Equation of the ellipse in coordinates $\tilde{\sigma}(t)$ and $\tilde{\varepsilon}(t)$ can be obtained by using formulae

$$\frac{\tilde{\varepsilon}(t)}{\varepsilon_0} = \sin\omega t, \tag{4.30}$$

$$\varepsilon_0 \cos\omega t = \pm\sqrt{1-\sin^2\omega t} = \pm\sqrt{\varepsilon_0^2 - \tilde{\varepsilon}(t)^2}$$

Taking into account this relations the equation (4.29) can be rearranged as follows

$$\tilde{\sigma}(t) = E'\tilde{\varepsilon}(t) \pm E''\sqrt{\varepsilon_0^2 - \tilde{\varepsilon}(t)^2} \tag{4.31}$$

Here for positive motion with the angular velocity ω only (+) sign can be used

$$\tilde{\sigma}(t) = E'\tilde{\varepsilon}(t) + E''\sqrt{\varepsilon_0^2 - \tilde{\varepsilon}(t)^2} \tag{4.32}$$

It is seen that this equation describes the elliptical hysteresis loop. The hysteresis loop is representation of steady state cyclic behaviour, i.e. the stress and strain vectors are rotating with the angular velocity ω so, that

in the material there is periodic motion with the period $T = 2\pi/\omega$. In the period T of one cycle one loop is closed.

It is of interest to calculate the energy dissipation ΔU per one cycle of vibrations. The energy dissipation is area of the hysteresis loop

$$\Delta U = \oint \tilde{\sigma} d\tilde{\varepsilon} = \int_0^{2\pi/\omega} \tilde{\sigma} \frac{d\tilde{\varepsilon}}{dt} dt = \tag{4.33}$$
$$= \int_0^{2\pi/\omega} (E'\varepsilon_0 \sin\omega t + \eta E'\varepsilon_0 \cos\omega t)\omega\varepsilon_0 \cos\omega t \; dt =$$
$$= \eta E'\varepsilon_0^2 \omega \int_0^{2\pi/\omega} \cos^2 \omega t \; dt = \pi\eta E'\varepsilon_0^2$$

In reality for the polymer and polymer composite materials the hysteresis loops determined experimentally are not of elliptical shape (see Figure 4.9). They have rather sharp corners at both ends and are nearly linear at the low-stress, low-strain region.

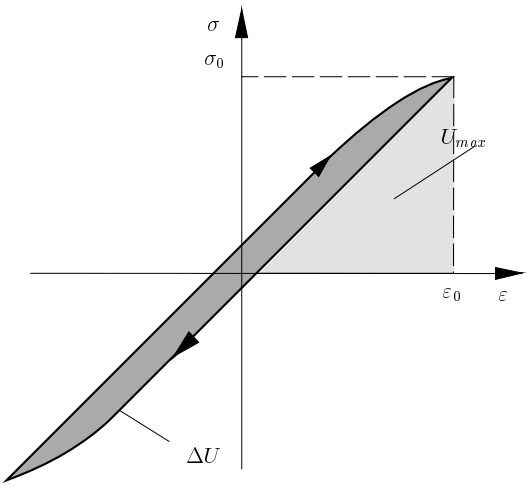

Figure 4.9: Hysteresis loop for polymer material and definition of specific damping capacity

Maximum of the stored elastic strain energy U in the one cycle of vibrations can be defined as

$$U = \frac{1}{2}\sigma_0\varepsilon_0 = \frac{1}{2}E'\varepsilon_0^2 \tag{4.34}$$

A specific damping capacity ψ is defined as ratio of dissipated energy ΔU (4.34) per one cycle of vibrations to the maximum stored elastic energy U (4.34)

$$\psi = \frac{\Delta U}{U} = 2\pi\eta \tag{4.35}$$

From this relation the loss factor in terms of energy can be calculated

$$\eta = \frac{\psi}{2\pi} = \frac{\Delta U}{2\pi U} \tag{4.36}$$

So, to characterize damping of the viscoelastic material we have some quantities - the logarithmic decrement δ (4.2), the loss factor η (4.20), the loss angle γ (4.20) and the specific damping capacity ψ (4.35). All these quantities are related by the expression

$$\eta = \frac{\delta}{\pi} = \frac{\psi}{2\pi} = \tan\gamma \tag{4.37}$$

Various techniques are used to determine these quantities experimentally (see, for example, ref. [9]). These material properties can be used in the analysis of structures performing the harmonic oscillations. Further in this textbook on the basis of model outlined above the damping analysis is carried out, i.e. on the basis of the complex modulus theory or the so called hysteretic damping model. This model better than other models, for example, viscous damping model, represents the damping properties of the polymer and polymer composite materials.

4.2 Finite Element Analysis of Damping

In the case when some constituents of the composite structure (fibres, matrix or single layers) are made from the viscoelastic material with damping properties characterised by the complex moduli instead of frequency equation for elastic vibrations (3.23) the frequency equation for damped vibrations should be be employed

$$\boldsymbol{M}\ddot{\boldsymbol{v}}(t) + \boldsymbol{K}^{*}\boldsymbol{v}(t) = 0 \tag{4.38}$$

where $\boldsymbol{K}^{*}$ is a complex stiffness matrix of the structure

$$\boldsymbol{K}^{*} = \boldsymbol{K}' + i\boldsymbol{K}'' \tag{4.39}$$

Here $\boldsymbol{K}'$ is a real part of the stiffness matrix associated with the storage moduli $C'_{ij}(\omega)$, and $\boldsymbol{K}''$ is an imaginary part of the stiffness matrix associated with the loss moduli $C''_{ij}(\omega)$. Note that the mass matrix $\boldsymbol{M}$ in the equation (4.38) is a real matrix. The nodal displacement vector $\boldsymbol{v}$ is complex quantity because the stiffness matrix is complex.

In general for the viscoelastic materials the complex moduli $C^{*}_{ij}(\omega) = C'_{ij}(\omega) + iC''_{ij}(\omega)$ are frequency dependent (see eq. (4.18)). So, the stiffness matrix in the frequency equation (4.38) also is frequency dependent

$$\boldsymbol{M}\ddot{\boldsymbol{v}}(t) + \boldsymbol{K}^{*}(\omega)\boldsymbol{v}(t) = 0 \tag{4.40}$$

It should be noted that in the equations of motion (4.38) or (4.40) the nodal displacements are not arbitrary functions of time but must be assumed only performing the harmonic oscillations in time

$$\boldsymbol{v}(t) = \boldsymbol{v}_0 e^{i\omega t} \tag{4.41}$$

Here $\boldsymbol{v}_0$ is complex amplitudes of the displacement vector. So, the equation of motion in complex form (4.38) or (4.40) can be used only in the case of free harmonic oscillations or for the forced vibrations under harmonic in time exitation force

$$\boldsymbol{M}\ddot{\boldsymbol{v}}(t) + \boldsymbol{K}^*(\omega)\boldsymbol{v}(t) = \boldsymbol{F}(t) \tag{4.42}$$

Here

$$\boldsymbol{F}(t) = \boldsymbol{F}_0 e^{i\Omega t}$$

where Ω is a freguency of the exitation force. Since the complex modulus is defined for the harmonic oscillations, in general the equation (4.42) can not be used in the case, when the loads F(t) are arbitrary, for example, for the transient dynamics problems. However, sometimes eq. (4.42) also is employed for analysis of the response of viscoelastic structures under impact loading.

Substituting eq. (4.41) into the eq. (4.38) one obtains

$$\boldsymbol{K}^*\boldsymbol{v}_0 = \lambda^*\boldsymbol{M}\boldsymbol{v}_0 \tag{4.43}$$

Here $\lambda^* = \omega^{*2}$ is a complex eigenvalue

$$\lambda^* = \lambda' + i\lambda'' \tag{4.44}$$

and ω^* is a complex (damped) eigenfrequency

$$\omega^* = \omega' + i\omega'' \tag{4.45}$$

Substituting eq. (4.41) into the eq. (4.40) one can obtain

$$\boldsymbol{K}^*(\omega)\boldsymbol{v}_0 = \lambda^*\boldsymbol{v}_0 \tag{4.46}$$

There are two cases of damped frequency analysis. The first case is when the material properties are frequency independent. In this case the damped frequencies can be calculated by using equation (4.43). It is a complex linear eigenvalue problem. The second case is when the material properties are frequency dependent. In this case for the frequency analysis we have equation (4.46). Obtaining the solution of eq. (4.46) is more complicated since this is a complex non-linear eigenvalue problem.

In the present textbook we have consider only the damped frequency analysis based on the equation (4.43). So, we have considered a viscoelastic material with frequency independent material damping properties. Even if the material damping properties are frequency dependent, the equation (4.43) can be used. In this case all frequency domain can be divided in the frequency subdomains (bands), in which the material damping properties are frequency independent. In each frequency band the comlex modulus is assumed to be constant

$$E_* = E' + iE'' = const \tag{4.47}$$

For solution of the eigenvalue problem (4.43) the Lanczos' method is used and complex eigenvalues (4.44) are found

$$\lambda_n^* = \lambda_n' + i\lambda_n'', \quad (n = 1, 2, ..., N)$$

Corresponding complex frequencies are calculated by the formula

$$\omega_n^* = \sqrt{\lambda_n^*} \tag{4.48}$$

Here $\omega_n^* = \omega_n' + i\omega_n''$ is nth complex frequency, which is associated with the corresponding complex eigenvector

$$\mathbf{\Phi}_n^* = \mathbf{\Phi}_n' + \mathbf{\Phi}_n'', \quad (n = 1, 2, ..., N)$$

These eigenvectors characterize a damped vibration modes and satisfy the equation (4.43)

$$\boldsymbol{K}^* \mathbf{\Phi}_n^* = \lambda_n^* \boldsymbol{M} \mathbf{\Phi}_n^* \tag{4.49}$$

The damped frequency is a real part ω_n' of the complex frequency.

For each damped vibration mode $\mathbf{\Phi}_n^*$ and corresponding damped frequency ω_n^* the modal loss factor η_n can be calculated

$$\eta_n = \frac{\lambda_n''}{\lambda_n'} \tag{4.50}$$

The modal loss factor also can be determined throgh the complex frequency ω_n^*. For this expression (4.48) can be rearranged

$$\omega_n^* = \sqrt{\lambda_n^*} = \sqrt{\lambda_n'}\sqrt{1 + i\eta_n} \tag{4.51}$$

The square root can be represented in the trigonometric form of a complex number

$$\sqrt{1 + i\eta_n} = \sqrt[4]{1 + \eta_n^2}\, e^{\frac{i\eta_n}{2}} = \sqrt[4]{1 + \eta_n^2}(\cos\frac{\eta_n}{2} + i\sin\frac{\eta_n}{2})$$

Using this equation in (4.51) for the real and imaginary parts of the complex frequency ω_n^* we have two relations

$$\omega_n' = \sqrt{\lambda_n'}\sqrt[4]{1+\eta_n^2}\cos\frac{\eta_n}{2}, \omega_n'' = \sqrt{\lambda_n'}\sqrt[4]{1+\eta_n^2}\sin\frac{\eta_n}{2}$$

Dividing the second and the first relation, we have

$$\tan\frac{\eta_n}{2} = \frac{\omega_n''}{\omega_n'}$$

or

$$\eta_n = 2\arctan\frac{\omega_n''}{\omega_n'}$$

For structures with slight damping $\omega_n'' << \omega_n'$ and

$$\arctan\frac{\omega_n''}{\omega_n'} \approx \frac{\omega_n''}{\omega_n'}$$

In this case the modal loss factor can be calculated by simple expression

$$\eta_n = 2\frac{\omega_n''}{\omega_n'} \tag{4.52}$$

The method described above is called the complex eigenvalue method (CEM) for analysis of modal loss factors of the structure. In the case of frequency independent complex moduli this method can be qualified as exact method. Exact means in the sense of calculation of damping, because the finite element method is numerical method, i.e. approximate method. Lanczos' method for solution of the eigenvalue problem also is approximate method, i.e. the iteration method based on using the numerical procedures. It should be noted that the complex eigenvalue method needs rather large computational efforts. In some cases, for example, for slight damping more simple methods for calculation of modal loss factors can be used.

One of the simplest method for calculation of modal loss factors is based on using the energy concept proposed by Ungar and Kerwin [13]. In the case of slight damping the differences between elastic frequencies and modes, on the one hand, and the damped frequencies and modes, on the other hand, are small. The elastic frequencies ω_n and elastic vibration modes $\boldsymbol{\Phi}_n$ can be calculated from the equation (3.23)

$$\boldsymbol{K}\boldsymbol{v}_0 = \omega^2\boldsymbol{M}\boldsymbol{v}_0$$

Here $\boldsymbol{K} = \boldsymbol{K}'$ is a real part of the complex stiffness matrix $\boldsymbol{K}^* = \boldsymbol{K}' + i\boldsymbol{K}''$. By using a subspase iteration method the first N elastic frequencies ω_n, $(n = 1, 2, ..., N)$ and corresponding vibration modes $\boldsymbol{\Phi}_n$ are calculated.

There are two possibilities to obtain the modal loss factor for each vibration mode. The first possibility is using the Rayleigh's quotent. For this the Rayleigh's formula must be derived. In formula (4.49) it is assumed that the complex stiffness matrix $\boldsymbol{K}^* = \boldsymbol{K}'$ and the complex vibration mode $\boldsymbol{\Phi}_n^* = \boldsymbol{\Phi}_n$. In this case

$$\boldsymbol{K}'\boldsymbol{\Phi}_n = \lambda_n \boldsymbol{M}\boldsymbol{\Phi}_n \tag{4.53}$$

Both sides of this equation is multiplied by $\boldsymbol{\Phi}_n^T$

$$\boldsymbol{\Phi}_n^T \boldsymbol{K}'\boldsymbol{\Phi}_n = \lambda_n \boldsymbol{\Phi}_n^T \boldsymbol{M}\boldsymbol{\Phi}_n$$

From this equation the well known Rayleigh's quotent is obtained

$$\lambda_n = \frac{\boldsymbol{\Phi}_n^T \boldsymbol{K}'\boldsymbol{\Phi}_n}{\boldsymbol{\Phi}_n^T \boldsymbol{M}\boldsymbol{\Phi}_n} \tag{4.54}$$

If in this quotent to the stiffness matrix $\boldsymbol{K}'$ a small variations is applied $\boldsymbol{K}' + \delta\boldsymbol{K}'$, where $\delta\boldsymbol{K}'$ is imaginary part of the stiffness matrix, so that $\boldsymbol{K}' + \delta\boldsymbol{K}' = \boldsymbol{K}^* = \boldsymbol{K}' + i\boldsymbol{K}''$, then eigenvalues $\lambda_n^* = \lambda_n' + i\lambda_n''$ and eigenvectors $\boldsymbol{\Phi}_n^* = \boldsymbol{\Phi}_n' + i\boldsymbol{\Phi}_n''$ also have small variations and are complex. In this case the quotent (4.54) has a form

$$\lambda_n' + \lambda_n'' = \frac{\boldsymbol{\Phi}_n^{*T} \boldsymbol{K}'\boldsymbol{\Phi}_n^*}{\boldsymbol{\Phi}_n^{*T} \boldsymbol{M}\boldsymbol{\Phi}_n^*} + i\frac{\boldsymbol{\Phi}_n^{*T} \boldsymbol{K}'\boldsymbol{\Phi}_n^*}{\boldsymbol{\Phi}_n^{*T} \boldsymbol{M}\boldsymbol{\Phi}_n^*} \tag{4.55}$$

This expression can be considered as extension of Rayleigh's quotent to the complex stiffness matrix. Further the expression (4.55) is simplified substituting here instead of damped vibration modes $\boldsymbol{\Phi}_n^*$ the elastic vibration modes $\boldsymbol{\Phi}_n$

$$\lambda_n' + i\lambda_n'' = \frac{\boldsymbol{\Phi}_n^T \boldsymbol{K}'\boldsymbol{\Phi}_n}{\boldsymbol{\Phi}_n^T \boldsymbol{M}\boldsymbol{\Phi}_n} + i\frac{\boldsymbol{\Phi}_n^T \boldsymbol{K}''\boldsymbol{\Phi}_n}{\boldsymbol{\Phi}_n^T \boldsymbol{M}\boldsymbol{\Phi}_n} \tag{4.56}$$

Equating in this approximate expression the real and imaginary parts one can obtain

$$\lambda_n' = \frac{\boldsymbol{\Phi}_n^T \boldsymbol{K}'\boldsymbol{\Phi}_n}{\boldsymbol{\Phi}_n^T \boldsymbol{M}\boldsymbol{\Phi}_n}, \quad \lambda_n'\eta_n = \frac{\boldsymbol{\Phi}_n^T \boldsymbol{K}''\boldsymbol{\Phi}_n}{\boldsymbol{\Phi}_n^T \boldsymbol{M}\boldsymbol{\Phi}_n} \tag{4.57}$$

Excluding λ_n' from these equations the modal loss factor η_n is obtained

$$\eta_n = \frac{\boldsymbol{\Phi}_n^T \boldsymbol{K}''\boldsymbol{\Phi}_n}{\boldsymbol{\Phi}_n^T \boldsymbol{K}'\boldsymbol{\Phi}_n} \tag{4.58}$$

This expression can be derived also in another way similarly as the expression for material loss factor (4.36). For each vibration mode $\boldsymbol{\Phi}_n$ the elastic

strain energy, the dissipated energy and loss factor can be calculated. It is assumed that instead of damped modes $\boldsymbol{\Phi}_n^*$ the elastic vibration modes $\boldsymbol{\Phi}_n$) are employed similarly as in formulae (4.34)-(4.36).

The elastic strain energy of the structure represented by assembly of the finite elements is defined by eq. (3.15)

$$U = \frac{1}{2}\boldsymbol{v}^T \boldsymbol{K} \boldsymbol{v}$$

For free elastic vibrations the strain energy of the structure at maximum of displacements (this maximum can be taken unity) can be calculated by using the vibration modes $\boldsymbol{\Phi}_n$. Thus, for the nth vibration mode the elastic strain energy U_n is given by

$$U_n = \frac{1}{2}\boldsymbol{\Phi}_n^T \boldsymbol{K}' \boldsymbol{\Phi}_n \tag{4.59}$$

Here $\boldsymbol{K}'$ is the real part of stiffness matrix associated with the storage moduli.

Dissipated energy ΔU per one cycle of vibrations is obtained similarly as eq. (4.33)

$$\Delta U_n = \oint \boldsymbol{F}_n^T d\boldsymbol{v}_n \tag{4.60}$$

Here $\boldsymbol{F}_n$ is vector of nodal forces for the nth vibration mode and $\boldsymbol{v}_n$ is vector of nodal displacements for nth vibration mode

$$\boldsymbol{v}_n(t) = \boldsymbol{\Phi}_n \sin \omega t \tag{4.61}$$

Expression for the nodal forces $\boldsymbol{F}_n$ is similar to the expressions (4.24) and (4.26) for the stresses in viscoelastic material

$$\boldsymbol{F}_n(t) = \boldsymbol{K}^* \boldsymbol{v}_n(t)$$

or

$$\boldsymbol{F}_n(t) = \boldsymbol{K}' \boldsymbol{v}_n(t) + \frac{\boldsymbol{K}''}{\omega} \frac{d\boldsymbol{v}_n(t)}{dt} \tag{4.62}$$

In deriving this expression it was taken into account that the displacements $\boldsymbol{v}_n(t)$ vary sinusoidally (4.61). Substituting eq. (4.61) into (4.62) similarly as eq. (4.29) the nodal forces is obtained

$$\boldsymbol{F}_n(t) = \boldsymbol{K}' \boldsymbol{\Phi}_n \sin \omega t + \boldsymbol{K}'' \boldsymbol{\Phi}_n \cos \omega t \tag{4.63}$$

For the vibration mode $\mathbf{\Phi}_n$ the energy dissipation ΔU_n per one cycle of vibrations is obtained by substituting eqs (4.61) and (4.63) into (4.60) and performing integration over the period $T = 2\pi/\omega$

$$\Delta U_n = \oint \boldsymbol{F}_n^T d\boldsymbol{v}_n = \int_0^{2\pi/\omega} \boldsymbol{F}_n^T \frac{d\boldsymbol{v}_n}{dt} dt = \tag{4.64}$$
$$= \int_0^{2\pi/\omega} \mathbf{\Phi}_n^T (\boldsymbol{K}' \sin\omega t + \boldsymbol{K}'' \cos\omega t)\omega \cos\omega t \mathbf{\Phi}_n \; dt =$$
$$= \Phi_n^T (\boldsymbol{K}'' \mathbf{\Phi}_n \omega \int_0^{2\pi/\omega} \cos^2\omega t \; dt = \pi \mathbf{\Phi}_n^T \boldsymbol{K}'' \mathbf{\Phi}_n$$

Here

$$\int_0^{2\pi/\omega} \sin\omega t \cos\omega t \; dt = 0$$

The specific damping capacity ψ_n for the vibration mode $\mathbf{\Phi}_n$ is defined similarly as (4.35)

$$\psi_n = \frac{\Delta U_n}{U_n} = \frac{2\pi \mathbf{\Phi}_n^T \boldsymbol{K}'' \mathbf{\Phi}_n}{\mathbf{\Phi}_n^T \boldsymbol{K}' \mathbf{\Phi}_n} \tag{4.65}$$

Taking into account the relation (4.36) between the specific damping capacity ψ and the loss factor η the modal loss factor η_n for the nth vibration mode $\mathbf{\Phi}_n$ is obtained

$$\eta_n = \frac{\psi_n}{2\pi} = \frac{\mathbf{\Phi}_n^T \boldsymbol{K}'' \mathbf{\Phi}_n}{\mathbf{\Phi}_n^T \boldsymbol{K}' \mathbf{\Phi}_n} \tag{4.66}$$

This expression is equal to the expression (4.58) obtained by using the Rayleigh's quotent.

Both expressions (4.58) and (4.66) were obtained on the basis of the energy concept of Ungar and Kerwin and on the basis of assumption that damping is small. In this case instead of the damped vibration modes the elastic vibration modes can be used. Therefore, the method described above is called energy method (EM). This is approximate method in comparison with the exact complex eigenvalue method. Comparison of results for the modal loss factors of sandwich beams obtained by both methods will be given in the next section.

4.3 Numerical Examples

Let us consider some numerical examples of analysis of sandwich beams with damping layers in order to estimate the influence of layer properties and layer

stacking sequence on modal loss factors of structure. For analysis the finite element $SI20$ based on broken line (zig-zag) model is used (see section 1.4). Elastic frequencies, damped frequencies and modal loss factors are calculated by using two methods - the energy method (EM) and the complex eigenvalue method (CEM), which were described in the section 4.2.

4.3.1 Symmetric sandwich cantilever with thin damping layer

Let us consider a symmetric sandwich cantilever having a stiff elastic isotropic face sheets made from aluminium alloy and a thin soft core made from isotropic polymer material with high damping (see Figure 4.10).

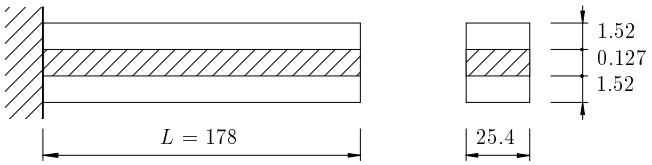

Figure 4.10: Sandwich cantilever beam with thin damping layer (dimensions are given in [mm])

Material properties and geometric parameters of layers are given by

$$\begin{aligned} h_1 = h_3 = 1.52 * 10^{-3} \text{ m}, \quad E_1 = E_3 = 6.9 * 10^4 \text{ MPa}, \\ \nu_1 = \nu_3 = 0.3, \quad \rho_1 = \rho_3 = 2800 \text{ kg/m}^3, \\ \eta_1 = \eta_3 = 0, \quad h_2 = 0.127 * 10^{-3} \text{ m}, \\ E_2 = 2.1 \text{ MPa}, \quad \nu_2 = 0.499, \quad \rho_2 = 970 \text{ kg/m}^3, \\ \eta_2 = 0.1; 0.3; 1.0; 1.5, \quad b = 25.4 * 10^{-3} \text{ m}, \quad L = 0.178 \text{ m} \end{aligned} \tag{4.67}$$

Results of elastic and damped frequency analysis are presented in Table 4.1.

All frequencies were calculated by using the finite element $SI20$ with the mesh $N = 10$. For comparison the results of the frequency analysis obtained by Rao [14] are presented. From analysis of the results presented in Table 4.1 it is seen that for the elastic sandwich beam ($\eta = 0$) both methods, the complex eigenvalue method (Lanczos method) and the energy method (subspace iteration method), gives the same results for elastic frequencies. It is seen that the damped frequencies are slightly higher than elastic frequencies. For slight damping ($0 \leq \eta \leq 0.3$) there are only small differencies between damped frequencies and elastic frequencies. For significant damping ($\eta = 1.5$) differences between the damped and the elastic frequencies also

η_2	Method	f_1	f_2	f_3	f_4	f_5
0	CEM	61.9	287.5	726	1367	2219
	EM	61.9	287.6	726	1367	2219
	Rao	64.1	296.4	743	1393	2261
0.1	CEM	62.0	287.6	726	1367	2219
	Rao	64.1	296.4	743	1394	2261
0.3	CEM	62.3	288.3	727	1367	2219
	Rao	64.4	297	744	1394	2261
1.0	CEM	65.6	294.8	732	1370	2221
	Rao	67.4	302.8	749	1397	2263
1.5	CEM	68.2	301.5	738	1373	2223
	Rao	69.9	308.9	754	1400	2265

Table 4.1: Elastic and damped frequencies in [Hz] of sandwich cantilever, finite element $SI20$, $N = 10$

does not exceed 10%. For the polymer materials, which are used as damping layers the loss factor is in the range $0.2 \leq \eta \leq 0.8$. So, in most cases for damping analysis of structures the most simple energy method can be used.

4.3.2 Sandwich cantilever with different cross sections

Let us consider an example of damping analysis of symmetric sandwich cantilever beam with different cross sections (see Figure 4.11).

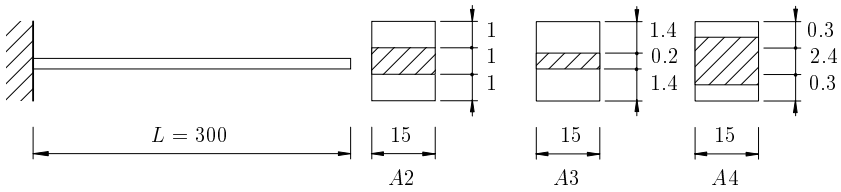

Figure 4.11: Sandwich cantilever beam with different cross sections (dimensions are given in mm)

There are three types of cross section of the beam. The first cross section ($A2$) is with layers of equal thickness $h_1 = h_2 = h_3$ mm, so that $h_1/h_2 = 1$. The second cross section ($A3$) is with relatively thick face sheets $h_1 = h_3 = 1.4$ mm and with thin damping layer $h_2 = 0.2$ mm, so that $h_1/h_2 = 7$. The third cross section ($A4$) is with relatively thin faces $h_1 = h_3 = 0.3$ mm and

with thick damping layer $h_2 = 2.4$ mm, so that $h_1/h_2 = 0.125$. Length of the beam is $L = 300$ mm $= 0.300$ m and width of the beam is $b = 15$ mm.

The face sheets are made from the glass-epoxy unidirectionally fibre reinforced composite with fibre volume fraction $\mu_f = 0.6$. Parameters of this unidirectional composite are as follows (axis 1 is in the fibre direction, axes 2 and 3 are in the transverse direction)

$$\begin{aligned} &E_{11} = 45540 \text{ MPa}, \quad E_{22} = 12808 \text{ MPa}, \quad G_{12} = 4190 \text{ MPa}, \\ &\nu_{21} = 0.33, \quad \nu_{32} = 0.5, \quad \rho = 2040 \text{ kg/m}^3 \end{aligned} \tag{4.68}$$

In the present analysis it is supposed that the face sheets are elastic ($\eta_1 = \eta_2 = 0$). However, a glass-epoxy composite offer a slight damping even in the fibre direction. Note that in the face sheets direction of fibres is in the direction of beam axis. So, the material constants used in the damping analysis are given by

$$E_1 = E_3 = E_{11}, \quad G_1 = G_3 = G_{12}, \quad \rho_1 = \rho_3 = \rho, \quad \eta_1 = \eta_3 = 0 \tag{4.69}$$

In sandwich beam the core is a damping layer, which is made from polymer material with high damping capacity. For all types of the cross section for the damping layer it is supposed that the loss factor is $\eta_2 = 1$. The density of damping layer is $\rho_2 = 1200$ kg/m^3. The loss factor equal to unity is assumed for purposes of more convinient comparison of different designs of the cross section. Actualy for damping layers the loss factor for different polymer materials is in the range $0.1 \leq \eta \leq 0.8$.

For each type of cross section the damping layers of two different stiffness are considered. The first design is with more soft damping layer and the second design is with more stiff damping layer. The parameters of material for the damping layer of different cross sections are given by

$$\begin{aligned} A2A: &\quad G_2 = 0.19 \text{ MPa}, \quad \nu_2 = 0.5, \quad E_2 = 0.57 \text{ MPa}; \\ A2B: &\quad G_2 = 2.53 \text{ MPa}, \quad \nu_2 = 0.5, \quad E_2 = 7.6 \text{ MPa}; \\ A3A: &\quad G_2 = 0.078 \text{ MPa}, \quad \nu_2 = 0.5, \quad E_2 = 0.234 \text{ MPa}; \\ A3B: &\quad G_2 = 0.708 \text{ MPa}, \quad \nu_2 = 0.5, \quad E_2 = 2.125 \text{ MPa}; \\ A4A: &\quad G_2 = 0.036 \text{ MPa}, \quad \nu_2 = 0.5, \quad E_2 = 0.109 \text{ MPa}; \\ A4B: &\quad G_2 = 1.82 \text{ MPa}, \quad \nu_2 = 0.5, \quad E_2 = 5.46 \text{ MPa}; \end{aligned} \tag{4.70}$$

Damping analysis of the sandwich beams considered in the present example was previously performed by Moser [15, 16] using a well known finite element code ADINA. In the analysis performed by Moser for face sheets the Bernouli-Euler's beam finite element was used. The core was modelled by a two dimensional (2D) finite elements.

Beam	Method	ω_1	ω_2	ω_3	η_1	η_2	η_3
A2A	ADINA	85.2	361	891	0.500	0.290	0.140
	EM	81.4	352	880	0.499	0.268	0.125
	CEM	87.2	360	884	0.425	0.255	0.124
A2B	ADINA	144.4	616.4	1365	0.240	0.470	0.490
	EM	141.1	590	1305	0.271	0.475	0.482
	CEM	149.9	633	1385	0.171	0.398	0.431
A3A	ADINA	104.9	509	1335	0.340	0.16	0.070
	EM	101.6	502	1325	0.340	0.145	0.063
	CEM	107	508	1328	0.287	0.134	0.063
A3B	ADINA	143.3	674	1617	0.180	0.320	0.290
	EM	140.8	655	1575	0.201	0.318	0.274
	CEM	147.3	685	1623	0.129	0.270	0.253
A4A	ADINA	31.4	106	214	0.780	0.650	0.470
	EM	29.2	100	205	0.770	0.626	0.426
	CEM	31.6	106	211	0.717	0.587	0.421
A4B	ADINA	118.2	483	1003	0.240	0.610	0.740
	EM	109.6	410	825	0.352	0.674	0.796
	CEM	118.7	452	915	0.215	0.561	0.697

Table 4.2: Natural angular frequencies ω_n[rad/s] and modal loss factors η_n of cantilever sandwich beam

In the present investigation the finite element $SI20$ based on broken line model is used with the mesh $N = 10$. For the damping analysis two methods - the energy method (EM) and the complex eigenvalue method (CEM) are employed. Results of analysis for the first three angular frequencies ω_n, $(n = 1, 2, 3)$ and corresponding modal loss factors η_n are presented in Table 4.2.

From analysis of the results presented in Table 4.2 it is seen that modal loss factors are higher if the damping layer of sandwich beam is thicker. There is different behaviour of the sandwich beam for more soft and for more stiff damping layers. For more soft damping layer (beams $A2A$, $A3A$, $A4A$) the modal loss factor decreases when frequency increases. For the most stiff damping layer (beams $A2B$, $A3B$, $A4B$) the modal loss factor increases when frequency increases. There are rather good agreement of the results obtained by using the finite element code ADINA and the results obtained by using the methods described in the present textbook. Some differencies in frequency analysis are connected with differences of the kinematic models to be used. Moser [15, 16] was employing the Bernouli-Euler beam finite element for the face sheets and the two dimensional (2D) finite element for the core.

Beam	h_1, mm	h_2, mm	h_3, mm
1A	1.1	0.7	4.5
2A	2.0	0.8	5.5
4A	3.7	1.2	3.7
7A	5.0	2.7	1.0
10A	5.0	3.0	2.0
11A	4.0	1.7	4.0

Table 4.3: Specimens geometry

Our finite element $SI20$ is based on using the Timoshenko's hypothesis for each layer of the sandwich beam.

4.3.3 Beams with damping layers. Comparison with experiment

It is of interest to compare the theoretical and experimental results for the modal parameters of the beams with damping layers. Leibowitz and Lifshitz [17] have measured experimentally the natural frequencies and corresponding modal loss factors for sandwich beams with middle damping layer. The beams were made by molding a layer of Neoprene CR-602 between two layers of 2024 aluminium alloy sheets. The conditions in the experiment were such (details see in the paper [17]), that the sandwich beam can be considered as clamped cantilever of length $L = 180$ mm and width $b = 12$ mm. Six different beams were tested. The dimensions of the beams are listed in Table 4.3.

The middle layer of sandwich beam was made from viscoelastic polymer material Neoprene CR-602. Its dynamic shear modulus G_2 and loss factor η_2 were determined experimentally over a frequency range of 100-700 Hz. It was experimentally observed that the dynamic properties of the viscoelastic core have a linear frequency dependence in the test range. The dynamic shear modulus G_2 and the loss factor η_2 of the core are given by

$$G_2(f) = 1.007 \times 10^{-3} f + 1.386 \text{ MPa}, \quad \eta_2(f) = 1.608 \times 10^{-4} f + 0.256$$

Here f is the frequency in Hz. It is assumed that Poisson's ratio of the core is $\nu_2 = 0.3$ and density of the core is $\rho_2 = 970$ kg/m^3. Material properties of the aluminium face sheets are as follows

$$E_1 = E_3 = 7.1 * 10^4 \text{ MPa}, \quad G_1 = G_3 = 2.73 * 10^4 \text{ MPa},$$

Beam	Method	f_1[Hz]	%Deviation	η_1	%Deviation
1A	Exper.	115.5	-	0.052	-
	EM	118.0	2.2	0.0508	-2.3
	CEM	118.2	2.3	0.0503	-3.3
2A	Exper.	139.5	-	0.062	-
	EM	138.7	-0.6	0.0548	-11.6
	CEM	139.0	-0.4	0.0545	-12.1
4A	Exper.	107.5	-	0.072	-
	EM	110.5	2.8	0.0741	2.9
	CEM	110.7	3.0	0.0738	2.5
7A	Exper.	120.5	-	0.054	-
	EM	120.0	-0.4	0.0443	-18.0
	CEM	120.1	-0.3	0.0442	-18.0
10A	Exper.	115.0	-	0.060	-
	EM	116.1	0.9	0.0518	-13.7
	CEM	116.2	1.0	0.0517	-13.7
11A	Exper.	115.5	-	0.078	-
	EM	114.5	-0.9	0.0651	-16.5
	CEM	114.7	-0.7	0.0652	-16.5

Table 4.4: Experimental and theoretical modal parameters f_n and η_n of clamped cantilever for mode 1

$$\nu_1 = \nu_3 = 0.3, \quad \rho_1 = \rho_3 = 2700 \text{ kg/m}^3$$

Frequency and damping analysis was performed by using the finite element $SI20$ based on broken line (zig-zag) model. Finite element mesh was taken $N = 10$ finite elements on the beam length. Two methods - the energy method (EM) and the complex eigenvalue method (CEM) were used.

Experimental and theoretical results for the first natural frequency (mode 1) and corresponding loss factor are presented in Table 4.4.

Experimental and theoretical results for the second natural frequency (mode 2) and corresponding loss factor are presented in Table 4.5. In Tables 4.4 and 4.5 the deviation in percents of the theoretical results from the experiment also is presented.

From analysis of the results presented in Tables 4.4 and 4.5 it is seen that both methods - the energy method (EM) and the complex eigenvalue metod give practically the same results. It is evident because the damping of the beams experimentally tested is relatively small. In this case the approximate energy method can be used successfuly. Damped and elastic frequencies

Beam	Method	f_2[Hz]	%Deviation	η_2	%Deviation
1A	Exper.	628.5	-	0.041	-
	EM	663.0	5.5	0.0258	-37.1
	CEM	663.5	5.5	0.0256	-37.1
2A	Exper.	765	-	0.049	-
	EM	784.3	2.5	0.0263	-46.3
	CEM	784.8	2.5	0.0262	-46.3
4A	Exper.	581.0	-	0.035	-
	EM	605.0	4.1	0.0322	-8.0
	CEM	605.3	4.1	0.0322	-8.0
7A	Exper.	674	-	0.036	-
	EM	696.3	3.3	0.0179	-50.3
	CEM	696.5	3.3	0.0179	-50.3
10A	Exper.	631	-	0.036	-
	EM	666.9	5.7	0.0201	-44.2
	CEM	666.9	5.7	0.0201	-44.2
11A	Exper.	612.0	-	0.049	-
	EM	641.2	4.8	0.0267	-45.5
	CEM	641.4	4.8	0.0267	-45.5

Table 4.5: Experimental and theoretical modal parameters f_n and η_n of clamped cantilever for mode 2

practicaly are equal. For the natural frequencies there are good agreement of theoretical and experimental results. For the first frequencies for the beams tested the deviation does not exceed 3%. For the second frequencies the deviation does not exceed 5.7%.

Relatively good agreement of theoretical and experimental results are also for the modal loss factor η_1 for the vibration mode 1. The deviation does not exceed 18%. For the modal damping parameters this is rather good result. Significant differences (till 50.3%) of the theoretical and experimental results are for the modal loss factor η_2 of the vibration mode 2. Note that for all beams tested the modal loss factors η_2 obtained from theoretical calculations are smaller that those obtained experimentally. It could be due to additional damping in the supports for the higher frequencies.

Chapter 5

Stability Analysis of Columns

Two types of non-linearities occur in the structural problems. The first type is reffered to as material non-linearity and is due to the non-linearly elastic or plastic behaviour of the material. In the present textbook the composite materials are investigated on the basis of linear elastic or viscoelastic behaviour. The second type of non-linearity reffered to as geometric non-linearity, and it occurs when the deflections are large enough to cause significant changes in the geometry of structure. In this case the equations of equilibrium must be formulated for the deformed configuration.

For the composite structures, which mainly are used as lightweight structures, the geometric non-linearity is most important in comparison with non-linearity of the material. Typical non-linear behaviour is in the case of stability or buckling of the composite columns, plates and shells.

Stability analysis of columns, plates and sometimes even shells can be performed on the basis of simplified or the Euler's approach. It is called the Euler's approach because in 1737 Euler was the first who investigated the buckling of columns. He has obtained a solution, which today is known for all students in mechanical and civil engineering. The Euler's problem of buckling of the pin-ended column is presented in Figure 5.1.

In Euler's approach or the so called linearised approach, which can be used instead of the large-deflection analysis for structural stability, the eigenvalue equations are formulated. Stability analysis of the column can be performed by using the Ritz's or the finite element method. For simplest cases of boundary conditions the Ritz's method can be used. More complicated cases of loading and boundary conditions can be solved by using the finite element method.

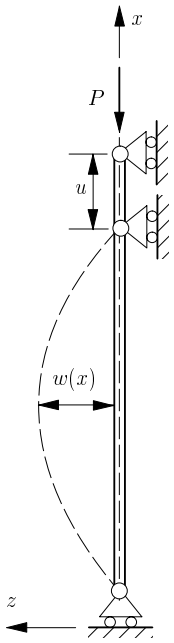

Figure 5.1: Buckling of the column

5.1 Solution by Ritz's Method

Buckling analysis of the pin-ended column (see Figure 5.1) can be performed by using the Ritz's method. In this case the total potential energy Π of the column can be written as

$$\Pi[w(x), \gamma_x(x)] = U - W \tag{5.1}$$

Here the strain energy U for the composite or sandwich column obtained by using the Timoshenko's model is presented by the same functional (3.2) as for the case of bending and vibrations of the beam

$$U = \frac{1}{2} \int_0^L \left[D_{11} \left(\frac{\partial \gamma_x}{\partial x} \right)^2 + kQ_{55} \left(\gamma_x + \frac{\partial w}{\partial x} \right)^2 \right] dx \tag{5.2}$$

The work W done by the external force P after buckling of the column is given by

$$W = Pu \tag{5.3}$$

Here u is vertical displacement after buckling of the column. This displacement can be calculated from the lateral deflection w in the routine way.

The differential element ds of the buckled column (see Figure 5.1) can be calculated

$$(ds)^2 = (dx)^2 + (dw)^2$$

Thus

$$ds = dx\sqrt{1 + w'^2} \approx dx\left(1 + \frac{1}{2}w'^2\right)$$

Since $du = ds - dx \approx (1/2)w'^2 dx$ and

$$u(L) = \int_0^L du$$

the following expression for the vertical displacement can be obtained

$$u = \frac{1}{2}\int_0^L \left(\frac{\partial w}{\partial x}\right)^2 dx \tag{5.4}$$

So, the work of external force can be represeted as functional of the lateral displacement w after buckling of the column

$$W = \frac{P}{2}\int_0^L \left(\frac{\partial w}{\partial x}\right)^2 dx \tag{5.5}$$

Essential boundary conditions for the pin-ended column (see Figure 5.1) are as follows

$$w = \Big|_{x=0} = 0, \quad w = \Big|_{x=L} = 0 \tag{5.6}$$

Minimization of the functional (5.1) is performed by using the Ritz's method. Unknown functions w and γ_x are approximated as follows

$$\begin{aligned} w(x,t) &= a_1 \sin\left(\frac{\pi x}{L}\right), \\ \gamma_x(x,t) &= b_1 \cos\left(\frac{\pi x}{L}\right) \end{aligned} \tag{5.7}$$

Substituting these approximations into functional (5.1) and taking into account (5.2) and (5.5) after integration over the length of the column the total potential energy Π is obtained as function of the unknown Ritz's coefficients

$$\Pi = \Pi(a_1, b_1) \tag{5.8}$$

Minimum of this function can be obtained

$$\frac{\partial \Pi}{\partial b_1} = 0, \quad \frac{\partial \Pi}{\partial a_1} = 0 \tag{5.9}$$

These minimum conditions leads to a set of two linear homogeneous algebraic equations

$$\begin{array}{rcrcl} (D_{11}\left(\frac{\pi}{L}\right)^2 + kQ_{55})b_1 & + & kQ_{55}\frac{\pi}{L}a_1 & = & 0 \\ kQ_{55}\frac{\pi}{L}b_1 & + & \left[kQ_{55}\left(\frac{\pi}{L}\right)^2 - P\left(\frac{\pi}{L}\right)^2\right]a_1 & = & 0 \end{array} \tag{5.10}$$

For the non-trivial solution ($a_1 \neq 0, b_1 \neq 0$) the determinant D of the system of linear equations (5.10) must be zero

$$D = 0 \tag{5.11}$$

Under this condition the buckling load $P_{\rm cr}^{\rm T}$ of the Euler's column calculating by using the Timoshenko's model can be found

$$P_{\rm cr}^{\rm T} = \frac{D_{11}\left(\frac{\pi}{L}\right)^2}{\left[1 + \left(\frac{\pi}{L}\right)^2 \frac{D_{11}}{kQ_{55}}\right]} \tag{5.12}$$

In the classical Bernouli-Euler's beam theory the transverse shear deformations are neglected and the transverse shear stiffness of the beam is assumed to be infinity $kQ_{55} \to \infty$. In this case the buckling load $P_{\rm cr}^{\rm cl}$ (classical theory without shear deformations) can be obtained from formula (5.12)

$$P_{\rm cr}^{\rm cl} = D_{11}\left(\frac{\pi}{L}\right)^2 \tag{5.13}$$

For the column with uniform cross section the bending stiffness $D_{11} = EI$, where E is Young's modulus of the homogeneous material and I is moment of inertia of the cross section of the column. In this case expression (5.13) gives the well known Euler's formula

$$P_{\rm cr}^{\rm cl} = EI\left(\frac{\pi}{L}\right)^2 \tag{5.14}$$

To estimate the influence of the transverse shear deformations on the buckling load, formula (5.12) can be rearranged. In the case of rectangular cross

Euler's	Reuss'	Reissner's	Stamm and Witte [3]
$4.41 * 10^5$	$0.637 * 10^5$	$0.607 * 10^5$	$0.609 * 10^5$

Table 5.1: Buckling loads in [N] of the sandwich column

section $I = 1/12\ bh^3$ and $kQ_{55} = 5/6\ bhG$, where G is shear modulus, formula (5.12) can be written as follows

$$P_{\rm cr}^{\rm T} = \frac{EI\left(\frac{\pi}{L}\right)^2}{\left[1+\pi^2\left(\frac{h}{L}\right)^2\frac{E}{5/6\ G}\right]} \tag{5.15}$$

By using this formula it is easly to determine the influence on the buckling load of ratio E/G and slenderness h/L of the column.

5.1.1 Buckling of sandwich column

Let us calculate the buckling load of a sandwich column. Material properties were given by the eqs (3.27)

$$\begin{aligned} L = 1.08\ m,\quad b = 0.1\ \text{m},\quad h = 8.45 * 10^{-2}\ \text{m},\\ h_2 = 8.02 * 10^{-2}\ \text{m},\quad h_1 = h_3 = 0.225 * 10^{-2}\ \text{m},\\ E_1 = E_3 = 7.1 * 10^4\ \text{MPa},\quad E_2 = 22\ \text{MPa},\\ \nu_1 = \nu_2 = \nu_3 = 0.315,\\ \rho_1 = \rho_3 = 2700\ \text{kg/m}^3,\quad \rho_2 = 40\ \text{kg/m}^3,\\ k_{\rm Reuss} = 0.637 * 10^{-2},\quad k_{\rm Reissner} = 0.602 * 10^{-2} \end{aligned} \tag{5.16}$$

The buckling load of this sandwich column with the soft core and thin face sheets is determined by using in the formula (5.12) the shear correction coefficient calculated by the Reuss' formula (1.45) and by the Reissner's formula (1.39). Results are presented in Table 5.1.

For comparison in Table 5.1 the buckling load calculated by classical (Euler's) formula 5.13) is presented. The value of buckling load calculated by classical sandwich theory (see Stamm and Witte [3]) also is presented. Classical sandwich theory was developed on the basis of assumption that there is membrane stress state (without bending) in the face sheets. Such assumption can be used for very thin face sheets. In this case the buckling

load of the pin-ended column is as follows (see Stamm and Witte [3])

$$P_{\rm cr}^{\rm sandw} = \frac{\pi^2 B_s}{\left[L^2 + \pi^2 \dfrac{B_s}{A_s}\right]} \tag{5.17}$$

Here A_s is transverse shear stiffness of the core

$$A_s = G_2 \frac{b(h_2 + h_1)^2}{h} \tag{5.18}$$

and B_s is the bending stiffness of the sandwich column, where only membrane stress-state is taken into account in the face sheets

$$B_s = \frac{1}{2} E_1 b h_1 (h_2 + h_1)^2 \tag{5.19}$$

Here the values of the geometry of cross section of the sandwich beam were defined in the Figure 1.5. From analysis of the results presented in Table 5.1 it is seen that classical beam theory overestimate the value of the buckling load 6.92 times. In the same time the results obtained by using the Timoshenko's model with shear correction by the Reuss' or by the Reissner's formulae is in good agreement with the results obtained by classical sandwich beam theory, which was outlined in the textbook by Stamm and Witte [3].

5.2 Solution by Finite Element Method

In the finite element method the column can be represented as assembly of finite elements. The column of length L can be discretised by N finite elements of length $l = L/N$. For each finite element the strain energy (5.2) is represented in the discrete form (1.59)

$$U_e = \frac{1}{2} \boldsymbol{v}_e^T \boldsymbol{K}_e \boldsymbol{v}_e \tag{5.20}$$

The functional of the work of external load (5.5) for one finite element is given by

$$W_e = \frac{P}{2} \int_0^l \left(\frac{\partial w}{\partial x} \right)^2 \, dx \tag{5.21}$$

This functional can be represented in matrix form

$$W_e = \frac{P}{2} \int_0^l \boldsymbol{u}^T \boldsymbol{L}_1^T \boldsymbol{L}_1 \boldsymbol{u} \, dx \tag{5.22}$$

Here $\boldsymbol{u}^T = [w, \gamma_x]$ was introduced by formula (1.50) and

$$\boldsymbol{L}_1 = \begin{bmatrix} \dfrac{\partial}{\partial x} & 0 \end{bmatrix} \tag{5.23}$$

Substituting the approximation (1.52) into the functional (5.22) one obtains

$$W_e = \frac{P}{2} \boldsymbol{v}_e^T \boldsymbol{K}_e^G \boldsymbol{v}_e \tag{5.24}$$

where $\boldsymbol{K}_e^G$ is a geometrical stiffness matrix of the finite element

$$\boldsymbol{K}_e^G = \int_0^l \boldsymbol{N}^T \boldsymbol{L}_1^T \boldsymbol{L}_1 \boldsymbol{N} \, dx \tag{5.25}$$

Here the shape functions $\boldsymbol{N}$ was defined by expressions (1.54)-(1.56). For the assembly of N finite elements the potential energy of the column is given by

$$\Pi = \sum_{e=1}^{N} (U_e - W_e) = \frac{1}{2} \boldsymbol{v}^T \boldsymbol{K} \boldsymbol{v} - \frac{P}{2} \boldsymbol{v}^T \boldsymbol{K}_G \boldsymbol{v} \tag{5.26}$$

Here $\boldsymbol{K}$ and $\boldsymbol{K}_G$ is the stiffness and the geometrical stiffness matrices of the whole structure, respectively

$$\boldsymbol{K} = \sum_{i=1}^{N} \boldsymbol{K}_{i,e}, \quad \boldsymbol{K}_G = \sum_{i=1}^{N} \boldsymbol{K}_{i,e}^G \tag{5.27}$$

The minimum of potential energy (5.26) gives a system of linear homogeneous equations

$$\boldsymbol{K} \boldsymbol{v} - P \boldsymbol{K}_G \boldsymbol{v} = 0 \tag{5.28}$$

By solving the eigenvalue problem the buckling load P_{cr} can be determined. The first eigenvalue of the equation (5.28) coresponds to the critical (buckling) load. By using the finite element method the buckling loads for more complicated structures, for example, frames, space trusses etc. can be determined.

Bibliography

[1] Altenbach, H., Altenbach, J. & Rikards, R. *Einfürung in die Mechanik der Laminat- und Sandwichtragwerke*, Deutscher Verlag für Grundstoffindustrie, Stuttgart, 1996.

[2] Zenkert, D. (Editor). *The Handbook of Sandwich Construction*, EMAS Publishing, Cradley Heath, West Midlands, UK, 1997.

[3] Stamm, K. & Witte, H. *Sandwichkonstruktionen*, Springer, Wien, New York, 1974.

[4] Pagano, N. J., Exact solutions for composite laminates in cylindrical bending. *J. Comp. Mater.*, **3**, 1969, 398–411.

[5] Bathe, K.-J., *Finite Element Procedures in Engineering Analysis*, Prentice-Hall, Englewood Cliffs, 1982.

[6] Jones, R. M., *Mechanics of Composite Materials*, MCGraw-Hill, Washington, 1975.

[7] Washizu, K., *Variational Methods in Elasticity and Plasticity*, Pergamon Press, Oxford, 1982.

[8] Fages, A. and Verchery, G., Influence de la prise en compte du cisaillament transversal sur le calcul des fréquences propres de poutres sandwiches. *J. Mécanique théorique et appliqueé*, **5**(1), 1986, 73–93.

[9] Nashif, A.D., Johnes, D.I.G. & Henderson, J.P., *Vibration Damping,* John Wiley & Sons, New York, 1985.

[10] Sun, C.T. & Lu, Y.P., *Vibration Damping of Structural Elements,* Prentice Hall, Englewood Cliffs, New Jersey, 1995.

[11] Christensen, R. M., *Theory of Viscoelasticity,* Academic Press, New York, London, 1971.

[12] Gibson, R. F., *Principles of Composite Material Mechanics,* McGraw-Hill, New York, 1994.

[13] Ungar, E. E., Kerwin, E. M., Loss factors of viscoelastic systems in terms of energy concepts. *J. Acoustical Soc. America*, **36**(7), 1962, 954–957.

[14] Rao, D. K., Frequency and loss factors of sandwich beams under various boundary conditions. *J. Mech. Engng. Sci.*, **20**, 1978, 271–282.

[15] Moser, K. & Lumassegger, M., Increasing the damping of flexural vibrations of laminated FPC structures by incorporation of soft intermediate plies with minimum reduction of stiffness. *Composite Struct.*, **10**, 1988, 321–333.

[16] Moser, K., *Faser Kunststoff Verbund*, VDI-Verlag, Düsseldorf, 1992.

[17] Leibowitz, S. G., Lifshitz, J. M., Experimental verification of modal parameters for 3-layered sandwich beams. *Int. J. Solids Struct.*, **26**(2), 1990, 175–184.

[18] Chandrupatla, T. R. & Belegundu, A. D., *Introduction to Finite Elements in Engineering* Prentice-Hall, Englewood Cliffs, 1997.

[19] Kachanov, L. M., *Delamination Buckling of Composite Materials*, Kluwer Academic Publishers, Dordrecht-Boston-London, 1988.

[20] Reddy, J. N., *Mechanics of Laminated Composite Plates. Theory and Analysis*, CRC Press, Boca Raton, 1996.

[21] Reddy, J. N., Miravete, A., *Practical Analysis of Composite Laminates*, CRC Press, Boca Raton, 1995.